Summer 7-28-2018

The fate of xylem-transported CO2 in plants

Samantha S. Stutz
University of New Mexico

David T. Hanson
University of New Mexico - Main Campus

Follow this and additional works at: https://digitalrepository.unm.edu/biol_etds

Part of the Biology Commons, Botany Commons, and the Other Plant Sciences Commons

Samantha S. Stutz
Candidate

Biology
Department

This dissertation is approved, and it is acceptable in quality and form for publication:

Approved by the Dissertation Committee:

David Hanson, Chairperson

Nate McDowell

Robert Teskey

Kathy Steppe

THE FATE OF XYLEM-TRANSPORTED CO₂ IN PLANTS

by

SAMANTHA S. STUTZ

B.S. Botany, University of Wyoming, 2010
M.Sc. Botany, Washington State University, 2012

DISSERTATION

Submitted in Partial Fulfillment of the
Requirements for the Degree of

Doctor of Philosophy
Biology

The University of New Mexico
Albuquerque, New Mexico

July, 2018

Acknowledgments

The fate of xylem-transported CO_2 in plants

by

Samantha S. Stutz

B.S. Botany, University of Wyoming, 2010
M.Sc. Botany, Washington State University, 2012
Ph.D. Biology, University of New Mexico, 2018

Abstract

The concentration of carbon dioxide in tree stems can be ~30-750 times higher than current atmospheric [CO_2]. Dissolved inorganic carbon enters the xylem from root and stem respiration and travels with water through the plant. However, the fate of much of this xylem-transported CO_2 is unknown. In these studies I examined the fate of xylem-transported CO_2 traveling through the petiole and leaf. This was accomplished by placing cut leaves from a woody and herbaceous C_3 species, and a Kranz-type C_4 species, in a solution of dissolved $NaH^{13}CO_3$ at concentrations similar to those measured in nature. This allowed me to track the efflux of $^{13}CO_2$ using tunable diode laser absorption spectroscopy and compare this with $^{12}CO_2$ fluxes derived from plant metabolism.

The objective of the first study was to measure the efflux of xylem-transported CO_2 out of the woody species *Populus deltoides* and the herbaceous C_3 species *Brassica napus* in the dark by testing the relationship among the concertation of bicarbonate in the xylem, the rate of transpiration, and the rate of gross CO_2 efflux. I found when the concentration of CO_2 in the xylem is high and when the rate of transpiration is also high, the magnitude of $^{13}CO_2$ efflux can approach half of the rate of respiration in the dark.

The second study extends measurements of the fate of xylem-transported CO_2 into lighted conditions where photosynthesis is active. I measured $^{12}CO_2$ and $^{13}CO_2$ fluxes across light- and CO_2-response curves with the objectives of: 1) determining how much and under what conditions xylem-transported CO_2 exited cut leaves in the light, and 2) determining how much xylem-transported CO_2 was used for photosynthesis and when the overall contribution to photosynthesis was most important. I found that in the light the contribution of xylem-transported CO_2 is most important when intercellular $[CO_2]$ is low which occurs under high irradiance and low $[CO_2]$.

The last study focused on the efflux and use of xylem-transported CO_2 in the Kranz-type C_4 species, *Amaranthus hypochondriacus*. Species with Kranz anatomy have highly active photosynthetic cells surrounding the vascular bundle, which is where xylem-transported CO_2 would first interact with photosynthetic cells. The objectives of this study were to determine: 1) the rate and total efflux of xylem-transported CO_2 exiting a cut leaf of the Kranz-type C_4 species, *A. hypochondriacus*, in the dark and 2) the rate and contribution of xylem-transported CO_2 to total assimilation in the light for *A. hypochondriacus*. Rates of dark efflux of xylem-transported CO_2 out of *A. hypochondriacus* leaves were lower in the dark compared to rates observed in *B. napus* across the same rates of transpiration and bicarbonate concentrations. In the light a higher portion of xylem-transported CO_2 was used for photosynthesis in *A. hypochondriacus* compared to *B. napus* suggesting that Kranz anatomy influences how C_4 plants use xylem-transported CO_2 for photosynthesis.

Table of Contents

List of Figures

List of Tables

Chapter 1

Introduction

        Concentrations of dissolved inorganic carbon in tree stems range from ~0.05 to ~13 mmol l^{-1} (Teskey *et al*., 2008); ~30-750 times higher than current atmospheric $[CO_2]$. Dissolved inorganic carbon (the sum of $[CO_2]_{aq}$, $[HCO_3^-]$, $[H_2CO_3]$, and $[CO_3^{2-}]$) enters the xylem from root and stem respiration and travels through the plant body in the transpiration stream. Xylem-transported CO_2 has two fates 1) it can exit the plant through the stem, branches or leaves or 2) it can be used for photosynthesis by corticular and woody stem tissue (Teskey *et al*., 2008), branch tissue (Teskey & McGuire, 2002; McGuire *et al*., 2009; Bloemen *et al*., 2013a, b), or leaves (Stringer & Kimmerer, 1993: McGuire *et al*., 2009: Bloemen *et al*., 2013a, b; Bloemen *et al*., 2015). In the dark, xylem-transported CO_2 travels through a plant and exits from tissues far from the point of origin, thus changing estimates for the rate of respiration for different plant organs (*i.e.* if xylem-transported CO_2 generated from root respiration effluxes from the stem then rates of stem respiration would be overestimated while rates of root respiration would be underestimated). In the light, assimilation of xylem-transported CO_2 represents carbon fixation invisible to standard measurements of photosynthetic activity, and may contribute significantly to total plant carbon capture. Therefore, the objectives of this dissertation are to achieve a better understanding of 1) how xylem-transported CO_2 changes our understanding of respiration, by measuring the efflux of xylem-transported CO_2 from cut leaves in the dark, 2) how cut leaves utilize xylem-transported CO_2 for photosynthesis and contribute to measurements of CO_2 efflux from leaves in the light, and 3) how Kranz anatomy associated C_4 metabolism impacts utilization of xylem-transported CO_2.

Models estimate that the current global contribution of leaf respiration accounts for 21-28 Pg C yr^{-1}, which is approximately 3-4 times larger than all emissions from fossil fuel burning globally (Atkins *et al.* 2007, 2014). Models for leaf respiration assume that the CO_2 generated from respiration is produced in the mitochondria of leaf cells (Farquhar *et al.*, 1980); however, if CO_2 is transported to leaves in the xylem this may change the estimates of the rate of leaf respiration. Prior studies suggest this could be an important source of error. Bloemen *et al.* (2013a) placed cut *Populus deltoides* branches in a $^{13}CO_2$ solution in the dark and measured how much xylem-transported CO_2 was taken up by the branch in the dark under two $[^{13}CO_2^*]$ and across high and low vapor pressure differences (VPD). They found that more $^{13}CO_2$ effluxed out of the branch when the $^{13}CO_2^*$ was higher and when rates of transpiration were higher, which occurred under high VPD. Stringer & Kimmerer (1993) placed cut leaves of *P. deltoides* in a solution of $NaH^{14}CO_3$ and found in the dark that 83% of the label exited the leaves as $^{14}CO_2$ in the dark. However, in the light, it is likely that the efflux of xylem-transported CO_2 exiting leaves is lower since xylem-transported CO_2 is consumed for photosynthesis.

Bloemen *et al.* (2013b) added $^{13}CO_2$ to the base of stems of *P. deltoides* saplings in the field and found in a low-label treatment that only 17.4% of the label was incorporated into plant tissue and in a high label treatment that only 5.6% of the label was incorporated into the plant tissue. The bulk of what was used for photosynthesis was located in the stem and branches. Leaves accounted for the smallest portion of xylem-transported CO_2 fixed in both the low- and high-labels. Using a leaf cutting and feeding approach, Stringer & Kimmerer (1993) also determined that only a small portion of xylem-transported CO_2 is used by a plant for photosynthesis. They found that not accounting for the contribution of xylem-transported CO_2 to photosynthesis underestimated net photosynthesis by 0.5% and that the contribution of xylem-

transported CO_2 to photosynthesis accounted for 2.2% of the atmospheric uptake by the leaf under a low concentration of xylem-transported CO_2.

Xylem-transported CO_2 research has focused on C_3 species; however, it is not known how Kranz-type C_4 plants use xylem-transported CO_2 for photosynthesis. Vascular bundles in Kranz-type C_4 plants are surrounded by two layers of specialized cells containing carboxylation enzymes, bundle-sheath cells which contain ribolose-1,5-bisphosphate-carboxylase/oxygenase (Rubisco) and mesophyll cells which contain phosphoenolphyruvate carboxylase (PEPC). In Kranz-type C_4 species there is a high probability that xylem-transported CO_2 will be captured by Rubisco or PEPC before exiting the leaf as CO_2. This is in contrast to C_3 leaf anatomy where vascular bundles are loosely surrounded by photosynthetic cells with intercellular air spaces, allowing more opportunities for xylem-transported CO_2 to exit the vascular bundle and then the leaf without interacting with photosynthetic cells. Kranz anatomy may represent a mechanism by which C_4 plants increase their carbon use efficiency over their C_3 counterparts, further improving C_4 water use efficiency in the light.

Xylem-transported CO_2 is an emerging area of research that has the potential to change our understanding of plant respiration and photosynthesis. For instance, in the dark, if the efflux of xylem-transported CO_2 out of the leaf is large, rates of leaf respiration maybe over estimated. While in the light, if the concentration of xylem-transported CO_2 is high current models of leaf intercellular $[CO_2]$ may not be accurate, or if the contribution of xylem-transported CO_2 to leaf photosynthesis is high then models for leaf photosynthesis may need to be adjusted. Xylem-transported CO_2 has not been studied in C_4 plants and may have a large impact on understanding how Kranz-type C_4 plants increase their water and carbon use efficiencies. While previous studies have only been able to determine where xylem-transported CO_2 is consumed and

incorporated into plant tissues; the method used in these studies allows for real-time measurements of xylem-transported CO_2 assimilation using a tunable diode laser coupled to a portable photosynthesis machine to measure the efflux of xylem-transported CO_2 out of a plant along with the rate of assimilation using ^{13}C labeled xylem-transported CO_2. The first study sought to measure the efflux of xylem-transported CO_2 exiting cut leaves of the woody *P. deltoides* or the herbaceous plant *Brassia napus* in the dark in real-time. In the second study the objective was to measure the efflux of xylem-transported CO_2 out of a cut leaf in real-time and measure how much xylem-transported CO_2 is used for leaf photosynthesis in *P. deltoides* and *B. napus* across both a light- and CO_2-response curve. The final study estimated how much xylem-transported CO_2 exits Kranz-type C_4 leaves in the dark and how Kranz-type C_4 plants use xylem-transported CO_2 for photosynthesis.

References

Atkin OK, Meir P, Turnbull MH. 2014. Improving representation of leaf respiration in largescale predictive climate-vegetation models. *New Phytologist* **202,** 743-748.

Atkin OK, Scheurwater I, Pons TL. 2007. Respiration as a percentage of daily photosynthesis in whole plants is homeostatic at moderate, but not high, growth temperatures. *New Phytologist* **174,** 367-380.

Bloemen JB, McGuire MA, Aubrey DP, Teskey RO, Steppe K. 2013a. Assimilation of xylem-transported CO_2 is dependent on transpiration rate but is small relative to atmospheric fixation. *Journal of Experimental Botany* **64,** 2129-2138.

Bloemen JB, McGuire MA, Aubrey DP, Teskey RO, Steppe K. 2013b. Transport of rootrespired CO_2 via the transpiration stream affects aboveground carbon assimilation and CO_2 efflux in trees. *New Phytologist* **197,** 555-565.

Bloemen JB, McGuire MA, Aubrey DP, Teskey RO, Steppe K. 2015. Assimilation of xylem-transported CO_2 is dependent on transpiration rate but is small relative to atmospheric fixation. *Journal of Experimental Botany* **64,** 2129-2138.

Farquhar GD, von Caemmerer S, Berry JA. 1980. A biochemical model of photosynthetic CO_2 assimilation in leaves of C_3 species. *Planta* 149: 78-90.

McGuire MA, Marshall JD, Teskey RO. 2009. Assimilation of xylem-transported ^{13}C-labelled CO_2 in leaves and branches of sycamore (*Platanus occidentalis* L.). *Journal of Experimental Botany* **60,** 3809-3817.

Stringer JW, Kimmerer TW. 1993. Refixation of xylem sap CO_2 in *Populus deltoides*. *Physiologia Plantarum* **89,** 243-251.

Teskey RO, McGuire MA. 2002. Carbon dioxide transport in xylem causes errors in estimation of rates of respiration in stems and branches of trees. *Plant, Cell & Environment* **25**: 1571-1577.

Teskey RO, Saveyn A, Steppe K, McGuire MA. 2008. Origin, fate and significance of CO_2 in tree stems. *New Phytologist* **117,** 17-32.

Chapter 2

Inside out: efflux of carbon dioxide from leaves represents more than leaf metabolism

SAMANTHA S. STUTZ[1], JEREMIAH ANDERSON[1], RACHAEL ZULICK[1], DAVID T. HANSON[1]

[1]*Department of Biology, University of New Mexico, MSC03-2020, 1 University of New Mexico, Albuquerque, NM 87131, USA*

Highlight

Respired CO_2 is transported through xylem and effluxes far from its point of origin. We supplied ^{13}C to leaves to show the effect of transported CO_2 on measured leaf respiration.

Abstract

High concentrations of inorganic carbon in the xylem, produced from root, stem, and branch respiration, travel via the transpiration stream and eventually exit the plant through distant tissues as CO_2. Unlike previous studies that focused on the efflux of CO_2 from roots and woody tissues, we focus on efflux from leaves and the potential effect on leaf respiration measurements. We labeled transported inorganic carbon, spanning reported xylem concentrations, with ^{13}C and then manipulated transpiration rates in the dark in order to vary the rates of inorganic carbon supply to cut leaves from *Brassica napus* and *Populus deltoides*. We used tunable diode laser absorbance spectroscopy to directly measure the rate of gross $^{13}CO_2$ efflux, derived from inorganic carbon supplied from outside of the leaf, relative to gross $^{12}CO_2$ efflux generated from leaf cells. These experiments showed that $^{13}CO_2$ efflux was dependent upon the rate of inorganic carbon supply to the leaf and the rate of transpiration. Our data show that the gross leaf efflux of xylem-transported CO_2 is likely small in the dark when rates of transpiration are low. However, gross leaf efflux of xylem-transported CO_2 could approach half the rate of leaf respiration in the light when transpiration rates and branch inorganic carbon concentrations are high, irrespective of the grossly different petiole morphologies in our experiment.

INTRODUCTION

Environmental control of leaf-level respiration is poorly understood and the global flux of

respired CO_2 from leaves is massive. Current estimates indicate that global leaf respiration is 21-

28 Pg C yr^{-1}, which is approximately 3-4 times larger than all emissions from fossil fuel burning

globally (Atkin *et al*., 2007; Atkin *et al*., 2014). The combination of uncertainty and small errors

in the measurement of respiration can have large consequences (Hanson *et al.*, 2016). For

example, a 1% error in predictions of leaf respiration (*i.e.* 0.21-0.28 Pg C yr^{-1}) would account for

about a third of the 0.7 Pg C yr^{-1} uncertainty in global carbon models (Canadell *et al*., 2007).

Such a large role of leaf respiration is consistent with analyses showing that behavior of the

carbon cycle is the second greatest source of uncertainty in climate model predictions of global

temperature. Over 15% of this uncertainty can be attributed to temperature feedbacks on

respiration and net primary productivity (Bodman *et al*., 2013). Coupled climate Earth System

Models and Terrestrial Biosphere Models have made some advances that improve the modeling

of respiration (King *et al*., 2006; Atkin *et al*., 2008; Wythers *et al.*, 2013; Atkin *et al*. 2015;

Wullschleger *et al*., 2015), while also highlighting the need for more data (King *et al*., 2006;

Atkin *et al*., 2008; Reich, 2010; Atkin *et al*., 2015; Wullschleger *et al.*, 2015).

All methods for measuring or modeling the rate of gross non-photorespiratory CO_2 efflux

(respiration) from leaves implicitly assume that all CO_2 efflux is derived from metabolism

occurring in leaf cells (*e.g.* Farquhar *et al*. 1980). Similarly, it has often been assumed that in

roots, internally generated CO_2 diffuses into the soil before diffusing into the atmosphere

(Kuzyakov, 2006). However, studies with woody plants show that a large fraction of CO_2

generated by root and stem respiration can be transported through the xylem and efflux from the

plant to the atmosphere through the stem and branches at a point remote from its production

(Levy et al., 1999; McGuire and Teskey, 2002; McGuire et al., 2009; Aubrey and Teskey, 2009; Bloemen et al., 2013a, b; Bloemen et al., 2015a; Steppe et al., 2015) (Fig. 1). The efflux of xylem-transported CO_2 can be large because the total inorganic carbon concentration ($[CO_2^*]$, the sum of $[CO_2]_{aq}$, $[H_2CO_3]$, $[HCO_3^-]$ and $[CO_3^{2-}]$) in the xylem ranges from ~0.05 mmol l^{-1} to ~13 mmol l^{-1}, levels that are ~30-750 times higher than if equilibrated with current atmospheric $[CO_2]$ (Teskey et $al.$, 2008). Previous studies have found xylem-transported CO_2^* is recycled by photosynthesis in corticular and woody stem tissue (Teskey et $al.,$ 2008), branch tissue (McGuire and Teskey, 2002; McGuire et al., 2009; Bloemen et al., 2013a, b) and even leaves (Stringer and Kimmer, 1993; McGuire et al., 2009; Bloemen et al., 2013a, b; Bloemen et $al.$, 2015a). The relative magnitude of this recycling in each part of the tree was demonstrated by Bloemen et al. (2013b). They added $^{13}CO_2^*$ to the stems of $Populus$ $deltoides$ in the field under a low (1.4 mmol l^{-1} [$^{13}CO_2^*$]) and high (12 mmol l^{-1} [$^{13}CO_2^*$]) treatments, and used destructive sampling for mass balance calculations to track the fate of the labeled carbon. They concluded that 82.6% and 94.4% of $^{13}CO_2^*$ added to the stems of the low and high treatment, respectively, was transported through the transpiration stream and diffused into the atmosphere through some combination of the stem and branches over a period of two days. Most of the $^{13}CO_2^*$ retained by the plant was recycled by photosynthesis in the stem and branches, with a small fraction recycled by leaves (2.7% and 0.5% under the low- and high-labels, respectively—Bloemen et al., 2013b). Very little data exist to assess if the low rates of re-capture of xylem-transported CO_2 by leaves is the result of little xylem-transported CO_2^* reaching the leaves, or because only a small amount of what reaches leaves is captured before diffusing away. When supplying a solution of $H^{14}CO_3^-$ in water to excised leaves, Stringer and Kimmerer (1993) estimated that 0.14% and 0.38% diffused out of the leaf as $^{14}CO_2$ under 660 μmol quanta m^{-2} s^{-1} and 70 μmol quanta m^{-2} s^{-1}, respectively,

9

and about 83% diffused out in the dark. The large fraction exiting leaves in the dark would appear as leaf respiration, but would be under the control of transpiration and rates of respiration in the stem and roots. In the day, the gross flux would be much higher so a substantial amount of CO_2 derived from root and stem respiration could be used by leaves for photosynthesis or exit leaves and confound the measurement of leaf respiration in the light.

Unlike stem and root respiration, leaf respiration is thought to differ between day and night because of a reduction in the cyclic nature of the Krebs Cycle when leaves are illuminated (Tcherkez *et al.*, 2009). However, this has only been demonstrated in *Xanthium strumarium*, so its application across species is uncertain. Measurements of the inhibition of leaf respiration in the light range widely from 16-77% (Atkin *et al.*, 2000; Hurry *et al.*, 2005; Ayub *et al.*, 2011). Additionally, rates of leaf day and night respiration can respond differently to sustained drought, with day respiration inhibited by drought more than night respiration (Ayub *et al.*, 2011), and in some cases the ratio of light to dark respiration increases with rising leaf temperature through a reduction in the light suppression of respiration at high temperatures (Way *et al.*, 2015).

The objective of this study is to test the dynamic relationship among the $[CO_2^*]$ in the xylem, the rate of transpiration, and the rate of gross CO_2 efflux in a woody (*P. deltoides*) and an herbaceous plant (*Brassica napus*). We hypothesize that the efflux of xylem transported CO_2 from leaves could be large relative to respiration and will be controlled by $[CO_2^*]$ and transpiration rate, with some effect of leaf and petiole morphology. Additionally, data on these fluxes should facilitate future efforts to create mechanistic models of the gross CO_2 efflux from leaves in response to prevailing and predicted environmental conditions, filling in the gaps left by previous studies which have not looked at the efflux of xylem-transported CO_2 from the leaves.

MATERIALS AND METHODS

Growth conditions and plant propagation

Brassica napus (L. stellar DH GT060615) and *Populus deltoides* (W. Bartram ex

Marshall) were grown under natural light in an unshaded greenhouse in February and March

2013 and 2014, with mid-day photosynthetically active radiation (PAR) at pot level of 1200

μmol m^{-2} s^{-1} at the University of New Mexico in Albuquerque, NM, under ambient CO_2,

21ºC/18ºC and 24ºC/21ºC day/night for *B. napus* and *P. deltoides*, respectively.

B. napus was started from seed, and *P. deltoides* was clonally propagated by cuttings. *B.*

napus was sown in 500 mL pots with Metro-Mix 300 potting soil (Sun Gro Horticulture, Seba

Beach, AB, Canada). *P. deltoides* cuttings were initially placed in cone-tainers filled with

Metro-Mix 300 potting soil and allowed to grow for approximately two months before the soil

was washed off the roots and cuttings were transplanted into 3.8 L pots with a mixture of

approximately two parts vermiculite (Therm-O-Rock West Inc., Chandler, AZ, USA) to one part

perlite (Therm-O-Rock West Inc., Chandler, AZ, USA) and less than 5% Agrosoke crystals

(Agrosoke International Arlington, TX, USA). *B. napus* and *P. deltoides* were fertilized twice

weekly with Peters 20-20-20 fertilizer (Scotts Miracle-Gro, Marysville, OH, USA) and once

weekly with chelated liquid iron (ferti-lome, Bonham, TX, USA). *B. napus* plants were

measured between 14 and 25 days after geminating.

Tunable diode laser absorbance spectroscopy and leaf gas exchange measurements

A LI-6400 (LI-COR Biosciences, Lincoln, NE, USA) was coupled to a tunable diode

laser (TDL) absorbance spectrometer (model TGA 100; Campbell Scientific, Inc., Logan, UT,

USA) to measure online $^{12}CO_2$ and $^{13}CO_2$ exchange. Isotope calibration consisted of a high and a

low CO_2 tank that spanned the expected range of [CO_2] of each isotopologue for the LI-COR reference and sample (Barbour *et al.,* 2007). The TDL cycled between calibrations of the high and low CO_2 tank along with the LI-COR reference and sample line measuring for one minute at each site; however, only the last 10 seconds of data from each site were used for calculations via the tdllicor processing package (Erhardt and Hanson, 2013) in R (R Core Development Team, 2011). The TDL measures [$^{12}CO_2$] and [$^{13}CO_2$], so the net fluxes of each were calculated as in normal gas exchange, where total [CO_2] is measured in the air supplied to the leaf chamber and within the well-mixed leaf chamber. All data presented below reflects the $^{12}CO_2$ and $^{13}CO_2$ effluxes measured with the TDL.

The entire, highest, fully expanded *B. napus* leaf, with a petiole length between 6.5 cm and 8.5 cm, or a fully expanded *P. deltoides* leaf, with a petiole length between 4 cm and 7 cm, was placed in a large (80 cm^2) custom clear topped chamber attached to a LI-6400 (LI-COR Biosciences, Lincoln, NE, USA). An RGB LED light source (LI-COR Biosciences) set at 1200 µmol quanta m^{-2} s^{-1} or 1500 µmol quanta m^{-2} s^{-1} for *B. napus* and *P. deltoides*, respectively, was placed over the custom LI-6400 leaf chamber with 25ºC (leaf temperature) and 3.8 Pa (380 µmol mol^{-1}) CO_2 reference. The leaves were photographed, and projected leaf area was estimated using ImageJ (US National Institutes of Health, Bethesda, MD, USA).

Once photosynthesis reached a steady state, the leaf was detached from the plant and the petiole was placed in a 40 mmol l^{-1} KCl solution. The detached leaf remained in the KCl solution for ~10 minutes while rates of transpiration and photosynthesis were monitored. Photosynthesis did not change when the leaf was cut, while transpiration increased by ~0.2 mmol H_2O m^{-2} s^{-1}. The KCl solution was swapped for a solution containing 99 atom % ^{13}C sodium bicarbonate dissolved in 40 mmol l^{-1} KCl at one of three [$^{13}CO_2^{*}$]: 1.19, 5.95, or 11.9 mmol l^{-1}.

Individual leaves were only provided a single [$^{13}CO_2^*$]. These concentrations span the range of

observed values from previous field studies for tree xylem [CO_2^*]. Approximately 90 seconds

after adding the $^{13}CO_2^*$ solution, a sharp increase in $^{13}CO_2$ efflux started and the light on the LI-

6400 was turned off. Throughout the measurement period, the rate of transpiration was

manipulated by switching the LI-COR desiccant between full scrub (*i.e.*, high VPD and higher

rates of transpiration) and full bypass (*i.e.*, low VPD and lower rates of transpiration). To further

increase the relative humidity when the desiccant was on full bypass, a condensing tube in a

water bath (VWR Scientific products, West Chester, PA, USA) was attached to the LI-COR inlet

to decrease VPD to 0.5 kPa or less.

The desiccant was left on full scrub or full bypass for approximately one hour. The

measurement cycle consisted of approximately 3-4 alternating high and low VPD periods. This

procedure was used to gain the widest range of transpiration values possible in the dark for

comparisons of transpiration and $^{13}CO_2$ efflux. Data consist of four replicates for each

bicarbonate concentration from four different individuals for each species.

Anaplerotic reactions calculations

The average natural abundance of $^{13}CO_2$ in the atmosphere is ~1.1% (Griffis *et al.*, 2004)

and we assumed the background rate of ^{13}C leaf respiration, *i.e.* the rate of $^{13}CO_2$ respiration

from an unlabeled leaf ($^{13}C_{RL}$), would be proportional to the rate of $^{12}CO_2$ respiration ($^{12}C_{RL}$)

according to the natural abundance for each isotopologue. Therefore, we approximated $^{13}C_{RL}$ as

1.1% of the total respiration rate ($^{12}C_{RL} + {}^{13}C_{RL}$) and used the measured $^{12}C_{RL}$ as the basis for

calculations. This approach gave data consistent with $^{12}CO_2$ and $^{13}CO_2$ respiration measured

from an unlabeled leaf. We calculated an expected ^{13}C efflux ($^{13}C_{cal\ efflux}$) that would occur if all

the $^{13}CO_2$ added to the cut leaf exited the leaf as $^{13}CO_2$. This was accomplished by multiplying

the $[^{13}CO_2^*]$ in the solution fed to the leaves by the rate of transpiration and adding it to the

background $^{13}C_{RL}$. After supplying $^{13}CO_2$ to the leaf we used the ratio of observed $^{13}CO_2$ efflux

($^{13}C_{efflux}$) to $^{13}C_{cal\ efflux}$ to determine the fraction of supplied $^{13}CO_2$ exiting the leaf and expressed

it as a percentage. We estimated the rate of anaplerotic reactions by taking the difference

between $^{13}C_{cal\ efflux}$ and observed $^{13}C_{efflux}$. For these calculations we assumed the transpiration

rate, along with the rate of ^{12}C and ^{13}C effluxes were constant across one TDL/LI-COR cycle (4

or 6 minutes). We excluded the first 30 minutes after the light was turned off for these

calculations to avoid potential complications from light enhanced dark respiration (LEDR) and to

allow the water in the leaf to be replaced with the water supplied to the petiole.

Stem [CO_2^*]

In situ stem CO_2 concentration and pH were measured according to McGuire and

Teskey (2002). To calibrate the CO_2 microelectrode (GS-136CO-1 Micro Carbon dioxide

electrode, Lazar Research Laboratories Inc., Los Angeles, CA, USA) four calibration tanks of 0,

0.33, 2.10, and 7.0% [CO_2] were dissolved into Milli-Q water with a glass bubbler for at least

one hour. Percent CO_2 gas by volume in stems is the value calculated in the airspace around the

xylem tissue that would exist when it is equilibrated with the total dissolved inorganic carbon in

xylem sap ($[CO_2^*] = [CO_2]_{aq} + [H_2CO_3] + [HCO_3^-] + [CO_3^{2-}]$). The pH of the calibration water

in the glass bubblers was measured in order to calculate all forms of inorganic carbon in solution.

Insertion of the CO_2 microelectrode was accomplished by making a hole slightly larger

than the microelectrode diameter in plant stems using a drill bit. For *B. napus* a hole was drilled

into the main stem, ~1.5 cm in diameter with well-developed secondary tissue growth. The drill

tip was inserted into the first layer of the stem (~0.25 cm, assumed to be phloem tissue) and hit a stiff inner section at ~0.50 cm, which was assumed to be secondary xylem tissue. For *P. deltoides* the drill was placed in a woody stem that was approximately 5 cm in diameter and was drilled until reaching woody tissue (~1 cm into the stem). For both plants, a micro pH electrode (0.1 mm immersion depth—PHR-146S micro pH electrode, Lazar Research Laboratories Inc., Los Angeles, CA, USA) was placed in the hole in the stem, and the pH was measured prior to insertion of the CO_2 microelectrode. Measurements with the CO_2 microelectrode were recorded every minute until the mV reading was stable for ten minutes. Following the measurement with the CO_2 microelectrode, pH was again measured to see if the stem sap pH had changed. Stem measurements were collected to provide data on the range of values to expect in small potted plants grown in a greenhouse. We believe these represent a minimum value for what would be found in branch tips throughout a tree canopy (if no xylem-transported CO_2 from roots and stems arrived from outside the branch) and should be roughly similar to stem [CO_2] in a field-grown *B. napus*. The stem [CO_2] data were collected separately from the detached leaf measurements, using the same *P. deltoides* individuals and a separate cohort of *B. napus* plants.

Statistical Analyses

Statistical analyses were performed using R. Linear regression models were produced for rates of $^{12}C_{RL}$ and $^{13}C_{efflux}$ for all [$^{13}CO_2^*$] and both species. ANCOVAs were performed to detect any significant difference among [$^{13}CO_2^*$] treatments for the rates of $^{12}C_{RL}$ and $^{13}C_{efflux}$ for both species. Two-way ANOVAs were used for percentage of $^{13}CO_2$ exiting the leaf, estimated rate of anaplerotic reactions and $^{13}C_{efflux}$ at a given rate of transpiration for both [$^{13}CO_2^*$] and species. Post-hoc analysis was performed using a Tukey HSD test.

RESULTS

Magnitude of xylem derived inorganic carbon efflux and retention in leaves

The gross rate of $^{13}C_{efflux}$ was dependent on the $[^{13}CO_2^*]$ supplied to the leaf when compared at a transpiration rate of 0.5 mmol H_2O $m^{-2}s^{-1}$ in both *B. napus* ($P<0.001$) and *P. deltoides* ($P<0.001$) (Fig. 2). Over-all the $^{13}C_{efflux}$ was significantly higher in *P. deltoides* than *B. napus* ($P=0.03$), but not for pairwise comparisons at each $[CO_2^*]$. The gross rate of $^{12}C_{RL}$ was not significantly affected by $[^{13}CO_2^*]$ (Fig. 2B) in either *B. napus* ($P=0.80$) or *P. deltoides* ($P=0.72$).

$^{13}CO_2^*$ provided to the petioles entered the darkened leaves through the xylem via the transpiration stream and exited the leaves as $^{13}CO_2$ (Fig. 3A, B). Approximately 50% of $^{13}CO_2^*$ at 1.19 mmol l^{-1} and 5.95 mmol l^{-1}, and ~70% at 11.9 mmol l^{-1} exited the leaf as $^{13}CO_2$ in *B. napus*. In *B. napus* the percent of $^{13}CO_2^*$ exiting the leaf at 11.9 mmol l^{-1} was significantly higher than both 1.19 mmol l^{-1} ($P<0.001$) and 5.95 mmol l^{-1} ($P<0.01$) (Fig. 3A). The percent $^{13}CO_2^*$ exiting the leaf as $^{13}CO_2$ for *P. deltoides* was ~80% across all bicarbonate concentrations (Fig. 3B). It was significantly different between 1.19 mmol l^{-1} and 5.95 mmol l^{-1} ($P<0.05$) but not between other concentrations (Fig. 3B). The percent efflux was higher overall in *P. deltoides* than *B. napus* ($P=0.001$) though not for the pairwise comparison at high $[CO_2^*]$ ($P=0.43$) (Fig. 3A, B).

The estimated retention rate of $^{13}CO_2^*$ by an individual leaf was similar across the higher $[^{13}CO_2^*]$ in *B. napus* (~0.05 µmol CO_2 m^{-2} s^{-1}) and was slightly lower in the lower $[^{13}CO_2^*]$ (~0.02 µmol CO_2 m^{-2} s^{-1}) (Fig. 3C). The estimated retention rate was significantly different between 1.19 mmol l^{-1} and 5.95 mmol l^{-1} ($P<0.05$) and 11.9 mmol l^{-1} ($P<0.01$) in *B. napus*. The retention rate increased between the lowest and highest $[^{13}CO_2^*]$ for *P. deltoides* (~0.01 µmol CO_2 m^{-2} s^{-1} to ~0.03 µmol CO_2 m^{-2} s^{-1}) ($P<0.01$) (Fig. 3D); however, differences between the

other concentrations were not significant. The retention rate differed overall between species ($P<0.001$) but did not show any consistent differences with respect to $[CO_2^*]$ (they are only significantly different at 5.95 mmol l^{-1} ($P<0.005$, using pairwise comparisons).

Transpiration decreased rapidly after turning off the light. This generated a range of transpiration rates where we could examine the relative magnitudes of $^{12}C_{RL}$ and $^{13}C_{efflux}$ (Fig. 4, 5). The gross rate of $^{13}C_{efflux}$ was dependent on both the $[^{13}CO_2^*]$ supplied to the xylem ($P<0.005$) (Fig. 4) and transpiration rate ($P<0.005$) (Fig. 4, 5). In contrast gross $^{12}C_{RL}$ was not significantly correlated with the transpiration rate in *B. napus* ($P=0.54$) or *P. deltoides* ($P=0.74$) (Fig. 5). Gross $^{12}C_{RL}$ was significantly higher during the first 30 minutes of the dark period where light enhanced dark respiration (LEDR) occurs in both *B. napus* and *P. deltoides* (Fig. 5) ($P<0.005$). As expected, the LEDR response did not affect the gross $^{13}C_{efflux}$ in either *B. napus* or *P. deltoides* ($P<0.0001$) (Fig. 5). We also found that $^{13}C_{efflux}$ approached ½ $^{12}C_{RL}$ in both species during our experiments. The rate of dark respiration when excluding LEDR was 1.26 ± 0.23 μmol CO_2 m^{-2} s^{-1} and 1.33 ± 0.21 μmol CO_2 m^{-2} s^{-1} in *B. napus* and *P. deltoides*, respectively. Linear regressions ($R^2=0.97$ for *B. napus* and $R^2=0.93$ for *P. deltoides*) show that for leaves supplied with 11.9 mmol l^{-1} $[^{13}CO_2^*]$, the gross efflux of xylem-transported CO_2 will equal ½R_d at a transpiration rate of 4 mmol H_2O m^{-2} s^{-1} and 3.69 mmol H_2O m^{-2} s^{-1} for *B. napus* and *P. deltoides*, respectively (Fig. 5). At all $[^{13}CO_2^*]$ for both species, gross $^{13}C_{efflux}$ was undetectable when transpiration was <0.1 mmol H_2O m^{-2} s^{-1}.

Stem $[CO_2^*]$

In greenhouse grown plants, the average $[^{13}CO_2^*]$ in the stem was 0.7 ± 0.2 mmol l^{-1} and 2.8 ± 3.5 mmol l^{-1} for *B. napus* and *P. deltoides*, respectively. Stem pH in *P. deltoides* ranged

between 5.1 and 6.4, with an average of 5.9 ± 0.3 and stem pH in *B. napus* ranged between 5.3

and 6.1 with an average of 5.7 ± 0.3.

DISCUSSION

Magnitude of xylem derived inorganic carbon efflux

      Our experimental approach allows simultaneous measurements of the gross efflux of

xylem-transported $^{13}CO_2^*$ (exiting leaves as $^{13}CO_2$) with transpiration, as well as the efflux of

$^{12}CO_2$ from leaf respiration in real-time. We applied this approach to excised leaves in order to

eliminate complications from radial diffusion through stems and branches. We also focused our

data collection on the dark conditions immediately after the light was turned off, in order to

compare CO_2 efflux with a wide range of transpiration rates, from typical night-time rates

through the low end of typical daytime rates. We demonstrated that transport of labeled $^{13}CO_2^*$

in xylem was highest when both the $[^{13}CO_2^*]$ (Fig. 2) and transpiration (Fig. 4) were high. The

broad range of transpiration values also allowed us to generate a robust relationship between

gross efflux of xylem-transported $^{13}CO_2^*$ ($^{13}C_{efflux}$) and transpiration that can be used to predict

$^{13}C_{efflux}$ in conditions where transpiration rate and xylem $[CO_2^*]$ are known. Considering the

very different petiole and leaf anatomies of *P. deltoides* and *B. napus*, we were surprised at how

similar this relationship was between species (Fig. 4).

      When $[CO_2^*]$ in stems is high (11.9 mmol l^{-1}) and when transpiration rates are high (>3

mmol H_2O m^{-2} s^{-1}) our estimates indicate the gross efflux of xylem-transported CO_2^* approaches

half the rate of leaf respiration (Fig. 5). Therefore, this efflux could account for some of the

variation observed in measurements of leaf respiration in the light. Measurements of stem

$[CO_2^*]$ in field grown *P. deltoides* have been reported to range from the low end between 2.8-9.5

mmol l^{-1} (Saveyn *et al.*, 2008) to the high end between 20 and 35 mmol l^{-1} (Aubrey and Teskey, 2009) while reported transpiration rates in *P. deltoides* ranged from 3.4 mmol H_2O m^{-2} s^{-1} (Bassman and Zwier, 1991) to 4.5 mmol H_2O m^{-2} s^{-1}(Barron-Gafford *et al.*, 2007), indicating our selection of [$^{13}CO_2^*$] were within the range of available data for *P. deltoides*. However, it should be noted that measurements of [$^{13}CO_2^*$] in *P. deltoides* are on the high end of reported tree values (Teskey *et al.* 2008).

However, most leaves are attached to small branches on trees or to the relatively small stems and branches of herbaceous plants, where [$^{13}CO_2^*$] has not been well characterized. Models of [CO_2^*] distribution throughout trees predict it increasing with distance from the ground since CO_2 is generated at higher rates than it diffuses out of a tree or shrub (Hölttä and Kolari, 2009). These predictions were supported by measurements in *Quercus pyrenaica* (Salomon *et al.*, 2016a). Hölttä and Kolari (2009) also modeled that [CO_2^*] declines as the stem tapers towards the top of the tree and may only end up around 5% of the basal [CO_2^*] at the leaf level. Surprisingly, no study has measured [CO_2^*] in the main stem near tree bases simultaneously with terminal branch data in order to validate these model predictions. Furthermore, there is almost no information on xylem [CO_2^*] in small tree branches or herbaceous plants. One study did find that terminal branch measurements of xylem [CO_2^*] in large *P. deltoides* trees were between 0.5 mmol l^{-1} and 0.9 mmol l^{-1} when growing in well drained soils and up to 9.4 mmol l^{-1} in water logged soils (Stringer and Kimmerer, 1993). Our small potted plants grown in a greenhouse contained 0.7 ± 0.2 mmol l^{-1} and 2.8 ± 3.5 mmol l^{-1} [CO_2^*] for *B. napus* and *P. deltoides*, respectively. This is on the low end of our experimental design and may be a reasonable value for similarly sized plants in the field. However, terminal branches of mature trees would also contain high [CO_2^*] transported from respiration of larger

branches, stem, and even roots. Modeling the effect from the rest of the tree is not currently

possible because there is very little data on long-term (diurnal and seasonal) variation in stem

$[CO_2^*]$ in mature trees, and what data do exist show high variability (Etzold *et al.*, 2013;

Salomón *et al.*, 2016b). Therefore, using our approach to calculate gross efflux rates of the

xylem transported $[CO_2^*]$ arriving at a leaf would also require measurement of the $[CO_2^*]$ in the

branches near the leaf as well as the rate of transpiration.

Retention of xylem-transported CO$_2$ in darkened leaves

At high $[^{13}CO_2^*]$, the percentage of xylem-transported $^{13}CO_2^*$ exiting the leaf was fairly

high for both species (Fig. 3), and near the 83% Stringer and Kimmerer (1993) observed when

they supplied 1 mmol l^{-1} $^{14}CO_2^*$ to *P. deltoides* leaves. However, at lower $[^{13}CO_2^*]$ the percent

exiting the leaf was reduced in *B. napus* (*P*=0.001). As these results show, all $^{13}CO_2^*$ entering

the leaf did not exit as $^{13}CO_2$ during our measurements even though leaves were darkened during

labeling. Therefore, we used a mass balance approach to determine the rate of retention of

$^{13}CO_2^*$ supplied to the leaf to facilitate comparison with other fluxes. Interestingly, the retention

rate only gradually increases with higher supplied $[^{13}CO_2^*]$ (Fig. 3C, D). We hypothesize that

this retention represents the rate that anaplerotic reactions consumed the supplied $^{13}CO_2^*$. Our

estimated rate of retention by anaplerotic reactions for *P. deltoides* (0.003 μmol m^{-2} s^{-1}) at 1.19

mmol l^{-1} $[^{13}CO_2^*]$ is similar to the rate (0.002 μmol m^{-2} s^{-1}) calculated from data in Stringer and

Kimmerer (1993) for leaves supplied with 1 mmol l^{-1} $[^{14}CO_2^*]$. However, our estimated rate of

anaplerotic reactions is only about 1% the rate of phosphoenolpyruvate carboxylase (PEPC)

activity in previously published studies with *P. deltoides* plants exposed to ozone or varying light

treatments (Loreto *et al*., 2007).

We also calculated a significantly higher overall apparent rate of retention in *B. napus* than in *P. deltoides* ($P<0.001$), though not for pairwise comparisons (Fig. 3). It is possible that the thick, green petioles and the blade of the *B. napus* leaf have slightly higher rates of anaplerotic respiration, and the *B. napus* petioles have a little higher radial efflux of CO_2 than the thin, waxy petiole of *P. deltoides*. Measuring how much of the retained ^{13}C is acid stable, which parts of the leaf have label, and what compounds are labeled will be necessary to fully determine the fate of xylem-transported CO_2^*. If petiole efflux of [13]CO_2 is large, we would expect that the percent [13]CO_2 exiting the leaf would decrease with increasing [[13]CO_2^*] due to a higher concentration gradient between the petiole and the atmosphere; however, the percent [13]CO_2 exiting the leaf does not show consistent patterns with [[13]CO_2^*] supplied to the leaf.

Implications for understanding leaf and stem carbon fluxes

Leaf efflux of xylem-transported CO_2^* is controlled by the rate of transpiration and the xylem [CO_2^*] (Fig. 4), but this is not accounted for when characterizing leaf respiration. We believe a significant amount of the uncertainty in plant respiration could be due to limited efforts to quantify the effects of xylem-transported CO_2^*. There is potential for further characterization to improve our understanding of a wide range of leaf-level processes that have been hard to quantify such as: gross photosynthesis, the extent to which day respiration is down regulated in the light (Atkin *et al*., 2000; Hurry *et al*., 2005; Ayub *et al*., 2011), the response of respiration to stressors (e.g. drought) (Ayub *et al*., 2011; Rowland *et al*., 2015), the acclimation to environmental conditions (e.g. temperature) (Vanderwel *et al*., 2015), night respiration for species whose night-time transpiration is high and/or variable (Snyder *et al*., 2003; Resco de Dios *et al.* 2015), variation in the acclimation rates of respiration and photosynthesis to

21

temperature between plant functional types (Campbell *et al.*, 2007), the amount of CO_2 recycling in leaves (including the potential recycling of xylem-transported CO_2^*) (Busch *et al.*, 2013), the diffusion of CO_2 in leaves (Evans and von Caemmerer, 2013), and the activity of alternative decarboxylations associated with photorespiration (Cousins *et al.*, 2008; Cousins *et al.*, 2011).

Essentially, any measurement of leaf respiration that induces or includes changes in transpiration is susceptible to this error for species where xylem $[CO_2^*]$ is high (Fig. 1). For example, the efflux of xylem-transported CO_2^* may interfere with methods for measuring day respiration in leaves. The two most common methods require varying photosynthesis at low light or low $[CO_2]$ (Kok, 1949; Laisk, 1977). These measurements are time consuming and require highly accurate measurements of small fluxes that would be compromised if transpiration varies during the measurement (e.g. due to light or CO_2 affecting stomatal aperture). Measurements of leaf photosynthesis are also directly affected since some of the xylem-transported CO_2^* is recycled by leaves (Stringer and Kimmerer, 1993; McGuire and Teskey, 2002; Bloemen *et al.*, 2013a, b; Bloemen *et al.*, 2015b) and model assumptions would be violated if some escaped the leaf without passing through chloroplasts (von Caemmerer, 2013).

In addition, any changes in root, stem, or branch respiration occurring during the measurement of small leaf fluxes would cause errors in leaf respiration when transpiration is sufficient. There are significant uncertainties surrounding the efflux of CO_2 from stems as well as the rate of anaplerotic reactions, and the effects of both on the measurement of stem respiration (Teskey *et al.*, 2008; Bloemen *et al.*, 2015a). These uncertainties include diurnal variation in stem and root respiration, which is well documented but poorly understood, showing some linkage to diurnal patterns of carbon supply from shoots as well as other drivers (Bloemen *et al.*, 2015b; Snell *et al.*, 2015; Steppe *et al.*, 2015). Our method of adding labeled bicarbonate

to leaves could be applied to stems to improve estimates of the gross efflux of CO_2 and the rates of gross stem photosynthesis in real-time by helping to partition the rates of radial efflux through the stem relative to the vertical transport of CO_2^* away from the site of respiration.

What would it take for this flux to be significant globally?

Although we have point data on stem $[CO_2^*]$ for over two dozen tree species (Teskey *et al.*, 2008) we still need more data on the relationship between stem and branch tip $[CO_2^*]$ as well as their diurnal and seasonal patterns before we can make a solid prediction of what the contribution is from the ~3 trillion trees on Earth (Crowther *et al*., 2015). However, if $[CO_2^*]$ averages near 1 mmol l^{-1} (a common value on the low end reported for tree stems – see Teskey *et al.*, 2008) at the point where petioles attach to the stem or branch, and if average transpiration rates are around 0.5 mmol H_2O m^{-2} s^{-1} (much closer to night-time than daytime rates, though see Rescos de Dios *et al*. 2015 for regulation of night-time transpiration), then our data (Fig. 2) and those from Stringer and Kimmerer (1993) predict the efflux to be just over 1.5% of respiration. At the global scale, an error in respiration this size would account for a large portion of the error in global carbon cycle models (Hanson *et al.,* 2016).

CONCLUSIONS

Using our novel online TDL gas exchange method paired with $^{13}CO_2^*$ labeling, we found that when xylem $[CO_2^*]$ and transpiration are high, the efflux of xylem-transported CO_2^* could cause large errors in observed leaf respiration. This would be most likely in the daytime when stomata are open, complicating the measurement of day respiration. We observed a fairly similar efflux of xylem-transported CO_2^* from *P. deltoides* and *B. napus* leaves, which suggests the effect of

leaf and petiole morphology on the efflux is modest. However, data from many more species that include the diurnal and seasonal patterns of xylem [CO_2^*] in branch tips (where leaves attach) are needed to ascertain how often xylem-transported CO_2^* interferes with measurements of leaf respiration or estimations of regional or global carbon fluxes. Future work with this approach will allow examination of the dynamics of the rate of xylem [CO_2^*] transport, radial efflux, and internal re-fixation by stem, branches, and leaves relative to rates of respiration and photosynthesis occurring in each organ.

ACKNOWLEDGEMENTS

REFERENCES

Atkin OK, Atkinson LJ, Fisher RA, Campbell CD, Zaragoza-Castells J, Pitchford JW, Woodward FI, Hurry V. 2008. Using temperature-dependent changes in leaf scaling relationships to quantitatively account for thermal acclimation of respiration in a coupled global climate-vegetation model. Global Change Biology **14,** 2709-2726.

Atkin OK, Bloomfield KJ, Reich PB, Tjoelker MG, Asner GP, Bonal D, Bönisch G, Bradford MG, Cernusak LA, Cosio EG, *et al*. 2015. Global variability in leaf respiration in relation to climate, plant functional types and leaf traits. New Phytologist **206,** 614-636.

Atkin OK, Edwards EJ, Loveys BR. 2000. Response of root respiration to changes in temperature and its relevance to global warming. New Phytologist **147,** 141-154.

Atkin OK, Meir P, Turnbull MH. 2014. Improving representation of leaf respiration in largescale predictive climate-vegetation models. New Phytologist **202,** 743-748.

Atkin OK, Scheurwater I, Pons TL. 2007. Respiration as a percentage of daily photosynthesis in whole plants is homeostatic at moderate, but not high, growth temperatures. New Phytologist **174,** 367-380.

Aubrey DP, Teskey RO. 2009. Root-derived CO_2 efflux via xylem stream rivals soil CO_2 efflux. New Phytologist **184,** 35-40.

Ayub G, Smith RA, Tissue DT, Atkin OK. 2011. Impacts of drought on leaf respiration in darkness and light in *Eucalyptus saligna* exposed to industrial-age atmospheric CO_2 and growth temperature. New Phytologist **190,** 1003-1018.

Barbour MM, McDowell NG, Tcherkez G, Bickford CP, Hanson DT. 2007. A new measurement technique reveals rapid post-illumination changes in the carbon isotope composition of leaf-respired CO_2. Plant, Cell & Environment **30,** 469-482.

Barron-Gafford GA, Griever KA, Murthy R. 2007. Leaf- and stand-level responses of a forested mesocosm to independent manipulations of temperature and vapor pressure deficit. New Phytologist **174,** 614-625.

Bassman JH, Zwier JC. 1991. Gas exchange characteristics of *Populus trichocarpa*, *Populus deltoides* and *Populus trichocarpa* x *P. deltoides* clones. Tree Physiology **8,** 145-159.

Bloemen J, Bauweraerts I, De Vos F, Vanhove C, Vanderberghe S, Boeckx P, Steppe K. 2015a. Fate of xylem-transported [11]C- and ^{13}C-labeled CO_2 in leaves of poplar. Physiologia Plantarum **153,** 555-564.

Bloemen JB, McGuire MA, Aubrey DP, Teskey RO, Steppe K. 2013a. Assimilation of xylem-transported CO_2 is dependent on transpiration rate but is small relative to atmospheric fixation. Journal of Experimental Botany **64,** 2129-2138.

Bloemen JB, McGuire MA, Aubrey DP, Teskey RO, Steppe K. 2013b. Transport of rootrespired CO_2 via the transpiration stream affects aboveground carbon assimilation and CO_2 efflux in trees. New Phytologist **197,** 555-565.

Bloemen J, Teskey RO, McGuire MA, Aubrey DP, Steppe K. 2015b. Root xylem CO_2 flux: an important but unaccounted-for component of root respiration. Trees DOI 10.1007/s00468-015-1185-4.

Bodman RW, Rayner PJ, Karoly DJ. 2013. Uncertainty in temperature projections reduced using carbon cycle and climate observations. Nature Climate Change **3**, 725-729.

Busch FA, Sage TL, Cousins AB, Sage RF. 2013. C_3 plants enhance rates of photosynthesis by reassimilating photorespired and respired CO_2. Plant Cell and Environment **36,** 200-212.

von Caemmerer 2013. Steady-state models of photosynthesis. Plant, Cell & Environment **36,** 1617-1630.

Campbell C, Atkinson L, Zaragoza-Castells J, Lundmark M, Atkin O, Hurry V. 2007. Acclimation of photosynthesis and respiration is asynchronous in response to changes in temperature regardless of plant functional group. New Phytologist **176,** 375-389.

Candell JG, Le Quere C, Raupach MR, Field CB, Buitenhuis ET, Ciais P, Conway TJ, Gillett NP, Houghton RA, Marland G. 2007. Contributions to accelerating atmospheric CO_2 growth from economic activity, carbon intensity, and efficiency of natural sinks. Proceedings of the National Academy of Sciences **104,** 18866-18870.

Cousins AB, Pracharoenwattana I, Zhou W, Smith SM, Badger MR. 2008. Peroxisomal malate dehydrogenase is not essential for photorespiration in Arabidopsis but its absence causes an increase in the stoichiometry of photorespiratory CO_2 release. Plant Physiology **148,** 786-795.

Cousins AB, Walker BJ, Pracharoenwattana I, Smith SM, Badger MR. 2011. Peroxisomal hydroxypyruvate reductase is not essential for photorespiration in Arabidopsis but its absence causes an increase in the stoichiometry of photorespiratory CO_2 release. Photosynthesis Research **108,** 91-100.

Crowther TW, Glick HB, Covey KR, Bettigole C, Maynard DS, Thomas SM, Smith JR, Hintler G, Duguid MC, Amatulli G. 2015. Mapping tree density at a global scale. Nature **525,** 201-205.

Erhardt EB, Hanson, DT. 2013. tdllicor: TDL/Licor processing. R package version 0.1-22.
Etzold S, Zweifel R, Ruehr NK, Eugster W, Buchmann N. 2013. Long-term stem CO_2 concentration measurements in Norway spruce in relation to biotic and abiotic factors. New Phytologist **197**, 1173–1184.

Evans JR von Caemmerer S. 2013. Temperature response of carbon isotope discrimination and mesophyll conductance in tobacco. Plant, Cell & Environment **36,** 200-212.

Farquhar G, von Caemmerer S, Berry JA. 1980. A biochemical model of photosynthetic CO2 assimilation in leaves of C_3 species. Planta **149**, 78–90.

Griffis T, Baker J, Sargent S, Tanner B, Zhang J. 2004. Measuring field-scale isotopic fluxes with tunable diode laser absorption spectroscopy and micrometeorological techniques. Agricultural and Forest Meteorology **124**, 15–29.

Hanson DT, Stutz SS, Boyer JS. 2016. Why small fluxes matter: the case and approaches for improving measurements of photosynthesis and (photo)respiration. Journal of Experimental Botany **67**, 3027-3039.

Hölttä T, Kolari, P. 2009. Interpretation of stem CO_2 efflux measurements. Tree Physiology **29**, 1447-1456.

Hurry V, Igamberdiev AU, Keerberg O, Parnik T, Atkin OK, Zaragoza-Castells J, Gardestrom P. 2005. Respiration in photosynthetic cells: gas exchange components, interactions with photorespiration and the operation of mitochondria in the light. In Lambers H, Ribas-Carbo M, eds. *Plant Respiration: From Cell to Ecosystem*. Dordrecht, The Netherlands: Springer 43-61.

King AW, Gunderson CA, Post WM, Weston DJ, Wullschleger SD. 2006. Plant respiration in a warmer world. Science **536,** 2005-2007.

Kok B. 1949. On the interrelation of respiration and photosynthesis in green plants. Biochimica et Biophysica Acta **3,** 625-631.

Kuzyakon Y. 2006. Sources of CO_2 efflux from soil and review of partitioning methods. Soil Biology & Biochemistry **38,** 425-448.

Laisk AK. 1977. Kinetics of photosynthesis and photorespiration in C_3 plants. Nauka, Moscow, Russia.

Levy PE, Meir P, Allen SJ, Jarvis PG. 1999. The effect of aqueous transport of CO_2 in xylem sap on gas exchange in woody plants. Tree Physiology **19**, 53-58.

Loreto F, Centritto M, Barta C, Calfapietra C, Fares S, Monson RK. 2007. The relationship between isoprene emission rate and dark respiration rate in white poplar (*Populus alba* L.) leaves. Plant, Cell & Environment **30,** 662-669.

McGuire MA, Marshall JD, Teskey RO. 2009. Assimilation of xylem-transported ^{13}C-labelled CO_2 in leaves and branches of sycamore (*Platanus occidentalis* L.). Journal of Experimental Botany **60,** 3809-3817.

McGuire MA, Teskey RO. 2002. Microelectrode technique for in situ measurement of carbon dioxide concentrations in xylem sap of trees. Tree Physiology **22,** 807-811.

R Core Development Team. 2012. R: A Language and Environment for Statistical Computing. R Foundation for Statistical Computing, Vienna, Austria. ISBN 3-900051-07-0. Available at: http://www.R-project.org (accessed 19 August 2012).

Reich PB. 2010. The carbon dioxide exchange. Science **329,** 774-776.

Resco de Dios V, Roy J, Ferrio JP, Alday JG, Landais D, Milcu A, Gessler A. 2015. Processes driving nocturnal transpiration and implications for estimating land evapotranspiration. Scientific Reports, **5**:10975.

Rowland L, Lobo-do-Vale RL, Cristoffersen BO, Melem EA, Kruijt B, Vasconcelos SS, Domingues T, Binks OJ, Oliveira AAR, Metcalfe D, *et al*. 2015. After more than a decade of soil moisture deficit, tropical rainforest trees maintain photosynthetic capacity, despite increased leaf respiration. Global Change Biology **21,** 4462-4672.

Salomón R, Valbuena-Carabaña M, Gil L, McGuire, MA, Teskey RO, Aubrey DP, González-Doncel I, Rodríguez-Calcerrada J. 2016a. Temporal and spatial patterns of internal and external stem CO_2 fluxes in a sub-Mediterranean oak. Tree Physiology **36,** 1409-1421.

Salomón R, Valbuena-Carabaña M, Teskey R, McGuire MA, Aubrey D, González-Doncel I, Gil L, Rodríguez-Calcerrada J. 2016b. Seasonal and diel variation in xylem CO2 concentration and sap pH in sub-Mediterranean oak stems. Journal of Experimental Botany **67**, 2817–2827.

Saveyn A, Steppe K, McGuire M, Lemeur R, Teskey RO. 2008. Stem respiration and carbon dioxide efflux of young *Populus deltoides* trees in relation to temperature and xylem carbon dioxide concentration. Oecologia **154,** 637-649.

Snell HSK, Robinson D, Midwood AJ. 2015. Sampling root-respired CO_2 in-situ for ^{13}C measurement. Plant and Soil **393,** 259-271.

Snyder KA, Richards JH, Donovan LA. 2003. Night-time conductance in C_3 and C_4 species: do plants lose water at night? Journal of Experimental Botany **54,** 861-865.

Steppe K, Sterck F, Deslauriers A. 2015. Diel growth dynamics in tree stems: linking anatomy and ecophysiology. Trends in Plant Science **20,** 335-343.

Stringer JW, Kimmerer TW. 1993. Refixation of xylem sap CO_2 in *Populus deltoides*. Physiologia Plantarum **89,** 243-251.

Tcherkez G, Mahe A, Gauthier P, Mauve C, Gout E, Bligny R, Comic G, Hodges M. 2009. In folio respiratory fluxomics revealed by ^{13}C isotope labeling and H/D isotope effects highlight the noncyclic nature of the tricarboxylic acid "cycle" in illuminated leaves. Plant Physiology **151,** 620-630.

Teskey RO, Saveyn A, Steppe K, McGuire MA. 2008. Origin, fate and significance of CO_2 in tree stems. New Phytologist **117,** 17-32.

Vanderwel MC, Slot M, Lichstein JW, Reich PB, Kattge J, Atkin OK, Bloomfield KJ, Tjoelker MG, Kitajima K. 2015. Global convergence in leaf respiration from estimates of thermal acclimation across time and space. New Phytologist **117,** 17-32.

Way DA, Holly C, Bruhn D, Ball MC, Atkin OK. 2015. Diurnal and seasonal variation in light and dark respiration in field-grown *Eucalyputs pauciflora*. Tree Physiology **35,** 840-849.

Wullschleger SD, Warren JM, Thornton PE. 2015. Commentary leaf respiration (GlobResp)-global trait database supports Earth System Models. New Phytologist **206,** 483-485.

Wythers KR, Reich PB, Bradford JB. 2013. Incorporating temperature-sensitive Q10 and foliar respiration acclimation algorithms modifies modeled ecosystem responses to global change. Journal of Geophysical Research: Biogeosciences **118,** 77-90.

FIGURES

Fig. 1 Conceptual illustration of relative fluxes for respiration, transpiration, and transported CO_2 between day and night. Respiration in the root (R_{root}) causes high concentrations of CO_2 to accumulate in the roots and stem (large black oval) relative to the surroundings while the accumulation should be much lower in smaller roots (small black circle) due to lower resistance to efflux. Some CO_2 from R_{root} effluxes into the surrounding soil, joining the pool of soil respired CO_2 (R_{soil}). In small roots, some CO_2 from R_{soil} could enter the root if the root CO_2 concentration is lower than the soil concentration. A large fraction of the CO_2 from R_{root} is transported up the stem in the transpiration stream (blue lines). During the day, transpiration is large (E_{day}) and carries a large amount of xylem dissolved CO_2 to the leaf that can efflux into the atmosphere (xylem CO_2 day) if not captured by photosynthesis. Respiration of leaf cells (green lines) in the day (R_{day}) is thought to be much smaller than in the night (R_{night}). However, in the night transpiration (E_{night}) is much smaller than E_{day} so the efflux of xylem dissolved CO_2 (xylem CO_2 night) should be proportionately smaller than xylem CO_2 day.

Fig. 2 Response of gross $^{13}C_{efflux}$ and $^{12}C_{RL}$ in *B. napus* (closed triangle) and *P. deltoides* (open triangle) at a transpiration rate of 0.5 mmol H_2O m^{-2} s^{-1} for each [$^{13}CO_2^*$]. (A) response of gross $^{13}C_{efflux}$ to [$^{13}CO_2^*$], R^2 of 0.91 and 0.67 in *B. napus* and *P. deltoides*, respectively, (B) simultaneous response of $^{12}C_{RL}$ to [$^{13}CO_2^*$], R^2 of <0.01 and 0.02 in *B. napus* and *P. deltoides*, respectively. Measurements were made on cut leaves of *B. napus* and *P. deltoides* placed in one of the three $^{13}CO_2^*$ solutions. Measurements represent averages and standard deviation of four replicates at each [$^{13}CO_2^*$].

Fig. 3 The percentage of gross $^{13}CO_2^*$ exiting the leaf in the transpiration stream in (A) *B. napus* and (B) *P. deltoides* across three different $[^{13}CO_2^*]$. Estimated rate of anaplerotic reactions (i.e., retention of ^{13}C in the dark) in (C) *B. napus* and (D) *P. deltoides* across three different $[^{13}CO_2^*]$. Measurements represent averages and standard deviation of four replicates.

Fig. 4 Transpiration dependence of gross $^{13}C_{efflux}$ for three $[^{13}CO_2^*]$ measured with the TDL. (A) *B. napus* and (B) *P. deltoides*. In both panels grey circles represent 1.19 mmol l^{-1} $[^{13}CO_2^*]$ (*B. napus* y= 0.008x + 0.001, R^2=0.68; *P. deltoides* y=0.02x +0.01, R^2=0.98), closed circles are 5.95 mmol l^{-1} $[^{13}CO_2^*]$ (*B. napus* y= 0.07x − 0.01, R^2=0.82; *P. deltoides* y= 0.09x + 0.02, R^2=0.98), and open circles are 11.9 mmol l^{-1} $[^{13}CO_2^*]$ (*B. napus* y=0.15x + 0.02, R^2 =0.97; *P. deltoides* y= 0.18x +0.00, R^2=0.93). Measurements were made on excised leaves of *B. napus* and *P. deltoides* placed in one of the three $[^{13}CO_2^*]$ solutions. Measurements represent averages and standard deviation of four replicates. Transpiration was averaged over 0.1 mmol H_2O m^{-2} s^{-1} increments.

Fig. 5 Comparison of leaf respiration ($^{12}C_{RL}$ – closed squares) and gross $^{13}C_{efflux}$ (open circles) (A) *B. napus* and (B) *P. deltoides* leaves fed with 11.9 mmol l^{-1} $^{13}CO_2^*$. $^{12}LEDR$ (grey squares) and $^{13}LEDR$ (grey circles) represent the light enhanced dark respiration rate (the first 30 minutes after the light was turned off). The dotted line represents ½ steady leaf respiration, observed in (Fig. 2) of 0.63 µmol ± 0.12 CO_2 $m^{-2}s^{-1}$ and 0.67 ± 0.11 µmol CO_2 $m^{-2}s^{-1}$ in *B. napus* and *P. deltoides*, respectively. Measurements represent averages and standard deviation of four replicates. Transpiration was averaged over 0.1 mmol H_2O m^{-2} s^{-1} increments.

Figure 1
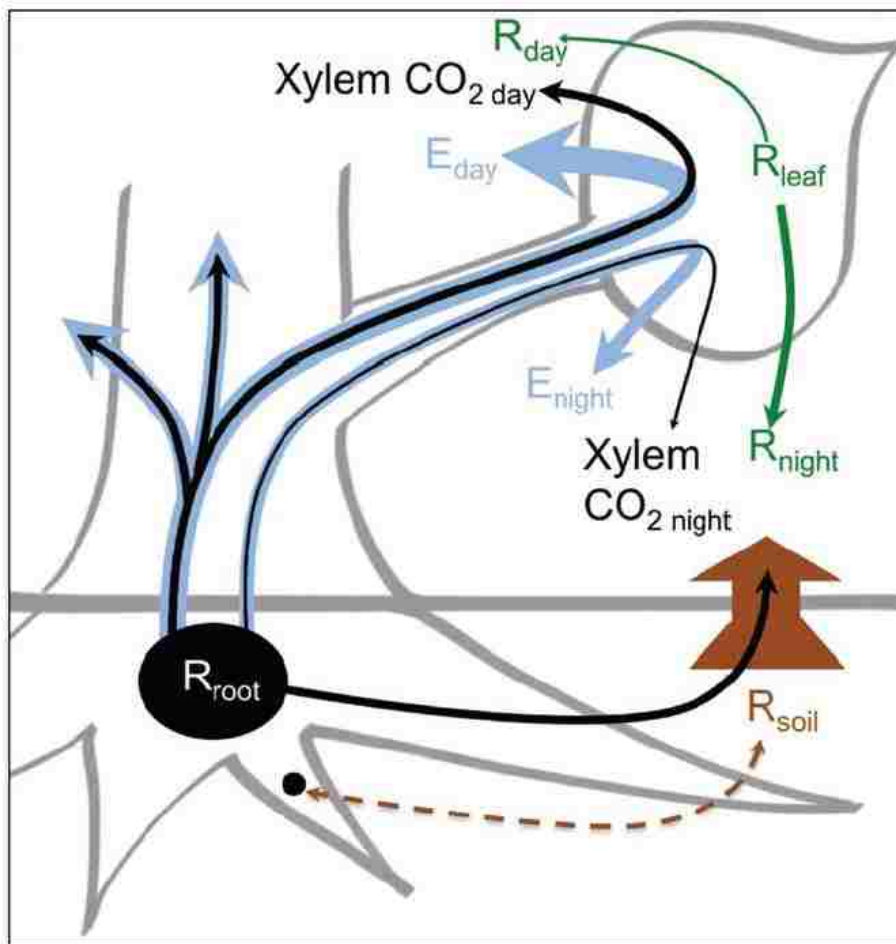
Figure 2
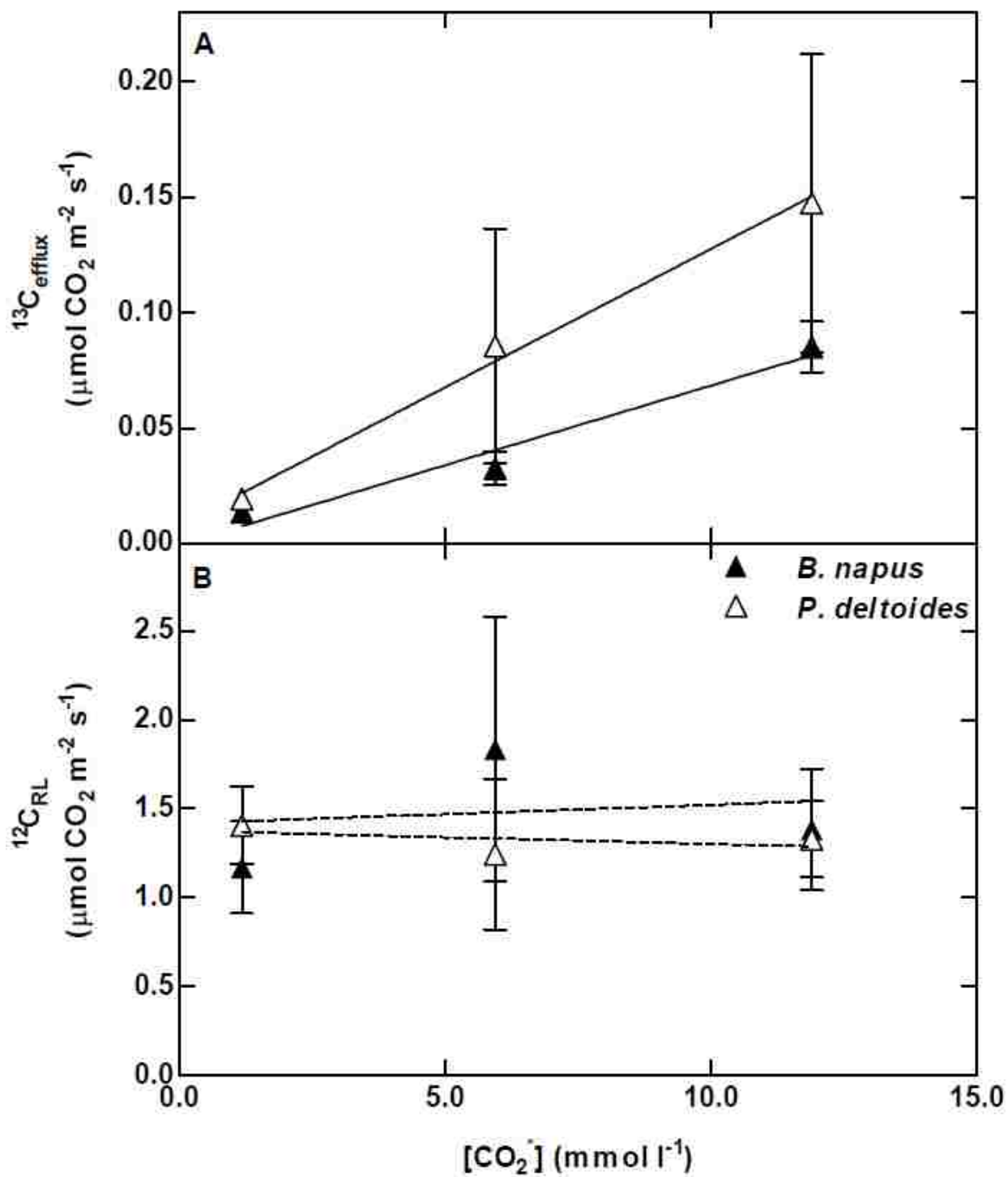
Figure 3
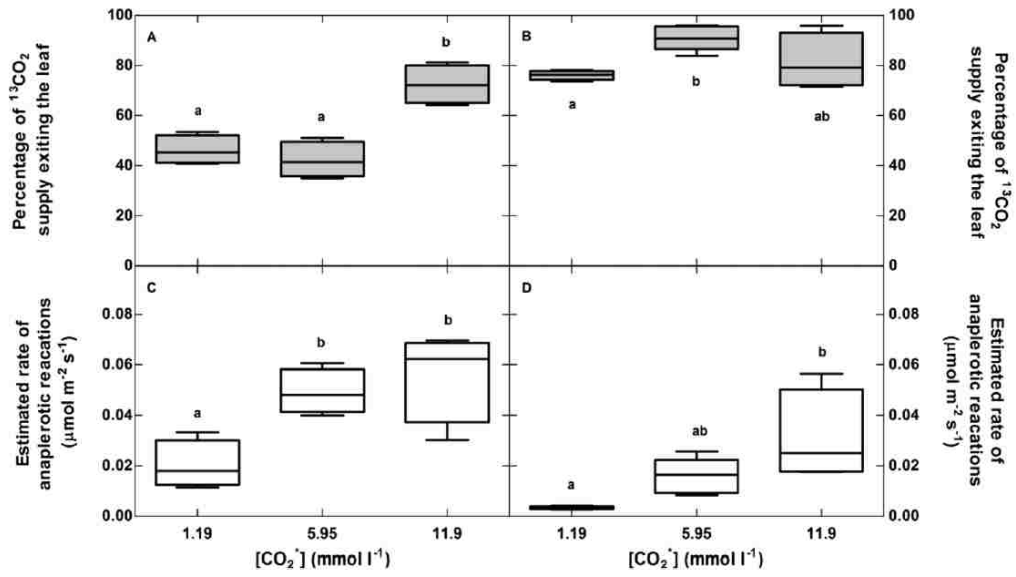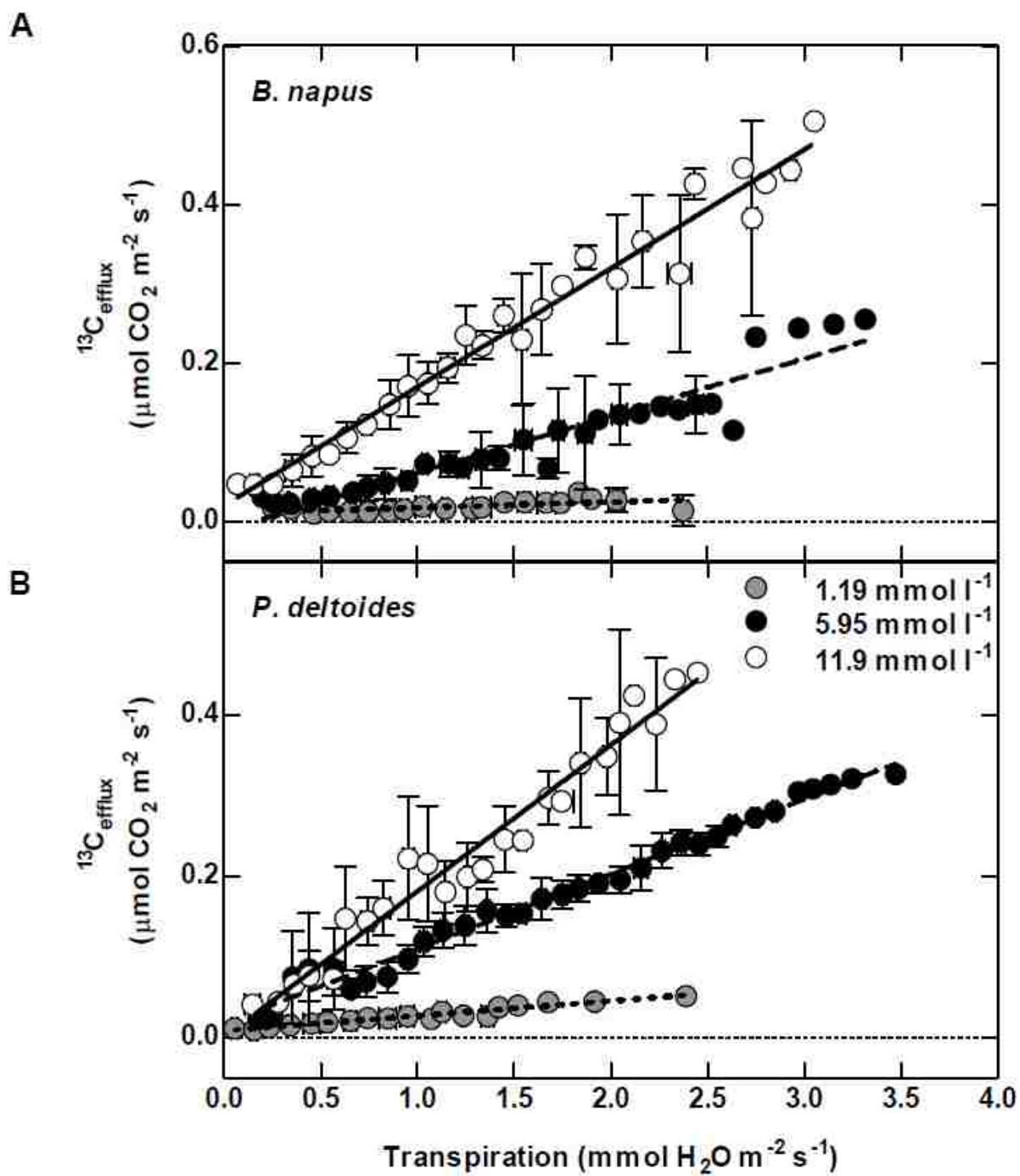
Figure 4

Figure 5
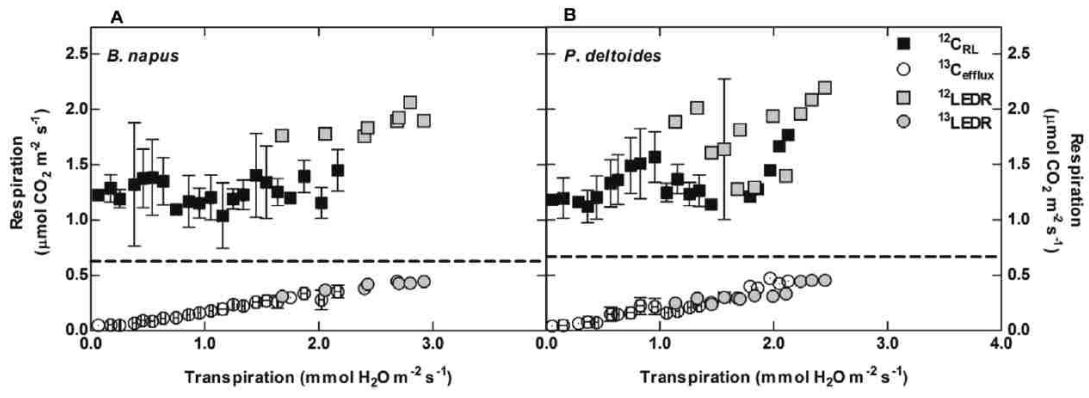
Chapter 3

Contribution and consequences of xylem-transported CO_2 assimilation for C_3 plants

Samantha S. Stutz[1]

[1]*University of New Mexico, Department of Biology, MSC03-2020, Albuquerque,*

NM 87131, USA

Summary

- Traditionally plants were thought to only use CO_2 derived from the atmosphere for photosynthesis; however, recent studies show that high concentrations of inorganic carbon dissolved in xylem water moves in bulk flow through a plant to the leaf where it is either used for photosynthesis or exits as CO_2 with the transpiration stream. However, the rate of assimilation and efflux of xylem-transported CO_2 out of leaves in the light are not known.

- Cut leaves of *Populus deltoides* and *Brassica napus* were placed in either a KCl solution or one of three [$NaH^{13}CO_3$] solutions dissolved in water; simultaneously the efflux of xylem-transported CO_2 exiting the leaf across light- and CO_2-response curves were measured in real-time using a tunable diode laser absorption spectroscope.

- Rates of assimilation and efflux of xylem-transported CO_2 increased with increasing xylem [$^{13}CO_2^*$]. Both the rate of assimilation and the efflux were highest when rates of transport were highest. Under saturating irradiance, rates of xylem-transported CO_2 assimilation accounted for ~2.5% of the total assimilation in both species in the highest [$^{13}CO_2^*$] treatment.

- It is unlikely that xylem-transported CO_2 changes current leaf-level models of photosynthesis; however, over the life of a plant, xylem-transported CO_2 assimilation may contribute greatly to carbon gain and allow plants to photosynthesize with lower stomatal conductance.

Key words: *Brassica napus*, CO_2 efflux, internally transported CO_2, leaf photosynthesis models, leaf respiration, *Populus deltoides*, stem [CO_2^*], tunable diode laser absorption spectroscopy, xylem-transported CO_2

INTRODUCTION

Traditionally, aside from mitochondrial respiration in the same cell, CO_2 for photosynthesis was assumed to diffuse from the atmosphere through the stomata into the intercellular air space. This CO_2 then diffuses into the mesophyll cells eventually making it to the site of ribulose-1,5-bisphosphate-carboxylase/oxygenase (Rubisco) where it will be used for photosynthesis. However, recent work has shown that the concentration of total dissolved inorganic carbon ([CO_2^*], the sum of [CO_2]$_{aq}$, [HCO_3^-], [H_2CO_3], and [CO_3^{2-}]) in the xylem ranges from ~0.05 to ~13 mmol l^{-1} (<1 to 26% CO_2 gas by volume in air equilibrated with xylem sap). These, levels are ~30-750 times higher than current atmospheric [CO_2] (Teskey *et al*., 2008). Dissolved CO_2 in the stem is derived from root and stem respiration and moves in bulk flow along with water through the plant to the leaf where it is either recaptured or exits via transpiration (Fig. 1). If the concentration of xylem-transported CO_2 is high and reaches the foliage it could provide a major substrate for Rubisco in leaf cells; it also has the potential to change the intercellular CO_2 (C_i) of a leaf, thus changing the current understanding of the Farquhar *et al*. (1980) model of leaf photosynthesis (Hanson & Gunderson, 2009). However, if little xylem-transported CO_2 is recaptured by photosynthesis, xylem-transported CO_2 exiting the leaf in the light may account for some of the variation seen in estimates of respiration in the light.

Previous studies have shown that plants utilize some xylem-transported CO_2 for photosynthesis by corticular and woody stem tissue (Teskey $et\ al.$, 2008), by branch tissue (Teskey & McGuire, 2002; McGuire $et\ al.$, 2009; Bloemen $et\ al.$, 2013a, b), and by leaves (Stringer & Kimmerer, 1993; McGuire $et\ al.$, 2009; Bloemen $et\ al.$, 2013a, b; Bloemen $et\ al.$, 2015). When cut $Platanus\ occidentalis$ branches with attaches leaves were placed in an ~11.6 mmol l^{-1} [$^{13}CO_2^{*}$], McGurie $et\ al.$ (2009,) found that leaf tissue accounted for ~31% while branch tissue accounted for ~50% of the xylem-transported CO_2 that was assimilated. While Bloemen $et\ al.$ (2013a) observed in $Populus\ deltoides$ branches with attached leaves placed in a low (3 mmol l^{-1}) and high (13 mmol l^{-1}) [$^{13}CO_2^{*}$] solutions that xylem-transported CO_2 assimilation accounted for ~0.75% and 2% of total photosynthesis in the branch and leaves combined in the low- and high-label treatments, respectively. These studies demonstrate that xylem-transported CO_2 will be taken up by a cut branch eventually making it to the leaves where it is used for photosynthesis. Using a destructive harvesting approach, Bloemen $et\ al.$ (2013b), found that, when a low (1.4 mmol l^{-1}) and high (12 mmol l^{-1}) [$^{13}CO_2^{*}$] label were applied to $P.\ deltoides$ sapling stems in the field, 17.4% and 5.6% of xylem-transported CO_2 was incorporated into the above ground portions of the plant, respectively. Of all the tissues measured for the presence of xylem-transported CO_2, the leaves accounted for the smallest percentage—2.7% in the low-label and 0.5% in the high-label (Bloemen $et\ al.$, 2013b).

In addition to studies measuring how much xylem-transported CO_2 is assimilated in branches with attached leaves and whole plants, several studies have focused on how cut leaves use xylem-transported CO_2 for photosynthesis. Stringer & Kimmerer (1993) applied a 1 mmol l^{-1} solution of $H^{14}CO_3^{-}$ dissolved in water to excised $P.\ deltoides$ leaves and found that 77% of the ^{14}C label was fixed in the tissues most proximal to the label with the remaining 23% located in

the minor veins and mesophyll cells. Bloemen *et al*. (2015) placed cut leaves in different

[$^{13}CO_2^*$] and found rates of assimilation using xylem-transported CO_2 were highest when the

vapor pressure difference was highest and under the high-label treatment. Similar to Stringer &

Kimmerer (1993), Bloemen *et al*. (2015), found that most of the xylem-transported CO_2 used for

photosynthesis was found in the petiole and the proximal primary veins with decreasing amounts

found in the more distal primary and secondary veins.

Presumably, if xylem-transported CO_2 is not used for photosynthesis, it will exit the leaf

in the light. If this flux is large it may account for some of the variation observed in rates of day

respiration. Current models of leaf photosynthesis incorporate CO_2 evolution from the

mitochondria in the light not associated with photorespiration (R_d) (Farquhar *et al*., 1980);

additionally, models assume that all fluxes of CO_2 exiting a leaf are derived from metabolism

occurring in leaf cells. While it is known that rates of respiration are lower in the light compared

to the dark (Kok, 1948, 1949; Tcherkez *et al*., 2017a), it is difficult to measure rates of

respiration in the light while leaves are photosynthesizing. This inhibition of leaf respiration in

the light is thought to be due to reductions in the TCA cycle (von Caemmerer, 2000; Tcherkez *et

al*., 2009). One explanation for the variation in the inhibition of leaf respiration in the light

maybe an efflux of xylem-transported CO_2 exiting a leaf. For instance, when rates of

assimilation are low, as occurs under low irradiance or low CO_2, the overall proportion of day

respiration is greater than under high irradiance and high CO_2 (Tcherkez *et al*., 2017b). If the

efflux of xylem-transported CO_2 out of a leaf is large when irradiance or [CO_2] are low this

efflux may change our current understanding of respiration in the light. Additionally, if the

efflux of xylem-transported CO_2 out of the leaf is high when irradiance is low, this efflux may

account for a portion of the Kok effect (Kok, 1949). Stringer & Kimmerer (1993) estimated that

less than 1% of xylem-transported CO_2 exited cut leaves in the light but found under low irradiance that a higher percentage of xylem-transported CO_2 exited the leaf compared to under high irradiance. Bloemen *et al*. (2015) found that xylem-transported CO_2 could exit labeled leaves in the light and then diffuse through the stomata of unlabeled leaves and be used for photosynthesis. However, neither of these studies had ways to estimate the dynamics of the efflux xylem-transported CO_2 exiting a leaf in the light.

While previous studies have used radio carbon or mass spectroscopy to determine how much labeled xylem-transported CO_2 is used for photosynthesis, these destructive techniques allow only a snapshot at a discrete point in time and do not allow for real-time measurements of rates of xylem-transported CO_2 assimilation or the efflux of xylem-transported CO_2 out of a leaf. Therefore, the goals of this study are to: 1) determine how much and under what conditions xylem-transported CO_2 is most important for leaf photosynthesis in excised leaves and if these fluxes change the modeling parameter for leaf-level photosynthesis, and 2) determine how much xylem-transported CO_2 ($^{13}C_{\text{light efflux}}$) exits a leaf in the light and if $^{13}C_{\text{light efflux}}$ has the potential to change estimates of day respiration in excised leaves of a woody and herbaceous C_3 plant, *P. deltoides* and *Brassica napus*, respectively. These objectives were accomplished by adding one of three [$NaH^{13}CO_3$] solutions to cut leaves of *P. deltoides* and *B. napus* and measuring rates of ^{12}C and ^{13}C assimilation and the efflux of xylem-transported CO_2 exiting the leaf across light- and CO_2-response curves in real-time using a tunable diode laser absorption spectroscope (TDL). We hypothesized that rates of assimilation using xylem-transported CO_2 would be greatest when intercellular [CO_2] were low and that the $^{13}C_{\text{light efflux}}$ would be highest when rates of transpiration were high.

MATERIALS & METHODS

Plant propagation and growth

Brassica napus (L. stellar DH GT060615) and *Populus deltoides* (W. Bartram ex Marshall) were propagated according to Stutz *et al*. (2017). All plants were grown under natural light in an unshaded greenhouse, with mid-day photosynthetically active radiation (PAR) at pot level of approximately 1200 μmol m^{-2} s^{-1} at the University of New Mexico in Albuquerque, NM, USA, under ambient CO_2, 24ºC/21ºC day/night.

Light-response curves

A LI-6400 (LI-COR Biosciences, Lincoln, NE, USA) was coupled to a tunable diode laser absorption spectroscope (TDL—model TGA 100; Campbell Scientific, Inc., Logan, UT, USA) to measure online $^{12}CO_2$ and $^{13}CO_2$ exchange. Isotope calibration consisting of a high and low CO_2 tank spanning the expected range of [CO_2] of each isotopologue for the LI-COR reference and sample was completed as previously described in Barbour *et al*. (2007) and Stutz *et al*. (2017). The TDL cycled among calibrations of the high and low CO_2 tank along with the LI-COR reference and sample line measuring for one minute at each site. However, only the last 10 seconds of data were used for calculations via the TDL LI-COR processing package (Erhardt & Hanson, 2013) in R (R Core Development Team, 2011). The highest fully expanded leaf for *B. napus* or a fully expanded *P. deltoides* leaf was placed in a clear topped, custom leaf chamber 38.5 cm^2 made to fit an RGB LED light source (LI-COR Biosciences, Lincoln, NE, USA) attached to a LI-6400 at 23ºC (leaf temperature), 380 μmol mol^{-1} CO_2 reference at 1200 μmol quanta m^{-2}s^{-1} or 1500 μmol quanta m^{-2}s^{-1} for *B. napus* and *P. deltoides*, respectively. Leaves were left in the chamber for approximately 30 minutes before being cut and placed in a 40 mmol

43

l^{-1} KCl solution. The KCl solution was swapped for 99% ^{13}C sodium bicarbonate (NaH^{13}CO$_3$—

Cambridge Isotope Laboratories, Inc. Andover, MA, USA) dissolved in 40 mmol l^{-1} KCl at one

of three [^{13}CO$_2^*$]: 1.19 (low-carbon—LC), 5.95 (medium-carbon—MC), or 11.9 (high-carbon—

HC) mmol l^{-1} [^{13}CO$_2^*$], or the leaf was left in the KCl solution for the measurement. Individual

leaves were only provided a single [^{13}CO$_2^*$] or left in the 40 mmol l^{-1}KCl solution according to

Stutz *et al.* (2017). Once cut and placed in the [^{13}CO$_2^*$] the leaf remained at the starting

irradiance (1200 μmol quanta m^{-2} s^{-1} *B. napus* or 1500 μmol quanta m^{-2} s^{-1} *P. deltoides*) until

δ^{13}C and [^{13}CO$_2$] peaked and either plateaued or decreased, which took approximately 20-30

minutes, before continuing with the light-response curve. The light-response curves were

measured in the following order for *B. napus*: 1200, 1000, 800, 500, 350, 250, 200, 175, 150,

125, 100, 75, 50, 35, 0 μmol quanta m^{-2} s^{-1} and the following order for *P. deltoides*: 1500, 1000,

800, 500, 250, 200, 175, 150, 125, 100, 75, 50, 35, 0 μmol quanta m^{-2} s^{-1}. Five measurements

were made at each irradiance. Five leaves from each species were measured in the KCl and each

[^{13}CO$_2^*$].

CO$_2$-response curves

For the CO$_2$-response curves, the highest fully expanded leaf for *B. napus* or a fully

expanded *P. deltoides* leaf, was placed in the same LI-6400 custom leaf chamber as was used for

the light-response curves at 23ºC (leaf temperature) at 1200 μmol quanta m^{-2}s^{-1} or 1500 μmol

quanta m^{-2}s^{-1} for *B. napus* and *P. deltoides*, respectively. The CO$_2$ reference on the LI-6400 was

set so the [CO$_2$] at the leaf level was approximately 400 μmol mol^{-1}, which was between 500 and

600 μmol mol^{-1} CO$_2$ reference [CO$_2$] for both species. As with the light-response curves, leaves

were left in the chamber for approximately 30 minutes before being cut and placed in a 40 mmol

l^{-1} KCl solution for approximately 16 minutes. The leaves were then transferred to a single 99%

^{13}C sodium bicarbonate (NaH^{13}CO$_3$) solution (LC, MC, or HC) or remained in the KCl solution,

as in the light-response curves. The leaf was left at the starting [CO$_2$] until the δ^{13}C and [^{13}CO$_2$]

readings on the TDL stabilized approximately 20 to 30 minutes for each leaf. The [CO$_2$] on the

LI-6400 reference were applied to the leaf in the following order: starting [CO$_2$], 200, 100, 50,

150, 300, starting [CO$_2$], 1000, 2000, 1500, 700 and starting [CO$_2$]. The leaf was left at each

[CO$_2$] for three cycles on the TDL except for the starting [CO$_2$] where the leaf was left until it

reached the starting rate of photosynthesis. Following the CO$_2$-response curve the light was

turned off and respiration was measured when the leaf had been in the dark for at least 30

minutes, to avoid light enhanced dark respiration (LEDR). Fives leaves from each species were

measured for each [^{13}CO$_2$*] and the KCl solution.

Estimating the rate of xylem-transported CO$_2$ assimilation

   The assimilation rate of xylem-transported CO$_2$ ($^{13}A_x$) was calculated as (Table 1, Fig. 1):

$$^{13}A_x = {}^{13}C_{pred\ efflux} - {}^{13}C_{observed\ light\ efflux} \qquad \text{Equation 1}$$

where $^{13}C_{pred\ efflux}$ (Table 1) is the predicted rate of xylem-transported CO$_2$ exiting the leaf if there

is no photosynthesis of xylem-transported CO$_2$, and is estimated from linear regression models of

xylem-transported CO$_2$ effluxes in the dark for both species (see Stutz *et al*., 2017). $^{13}C_{light\ efflux}$

is the efflux of xylem- transported ^{13}CO$_2$ in the light and is calculated as:

$$^{13}C_{light\ efflux} = {}^{13}A_{pred} - {}^{13}A_{obs} \quad \text{Equation 2}$$

where $^{13}A_{obs}$ is the rate of $^{13}CO_2$ assimilation measured with the TDL and $^{13}A_{pred}$ is the predicted

background rate of ^{13}C assimilation based on the atmospheric concentration of $^{13}CO_2$ and is

estimated as:

$$^{13}A_{pred} = {}^{12}A_{obs} * 0.011 \quad \text{Equation 3}$$

where $^{12}A_{obs}$ is the observed rate of $^{12}CO_2$ assimilation measured with the TDL. The natural

abundance of $^{13}CO_2$ is 1.1% of $^{12}CO_2$ in the atmosphere; therefore, the rate of $^{13}CO_2$ assimilation

will be approximately 0.011 of the rate of $^{12}CO_2$ assimilation under normal conditions (Griffis *et*

al., 2004).

Statistical analysis

Linear mixed effects models were produced for the following variables: $^{12}A_{obs}$, $^{13}A_x$,

$^{13}C_{light\ efflux}$ and the percentage of $^{13}A_x$ to total A, for both the light- and CO_2-response curves.

The fixed effects were species and $[^{13}CO_2{}^*]$ while the random effects were irradiance and $[CO_2]$,

for the light- and CO_2-response curves, respectively. Results were deemed significant at *P<0.05*.

No data were transformed based on the distribution of the residuals. All statistical analyses were

performed in R (version 3.4.2, R Development Core Team 2017).

RESULTS

Rates of assimilation

As expected, rates of photosynthesis using atmospheric CO_2 ($^{12}A_{obs}$) increased with

increasing irradiance and intercellular $[CO_2]$ (Fig. 2c, d, Fig. 3c, d) for both species. In *B. napus*,

rates of assimilation saturated at ~18 μmol CO_2 m^{-2} s^{-1} in the HC (high-carbon—11.9 mmol l^{-1})

and KCl treatments; while rates of saturation were ~22 μmol CO_2 m^{-2} s^{-1} in the LC (low-carbon—1.19 mmol l^{-1}) and MC (medium-carbon—5.95 mmol l^{-1}) treatments (Fig. 2c). In *P. deltoides*, rates of $^{12}A_{obs}$ saturated at ~18 μmol CO_2 m^{-2} s^{-1} across all treatments (Fig. 2d). In the CO_2-response curves, saturated rates of $^{12}A_{obs}$ in *B. napus* were ~30 μmol CO_2 m^{-2} s^{-1} in the HC and KCl treatments and ~40 μmol CO_2 m^{-2} s^{-1} in the LC and MC treatments (Fig. 3c). In *P. deltoides* the saturated rate of assimilation was ~13 μmol CO_2 m^{-2} s^{-1} (Fig. 3d) across all treatments.

Rates of xylem-transported CO_2 assimilation ($^{13}A_x$) increased with increasing irradiance and [$^{13}CO_2^*$] for both species (Fig. 2a, b). In *B. napus* rates of $^{13}A_x$ under saturating irradance were ~0.03 μmol CO_2 m^{-2} s^{-1}, ~0.22 μmol CO_2 m^{-2} s^{-1}, and ~0.42 μmol CO_2 m^{-2} s^{-1} in the LC, MC, and HC treatments, respectively (Fig. 2a); rates of $^{13}A_{obs}$ in the KCl treatment was ~0.18 μmol CO_2 m^{-2} s^{-1}. The rates of $^{13}A_x$ were significantly different among the three [$^{13}CO_2^*$] ($P<0.001$); the rate of $^{13}A_x$ and $^{13}A_{obs}$ in the MC and KCl treatments were significantly different ($P<0.05$). In *P. deltoides*, rates of $^{13}A_x$ were ~0.08 μmol CO_2 m^{-2} s^{-1}, ~0.25 μmol CO_2 m^{-2} s^{-1}, and ~0.44 μmol CO_2 m^{-2} s^{-1} in the LC, MC, and HC treatments, respectively; the rate of $^{13}A_{obs}$ in the KCl treatment was ~0.23 μmol CO_2 m^{-2} s^{-1} (Fig. 2b). Under saturating irradiance, rates of $^{13}A_x$ were significantly different among the three [$^{13}CO_2^*$] treatments ($P<0.001$). However, rates of $^{13}A_x$ and $^{13}A_{obs}$ were not significantly different between the MC and the KCl treatments ($P=0.062$) (Fig. 2b). Mean rates of $^{13}A_x$ in the LC treatment were more than five times greater in *P. deltoides* compared to *B. napus* when irradiance was saturating but were boardline significantly different ($P=0.051$). Rates of $^{13}A_x$ were similar and not significantly different between species in either the MC ($P=0.071$) or the HC ($P=0.370$) treatments. Rates of $^{13}A_{obs}$ in the KCl treatment were similar to to rates of $^{13}A_x$ in the MC treatment for both species,

indicating that under LC there is little additional contribution of $^{13}A_x$ compared to the background rate of photosynthesis using $^{13}CO_2$ derived from the atmosphere; however, when $[^{13}CO_2^*]$ is at least 5.95 mmol l^{-1}, not accounting for rates of xylem-transported CO_2, assimilation would underestimate total assimilation by approximately 1.1% (the rate of normal background assimation using $^{13}CO_2$), and this error would increase with increasing xylem $[CO_2^*]$.

In the CO_2-repsonse curves, rates of $^{13}A_{obs}$ in the KCl treatment increased with increasing $[CO_2]$ and saturated at an intercellular $[CO_2]$ of ~700 μmol mol^{-1} CO_2 for both species. However, in both species, across all $[^{13}CO_2^*]$, rates of $^{13}A_x$ increased with decreasing $[CO_2]$ and peaked at an intercellular $[CO_2]$ of ~150 μmol mol^{-1} (Fig. 3a, b). In *B. napus* the highest rates of $^{13}A_x$ were ~0.02 μmol CO_2 m^{-2} s^{-1}, ~0.14 μmol CO_2 m^{-2} s^{-1}, and ~0.28 μmol CO_2 m^{-2} s^{-1}, in the LC, MC, and HC treatments, respectively; the rate of $^{13}A_{obs}$ in the KCl treatment was ~0.36 μmol CO_2 m^{-2} s^{-1} (Fig. 3a). Rates of $^{13}A_x$ and $^{13}A_{obs}$ were significantly different among all treatments ($P<0.001$). In *P. deltoides* the highest rates of $^{13}A_x$ ~0.04 μmol CO_2 m^{-2} s^{-1}, ~0.17 μmol CO_2 m^{-2} s^{-1}, and ~0.28 μmol CO_2 m^{-2} s^{-1}, in the LC, MC, and HC treatments, respectively (Fig. 3b); rates of $^{13}A_{obs}$ were ~0.16 μmol CO_2 m^{-2} s^{-1} in the KCl treatment (Fig. 3b). However, rates of $^{13}A_x$ or $^{13}A_{obs}$ were only signficantly different in the MC treatment compared to the LC, HC and KCl treatments ($P<0.001$) (Fig. 3b). The saturating rate of $^{13}A_{obs}$ in the KCl treatment was similar to the highest observed rate of $^{13}A_x$ in the MC treatment; however, occuring at a different C_i. For both species, at an intercellular $[CO_2]$ of about 400 μmol mol^{-1} rates of $^{13}A_x$ started to decline and continued to decline once saturation was reached for $^{12}CO_2$. Rates of $^{13}A_x$ increased with increaing $[^{13}CO_2^*]$ and were significantly different among $[^{13}CO_2^*]$ ($P<0.001$). When $[CO_2]$ was saturating in *P. deltoides*, rates of $^{13}A_x$ in the LC, MC and HC were significantly lower than rates

of $^{13}A_{obs}$ in the KCl treatment ($P<0.05$) while rates of $^{13}A_x$ were significantly lower in *B. napus* in all $[^{13}CO_2{}^*]$ compared to the KCl treatment ($P<0.001$).

Efflux of xylem-transported CO_2 exiting the leaf in the light

Rates of $^{13}C_{light\ efflux}$ varried little across irradiance in both species (Fig. 4). In *B. napus* the highest rates of $^{13}C_{light\ efflux}$ were ~0.007 µmol CO_2 m^{-2} s^{-1}, ~0.11 µmol CO_2 m^{-2} s^{-1}, and ~0.2 µmol CO_2 m^{-2} s^{-1} in the LC, MC and HC treatments, respectively (Fig. 4a, c, e). In *B. napus* below the light-compensation point (<75 µmol quanta m^{-2} s^{-1}), $^{13}C_{light\ efflux}$ was not significantly different among treatments (Fig. 4a, c, e). However, above the light-compensation point the LC treatment was significantly different from the MC and HC treatments ($P<0.05$); while the MC and HC treatmentments were not significantly different across any irradiance.

The maximum rates of $^{13}C_{light\ efflux}$ in *P. deltoides* were ~0.013 µmol CO_2 m^{-2} s^{-1}, ~0.12 µmol CO_2 m^{-2} s^{-1}, and ~0.24 µmol CO_2 m^{-2} s^{-1} in the LC, MC and HC treatments, respectively (Fig. 4b, d, f). There were significant differences between the LC and HC treatments ($P<0.001$) and between the LC and MC treatments ($P<0.05$) across all irradiances. However, the LC and MC treatments were only significantly different under low (<175 µmol quanta m^{-2} s^{-1}) and high (>500 µmol quanta m^{-2} s^{-1}) irradiances (Fig. 4b, d). Higher rates of $^{13}C_{light\ efflux}$ were observed in leaves with higher transpiration rates within the MC and HC treatments compared to leaves with lower rates of transpiration within a single $[^{13}CO_2{}^*]$, leading to large error bars observed in *P. deltoides* (Fig. 4d, f). The $^{13}C_{light\ efflux}$ was significantly different among $[^{13}CO_2{}^*]$ ($P<0.001$) but not between species ($P=0.43$). Differences in $^{13}C_{light\ efflux}$ were most pronounced under low irradiance both among $[^{13}CO_2{}^*]$ and between species (Fig. 4). The rate of $^{13}C_{light\ efflux}$ was similar between species in the LC treatment; however maximum rates of $^{13}C_{light\ efflux}$ were higher in *P.*

deltoides compared to *B. napus* ($P<0.001$) in the MC treatment (Fig. 4c, d); while rates of $^{13}C_{light\ efflux}$ were higher in *B. napus* in the HC treatment compared to *P. deltoides* ($P<0.001$) (Fig. 4e, f).

In the CO_2-response curves, the maximum rates of $^{13}C_{light\ efflux}$ in *B. napus* were ~0.007 µmol CO_2 m^{-2} s^{-1}, ~0.07 µmol CO_2 m^{-2} s^{-1}, and ~0.24 µmol CO_2 m^{-2} s^{-1} in the LC, MC and HC treatments, respectively (Fig. 5a, c, e). The maximum rates of $^{13}C_{light\ efflux}$ in *P. deltoides* were ~0.014 µmol CO_2 m^{-2} s^{-1}, ~0.12 µmol CO_2 m^{-2} s^{-1}, and ~0.23 µmol CO_2 m^{-2} s^{-1} in the LC, MC and HC treatments, respectively (Fig. 5b, d, f). Rates of $^{13}C_{light\ efflux}$ were ten times higher going from the LC to the MC treatments for both species (Fig. 5a, b, c, d). $^{13}C_{light\ efflux}$ increased slightly with increasing intercellular [CO_2] for both species in the LC, and MC treatments and for *P. deltoides* in the HC treatment (Fig. 5a, b, c, d, f). In *B. napus* in the HC treatment $^{13}C_{light\ efflux}$ decreased with increasing intercellular [CO_2] (Fig. 5e). There were significant differences between species ($P<0.001$) and among [$^{13}CO_2^*$] ($P<0.001$).

How do rates of $^{13}A_x$ compare to rates of $^{13}C_{light\ efflux}$?

The rate of $^{13}C_{light\ efflux}$ was lower than the rate of $^{13}A_x$ across all irradiances in the LC and HC treatments, in *B. napus* (Fig. 4a, e). However, in the MC treatment, the rate of $^{13}C_{light\ efflux}$ was greater than the rate of $^{13}A_x$ when irradiance was less than 800 µmol quanta m^{-2} s^{-1} but under higher irradiances, this reversed (Fig. 4c).

In *P. deltoides,* in the MC and HC treatments, the rate of $^{13}C_{light\ efflux}$ was greater than $^{13}A_x$ when the irradiance was under 500 µmol quanta m^{-2} s^{-1}; however, when irradiance was greater than 500 µmol quanta m^{-2} s^{-1} rates of $^{13}A_x$ were greater (Fig. 4d, f). In the LC treatment, above the light-compensation point rates of $^{13}A_x$ were greater than the rate of $^{13}C_{light\ efflux}$ (Fig. 4b).

In the CO_2-response curves, rates of $^{13}A_x$ were always equal to or greater than rates of $^{13}C_{light\ efflux}$ across all $[^{13}CO_2^*]$ and C_i for both species (Fig. 5). With increasing C_i the rate of $^{13}A_x$ and $^{13}C_{light\ efflux}$ approached each other in the LC and MC treatments, in *B. napus* (Fig. 5a, c). However, in the HC treatment for *B. napus* both $^{13}A_x$ and $^{13}C_{light\ efflux}$ declined with increasing C_i (Fig. 5e).

Contribution of xylem-transported CO_2 assimilation to total assimiation

In both species the percentage of $^{13}A_x$ as a total contribution to photosynthesis increased with decreasing irradiance and peaked near the light-compensation point (Fig. 6a, b). In *B. napus*, the contrubution of $^{13}A_x$ to total photosynthesis increased with increasing $[^{13}CO_2^*]$. The highest percentage of $^{13}A_x$ to total photosynthesis were 0.98% (LC), 4.9% (MC) and 5.9% (HC) (Fig. 6a) which occurred near the light-compensation point. The contribution of xylem-transported CO_2 to total photosynthesis saturated at 0.3% (LC), 1% (MC), and 2.5% (HC); the contribution of xylem-transported CO_2 to total photosynthesis saturated at an irradiance of 250 μmol quanta m^{-2} s^{-1} in all treatments (Fig. 6a). In *P. deltoides* the contribution of $^{13}A_x$ to total photosynthesis was highest in the MC treatment with a total contribution of 8% while the contribution in the LC and HC treatments were 1.6% and 3.4%, respectively, which occurred near the light-compensation point (Fig. 6b). The contribution of xylem-transported CO_2 to total photosynthesis saturated at an irradiance of 250 μmol CO_2 m^{-2} s^{-1} (Fig. 6b) the contribution of $^{13}A_x$ to total photosynthesis were 0.4% (LC), 1.4% (MC) and 2.2% (HC) (Fig. 6b).

In the CO_2-response curves the percentage of $^{13}A_x$ as a total contribution of photosynthesis increased with decreasing $[CO_2]$ and peaked at the lowest $[CO_2]$ for both species acorss all $[^{13}CO_2^*]$. In *B. napus* the contribution of $^{13}A_x$ to total photosynthesis was 0.65% (LC),

3.6% (MC) and 8% (HC) (Fig. 7a); while in *P. deltoides* the contribution of $^{13}A_x$ to total photosynthesis was 3.6% (LC), 6.9% (MC) and 10% (HC) (Fig. 7b).

In order to determine if the $^{13}C_{light\ efflux}$ could ever reach the rate of respiration in the dark (R_d) or $\frac{1}{2}*R_d$ in the light, the rate of $^{13}C_{light\ efflux}$ from all $[^{13}CO_2^*]$ was plotted with the average rate of dark respiration across all $[^{13}CO_2^*]$ for each species (black line) and $\frac{1}{2}*R_d$ (dotted line) (Figs. 6c, d, 7c, d) for both the light- and CO_2-response curves. In the light-response curves, the rate of $^{13}C_{light\ efflux}$ is well below the rate of $\frac{1}{2}*R_d$ and R_d even under the HC for both species (Fig. 6c, d). Across all $[CO_2]$ and $[^{13}CO_2^*]$ the rate of $^{13}C_{light\ efflux}$ was well below the R_d and $\frac{1}{2}*R_d$ (Fig. 7c, d).

DISCUSSION

Our method, of placing a cut leaf in a solution of $[^{13}CO_2^*]$ and measuring gas exchange using a LI-6400 leaf chamber coupled to a tunable diode laser absorption spectroscope (TDL), allowed for real-time measurements of rates of assimilation of xylem-transported CO_2 ($^{13}A_x$) and the efflux of xylem-transported CO_2 ($^{13}C_{light\ efflux}$) out of the leaf in the light for both a woody species, *Populus deltoides* and a herbaceous species, *Brassica napus*. We found that xylem-transported CO_2 was most important when the intercellular $[CO_2]$ was low, which occurred under high irradiance and low $[CO_2]$ (Fig. 2a, b, 3a, b). While a portion of the xylem-transported CO_2 was used for photosynthesis, the contribution of $^{13}A_x$ to total photosynthesis in the light-response curves was only about 2.5% in *B. napus* and 2.2% in *P. deltoides* when the rates of $^{13}A_x$ were highest in the HC treatment (Fig. 6a, b); however, the percentage contribution of $^{13}A_x$ to total photosynthesis increased to 6% (high-carbon—HC) and 8% (medium-carbon—MC) in *B. napus* and *P. deltoides*, respectively, under low irradiance (Fig. 6a, b). In the CO_2-response curves the

contribution of $^{13}A_x$ to total photosynthesis was 0.9% (HC) and 1.5% (HC) at saturating $[CO_2]$ but increased with decreasing $[CO_2]$ to 8% (HC) and 10% (HC) in *B. napus* and *P. deltoides*, respectively (Fig. 7a, b). Rates and contributions of $^{13}A_x$ increased with increasing $[^{13}CO_2{}^*]$ for both species in both the light- and CO_2-response curves. Across all $[^{13}CO_2{}^*]$ in both the light- and CO_2-response curves, there was a small, but measurable efflux of $^{13}CO_2$ exiting the leaf (Fig. 6c, d, 7c, d) for both species in the light- and CO_2-response curves. The $^{13}C_{light\ efflux}$ increased with increasing $[^{13}CO_2{}^*]$ for both species in the light- and CO_2-response curves (Fig. 4, 5), with the maximum rate of $^{13}C_{light\ efflux}$ occurring in the HC treatments in both the light- (~0.2 µmol CO_2 m^{-2} s^{-1} in *B. napus* and ~0.3 µmol CO_2 m^{-2} s^{-1} in *P. deltoides*) and CO_2-response (~0.3 µmol CO_2 m^{-2} s^{-1} in *B. napus* and ~0.2 µmol CO_2 m^{-2} s^{-1} in *P. deltoides*) curves (Fig. 4e, f, 5e, f).

How large and is it possible to measure xylem-transported CO_2 exiting a leaf in the light?

Bloemen *et al*. (2013b) hypothesized that any xylem-transported CO_2 that reached the leaves of *P. deltoides* saplings would be inconsequential compared to the CO_2 that would enter the leaves from the atmosphere, thus, resulting in no net loss of xylem-transported CO_2 from leaves. However, when Bloemen *et al*. (2015) placed cut *P. deltoides* leaves either in a solution labeled with $^{13}CO_2$ or a solution of KCl in the same Plexiglass box for a 2 hour length of time they detected that between 6% and 15% of the total assimilates in unlabeled leaves originated from xylem-transported CO_2 that effluxed from the labeled leaves. Additionally, Stringer & Kimmerer (1993) measured the efflux of $^{14}CO_2$ in cut *P. deltoides* leaves and found that less than 1% of the $^{14}CO_2$ label escaped out the leaves in the light. We also observed a small but measurable efflux of xylem-transported CO_2 out of cut leaves in the light in the low-carbon (LC), MC and HC treatments ranging from <0.01 µmol CO_2 m^{-2} s^{-1} in the LC treatment for *B. napus* to

0.3 µmol CO_2 m^{-2} s^{-1} in the HC treatment for *B. napus* and *P. deltoides* (Fig. 4, 5) across both light- and CO_2-response curves. The $^{13}C_{light\ efflux}$ was dependent upon $[^{13}CO_2^*]$ and rates of transpiration. The highest rates of $^{13}C_{light\ efflux}$ in the light- and CO_2-reponse curves occurred under high irradiance and low $[CO_2]$ when rates of transpiration and stomatal conductance were highest, which occurred when vapor pressure difference (VPD) and C_i were lowest (Fig. 4, 5). Bloemen *et al*. (2013a) and Bloemen *et al*. (2015) observed VPD along with transpiration were the most important drives for how much xylem-transported CO_2 was assimilated in cut branches and leaves. We found that it was the rate of transpiration, controlled by stomatal conductance and VPD that indicated how much xylem-transported CO_2 exited the leaf in the light, which was also true for the dark (Stutz *et al*., 2017).

Rates of $^{13}C_{efflux}$ out of cut *Platanus occidentalis* branches were 52% lower in the light compared to the dark (McGuire *et al*., 2009) while Stringer & Kimmerer (1993) observed an 83% decrease in $^{14}CO_2$ efflux exiting cut leaves under an irradiance of 70 µmol quanta m^{-2} s^{-1} in the light compared to the dark. We observed a decline in $^{13}C_{light\ efflux}$ of 44% in the HC and 65% in the LC in the light compared to the dark in *P. deltoides* and a 9% in the HC and 39% in the LC in *B. napus*. With increasing $[^{13}CO_2^*]$, the amount of xylem-transported CO_2 used for photosynthesis declined while the amount of $^{13}CO_2$ exiting the leaf increased. Unlike previous studies we were able to measure in real-time the efflux of xylem-transported CO_2 exiting the leaf along with rates of xylem-transported CO_2 assimilation. High rates of $^{13}C_{light\ efflux}$ are not exclusive of low rates of $^{13}A_x$, instead the highest rates of $^{13}C_{light\ efflux}$ coincide with the highest rates of $^{13}A_x$. This indicates that the supply of xylem-transported CO_2 for photosynthesis, which is controlled by the rate of transpiration, is critical for controlling how much xylem-transported CO_2 is used for photosynthesis.

When is xylem-transported CO_2 assimilation most important

Rates of $^{13}A_x$ were measurable in all $[^{13}CO_2{}^*]$ and increased with increasing $[^{13}CO_2{}^*]$ provided through the xylem. High rates of $^{13}A_x$ occurred when the rate of transpiration was high and the intercellular $[CO_2]$ was low for both species. This occurs in the light-response curves, under high irradiance, and in the CO_2-response curves, under low $[CO_2]$. Xylem-transported CO_2 utilization followed similar patterns to $^{13}CO_2$ originating from the atmosphere in the light-response curves; however, the pattern of xylem-transported CO_2 utilization was completely different in the CO_2-response curves, indicating a balance of the supply and demand of xylem-transported CO_2 to photosynthesis. In *B. napus* rates of $^{12}A_{obs}$ were lower in the HC treatment compared to all other treatments in both the light- and CO_2-responses while there was no difference in *P. deltoides*. Suggesting a threshold of bicarbonate concentration was reached in *B. napus* which caused stomatal closure.

The balance of how much xylem-transported CO_2 is used for photosynthesis is dependent upon how much xylem-transported CO_2 is supplied to the leaf by the transpiration stream and the demand for CO_2. When rates of transpiration are high the $[CO_2{}^*]$ in the stem declines (Aubrey & Teskey, 2009); however, this increases the amount of xylem-transported CO_2 that reaches the leaves and is available for leaf photosynthesis. Bloemen *et al*. (2013a) found in cut branches with attached leaves that more ^{13}C was incorporated into leaf tissues when transpiration and VPD were both high. Our light-response curves showed a similar pattern, with a high supply rate of xylem-transported CO_2 to a leaf when irradiance and stomatal conductance were high as well a high demand for CO_2.

In the CO_2-response curves xylem-transported CO_2 was most important to overall photosynthesis when Rubisco was CO_2 limited (Sharkey *et al*., 2007). The CO_2-limited region

of a CO_2-response curve is considered to be below 200 μmol mol^{-1} CO_2 (Sharkey *et al*., 2007).

Rates of $^{13}A_x$ were highest below 200 μmol mol^{-1} CO_2, with the peak of $^{13}A_x$ occurring when

$[CO_2]$ was 100 μmol mol^{-1} CO_2 across all $[^{13}CO_2^*]$ and both species (Fig. 5). Below this $[CO_2]$

there was a decline in $^{13}A_x$ which is likely a result of deactivation of Rubisco (Sharkey *et al*.,

2007). The combination of low supply of atmospheric CO_2 (low intercellular CO_2) and high

rates of transpiration and stomatal conductance supplying high quantities of $[CO_2^*]$ to the leaf

resulted in the observed high rates of $^{13}A_x$ when the $[CO_2]$ was low. As the atmospheric $[CO_2]$

increased, the rate of transpiration supplying xylem-transported CO_2 to the leaf and stomatal

conductance declined. This diluted a proportion of xylem-transported CO_2 in the intercellular air

space and decreased the possibility of the xylem-transported CO_2 being used for photosynthesis.

Does xylem-transported CO_2 matter for photosynthesis?

The percentage of xylem-transported CO_2 contributing to total photosynthesis increased

with increasing $[^{13}CO_2^*]$ while also increasing with decreasing irradiance. When light was

saturating $^{13}A_x$ accounted for ~2.5% for *B. napus* and ~2.2% for *P. deltoides* in the HC

treatment. As irradiance decreased the contribution increased to ~5.8% in *B. napus* and ~9% in

P. deltoides. The same pattern is repeated across all $[^{13}CO_2^*]$. Stringer & Kimmerer (1993)

estimated that for an individual leaf not including xylem-transported CO_2 assimilation led to a

0.5% underestimation of net photosynthesis and that $^{13}A_x$ accounted for 2.2% of the atmospheric

uptake in intact leaves under a $[^{14}CO_2^*]$ of 1 mmol l^{-1}. Bloemen *et al*. (2013a) estimated that

xylem-transported CO_2 assimilation accounted for about 2.0% and 0.75% in their high- and low-

label treatments of cut *P. deltoides* branches and leaves combined. McGuire *et al*. (2009) found

that the assimilation of xylem-transported CO_2 accounted for 6% of the assimilation from the atmosphere.

It is well established that cut branches with attached leaves, as well as cut leaves can use xylem-transported CO_2 for photosynthesis (McGuire *et al*., 2009; Stringer & Kimmerer, 1993; Bloemen *et al.*, 2015); however, when labeled xylem-transported CO_2 is applied to the roots or shoots of a plant only small quantities of xylem-transported CO_2 is used for leaf photosynthesis (Bloemen *et al.*, 2013a, b) or not observed in leaf tissue (Powers & Marshall, 2011). However, no studies have measured $[CO_2^*]$ in the stem and branch tips simultaneously in order to determine how much xylem-transported CO_2 maybe reaching the leaves and available for leaf photosynthesis in a large tree. The real-time rates of xylem-transported CO_2 assimilation are low compared to assimilation rates using CO_2 from the atmosphere, especially when considering that most plants have $[CO_2^*]$ in the xylem near our LC treatment. On the high end of supplied $[CO_2^*]$, we observed a difference of less than 20 μmol mol^{-1} CO_2 in intercellular $[CO_2]$ (data not shown). Therefore, it is unlikely that xylem-transported CO_2 would significantly change our estimations of parameters for leaf-level photosynthesis models as Hanson & Gunderson (2009) postulated. However, when looking over the life-time of a plant xylem-transported CO_2 may play a significant role in total net photosynthesis. The carbon fixed using xylem-transported CO_2 can be used for a plant to grow a little more, for upkeep of respiring tissues or to put more energy into reproduction.

The rates of $^{13}C_{light\ efflux}$ in the HC treatment was approximately a tenth of the rate of dark respiration in *B. napus* and about a fifth the rate of dark respiration in *P. deltoides* therefore, xylem-transported CO_2 exiting the leaf will only affect estimates of respiration in the light for plants on the high end of measured xylem CO_2 concentrations. However, if assuming that rates

of day respiration being half the rate of dark respiration, the rate of $^{13}C_{light\ efflux}$ in the HC treatment would account for 40% of the efflux of CO_2 out of a leaf in the light in *B. napus* and 20% in *P. deltoides*.

CONCLUSION

Our technique of using an LI-6400 coupled to a TDL allows for real-time measurements of the rates of xylem-transported CO_2 assimilation and the efflux of xylem-transported CO_2 out of a cut leaf from both a herbaceous and woody C_3 plant leaves placed in a $[^{13}CO_2^*]$ solution. Rates of $^{13}A_x$ and $^{13}C_{light\ efflux}$ increased with increasing $[^{13}CO_2^*]$ for both the light- and CO_2-response curves. Both the woody species, *P. deltoides* and the herbaceous species, *B. napus* responded similarly to each other indicating that the effects of petiole morphology had little impact on how xylem-transported CO_2 was used for photosynthesis. The highest rates of $^{13}A_x$ and $^{13}C_{light\ efflux}$ occurred when the rate of transpiration was high which occurred when irradiance was high and $[CO_2]$ was low. The contribution of $^{13}A_x$ to total assimilation accounted for ~2.5% in *B. napus* and ~2.2% in *P. deltoides* of the total rate of assimilation under saturating irradiance in the HC treatment; however, the contribution of xylem-transported CO_2 to total photosynthesis was ~5.95% *B. napus* and ~8% in *P. deltoides* under low irradiance. It is unlikely that the contribution of xylem-transported CO_2 changes estimates of current models of leaf-level photosynthesis. However, xylem-transported CO_2 likely plays an important role and contribution to photosynthesis over the life of an individual plant and may allow a plant to survive adverse conditions and be helpful as climate change progresses.

ACKNOWLEDGMENTS

AUTHOR CONTRIBUTIONS

S.S.S. performed experiments and analyzed data. D.T.H. provided conceptual framework.

S.S.S. and D.T.H. wrote the manuscript.

REFERENCES

Aubrey DP, Teskey RO. 2009. Root-derived CO_2 efflux via xylem stream rivals soil CO_2 efflux. *New Phytologist* **184**: 35-40.

Barbour MM, McDowell NG, Tcherkez G, Bickford CP, Hanson DT. 2007. A new measurement technique reveals rapid post-illumination changes in the carbon isotope composition of leaf-respired CO_2. *Plant, Cell & Environment* **30**: 469-482.

Bloemen J, McGuire MA, Aubrey DP, Teskey RO, Steppe K. 2013a. Assimilation of xylem-transported CO_2 is dependent on transpiration rate but small relative to atmospheric fixation. *Journal of Experimental Botany* **64**: 2129-2138.

Bloemen J, McGuire MA, Aubrey DP, Teskey RO, Steppe K. 2013b. Transport of root-respired CO_2 via the transpiration stream affects aboveground carbon assimilation and CO_2 efflux in trees. *New Phytologist* **197**: 555-565.

Bloemen J, Bauweraerts I, De Vos F, Vanhove C, Vandenberghe S, Boeckx P, Steppe K. 2015. Fate of xylem-transported [11]C- and ^{13}C-labeled CO_2 in leaves of poplar. *Physiologia Plantarum* **153**: 555-564.

von Caemmerer S. 2000. Biochemical models of leaf photosynthesis. Collingwood, Vic., Austrailia: CSIRO Publishing.

Erhardt EB, Hanson DT. 2013. Tdllicor: TDL/Licor processing. R package version 0.1-22.

Farquhar GD, von Caemmerer S, Berry JA. 1980. A biochemical model of photosynthetic CO_2 assimilation in leaves of C_3 species. *Planta* 149: 78-90.

Griffis T, Baker J, Sargent S, Tanner B, Zhang J. 2004. Measuring field-scale isotopic fluxes with tunable diode laser absorption spectroscopy and micrometeorological techniques. *Agricultural and Forest Meterology* **124**: 15-29.

Hanson PJ, Gunderson CA. 2009. Root carbon flux: measurements versus mechanisms. *New Phytologist* **184**: 4-6.

McGuire MA, Marshall JD, Teskey RO. 2009. Assimilation of xylem-transported ^{13}C-labelled CO_2 in leaves and branches of sycamore (*Platanus occidentalis* L.). *Journal of Experimental Botany* **60**: 3809-3817.

Kok B. 1948. A critical consideration of the quantum yield of *Chlorella* photosynthesis. *Enzymologia* **13**: 1-56.

Kok B. 1949. On the interrelation of respiration and photosynthesis in green plants. *Biochimica et Biophysica Acta* **2**: 625-631.

Powers EM, Marshall JD. 2011. Pulse labeling of dissolved ^{13}C-carbonate into tree xylem: developing a new method to determine the fate of recently fixed photosynthate. *Rapid communications in mass spectrometry* **25**: 33-40.

R Core Development Team. 2012. R: A language and environment for statistical computing. Vienna, Austria: Ro Foundation for Statistical Computing. ISBN 3-900051-0700. Aviailable at: http://www.R-project.org (Accessed 19 August 2012).

Sharkey TD, Bernacchi CJ, Farquhar GDD, Singsaas EL. 2007. Fitting photosynthetic carbon dioxide response curves for C_3 leaves. *Plant, Cell & Environment* **30**: 1035-1040.

Stringer JW, Kimmerer TW. 1993. Refixation of xylem sap CO_2 in *Populus deltoides*. *Physiologia Plantarum* **89**: 243-251.

Stutz SS, Anderson J, Zulick R, Hanson DT. 2017. Inside out: efflux of carbon dioxide from leaves represents more than leaf metabolism. *Journal of Experimental Botany* **68**: 2849-2857.

Tcherkez G, Mahe A, Gauthier P, Mauve C, Gout E, Bligny R, Cornic G, Hodges M. 2009. In folio respiratory fluxomics revealed by ^{13}C isotopic labeling and H/D isotope effects highlight the noncyclic nature of the tricarboxylic acid "cycle" in illuminated leaves. *Plant Physiology* **151**: 620-630.

Tcherkez G, Gauthier P, Buckley TN, Busch FA, Barbour MM, Bruhn D, Heskel MA, Gong XY, Crous K, Griffin KL, Way DA, Turbull MH, Adams MA, Atkin OK, Bender M, Farquhar GD, Cornic G. 2017a. Tracking the origins of the Kok effect, 70 years after its discovery. *New Phytologist* **214**: 506-510.

Tcherkez G, Gauthier P, Buckley TN, Busch FA, Barbour MM, Bruhn D, Heskel MA, Gong XY, Crous KY, Griffin K, Way D, Turnbull M, Adams MA, Atkin OK, Farquhar GD, Cornic G. 2017b. Leaf day respiration: low CO_2 flux but high significance for metabolism and carbon balance. *New Phytologist* **216**: 986-1001.

Teskey RO, McGuire MA. 2002. Carbon dioxide transport in xylem causes errors in estimation of rates of respiration in stems and branches of trees. *Plant, Cell & Environment* **25**: 1571-1577.

Teskey RO, Saveyn A, Steppe K, McGuire MA. 2008. Origin, fate and significance of CO_2 in tree stems. *New Phytologist* **177**: 17-32.

TABLES

Table 1 Definitions and units for symbols in the text.
All units are μmol CO_2 m^{-2} s^{-1}.

Symbol	Definition	Equations/notes
$^{12}A_{obs}$	Net $^{12}CO_2$ assimilations	Measured with the TDL
$^{13}A_{obs}$	Net $^{13}CO_2$ assimilations	Measured with the TDL
$^{13}A_{pred}$	Predicted atmospheric $^{13}CO_2$ assimilation	Equation 3
$^{13}C_{pred\ efflux}$	Predicted rate of xylem $^{13}CO_2$ efflux assuming no xylem transported CO_2 is used for photosynthesis	See Stutz *et al*. 2017
$^{13}C_{light\ efflux}$	Calculated $^{13}C_{efflux}$ in the light	Equation 2
$^{13}A_x$	Assimilation of xylem transported CO_2	Equation 1

FIGURES

Fig 1 Experimental set up showing the different fluxes of xylem-transported CO_2 (blue, red and purple arrows) with the competing process of leaf photosynthesis with atmospheric CO_2 (purple arrow) and the net loss of CO_2 from respiration in the light (red arrow). CO_2 from root and stem respiration dissolves in xylem water and moves through the plant along with the bulk flow of water. Some of this xylem-transported CO_2 is used for photosynthesis in the stem and branches while some of it reaches the leaves (blue). This CO_2 is either used for leaf photosynthesis (purple arrow) or exits the leaf with the transpiration stream (blue arrow).

Fig. 2 Light-response curves for rates of photosynthesis with $^{13}CO_2$ ($^{13}A_x$—photosynthesis using xylem-transported CO_2, or background rates of $^{13}A_{obs}$ in KCl treatment) and $^{12}CO_2$ ($^{12}A_{obs}$—photosynthesis using CO_2 derived from the atmosphere). $^{13}A_x$ in (a) *B. napus* and (b) *P. deltoides*, KCl (open circles), LC (light gray circles), MC (dark gray circles), and HC (closed circles), and $^{12}A_{obs}$ for (c) *B. napus* and (d) *P. deltoides*, KCl (open triangles), LC (light gray triangles), MC (dark gray triangles) and HC (closed triangles). Measurements represent means and ±1 SD of five replicates for each treatment. The low-carbon (LC) was 1.19 mmol l^{-1}, medium-carbon (MC) was 5.95 mmol l^{-1}, and high-carbon (HC) was 11.9 mmol l^{-1}.

Fig. 3 CO_2-response curves for rates of photosynthesis with $^{13}CO_2$ ($^{13}A_x$—photosynthesis using xylem-transported CO_2 or background rates of $^{13}A_{obs}$ in KCl treatment) and $^{12}CO_2$ ($^{12}A_{obs}$—photosynthesis using CO_2 derived from the atmosphere). Rates of xylem-transported photosynthesis in (a) *B. napus* and (b) *P. deltoides*, KCl (open circles), LC (light gray circles), MC (dark gray), and HC (closed circles), and rates of $^{12}A_{obs}$ for (c) *B. napus* and (d) *P. deltoides*,

KCl (open triangles), LC (light gray triangles), MC (dark gray triangles) and HC (closed triangles). Measurements represent means and ±1 SD of five replicates for each treatment. The low-carbon (LC) was 1.19 mmol l^{-1}, medium-carbon (MC) was 5.95 mmol l^{-1} and high-carbon (HC) was 11.9 mmol l^{-1}. In the KCl treatment rates of $^{13}A_{obs}$ were measured in place of rates of $^{13}A_x$.

Fig. 4 Light-response curve for rates of xylem-transported CO_2 assimilation ($^{13}A_x$) (circles) and the efflux of $^{13}CO_2$ exiting the leaf in the light ($^{13}C_{light\ efflux}$) (upside down triangles) measured under (a, b) LC (light gray), (c, d) MC (dark gray) and (e, f) HC (closed). Measurements represent means and ±1 SD of five replicates for each treatment. The low-carbon (LC) was 1.19 mmol l^{-1}, medium-carbon (MC) was 5.95 mmol l^{-1} and high-carbon (HC) was 11.9 mmol l^{-1}.

Fig. 5 CO_2-response curve for rates of xylem-transported CO_2 assimilation ($^{13}A_x$) (circles) and the efflux of $^{13}CO_2$ exiting the leaf in the light ($^{13}C_{light\ efflux}$) (upside down triangles) measured under (a, b) LC (light gray), (c, d) MC (dark gray), and (e, f) HC (closed). Measurements represent means and ±1 SD of five replicates for each treatment. The low-carbon (LC) was 1.19 mmol l^{-1}, medium-carbon (MC) was 5.95 mmol l^{-1} and high-carbon (HC) was 11.9 mmol l^{-1}.

Fig. 6 Light-response curves for percentage of xylem-transported CO_2 assimilation ($^{13}A_x$) to total rates of photosynthesis under LC (gray hexagons), MC (closed hexagons) and HC (open hexagons) for (a) *B. napus* and (b) *P. deltoides*. Light-response curves for the efflux of $^{13}CO_2$ exiting the leaf in the light ($^{13}C_{light\ efflux}$) under LC (gray diamonds), MC (closed diamonds) and HC (open diamonds) for (c) *B. napus* and (d) *P. deltoides*. In plots c and d the black line

represents the average respiration in the dark (R_d) across all treatments for each species, 2.07 µmol CO_2 m^{-2} s^{-1} and 1.56 µmol CO_2 m^{-2} s^{-1} for *B. napus* and *P. deltoides*, respectively. While the dotted lines represent ½*R_d averaged across all treatments for each species, 1.04 µmol CO_2 m^{-2} s^{-1} and 0.78 µmol CO_2 m^{-2} s^{-1}, for *B. napus* and *P. deltoides*, respectively. Measurements represent means and ±1 SD of five replicates for each treatment. The low-carbon (LC) was 1.19 mmol l^{-1}, medium-carbon (MC) was 5.95 mmol l^{-1} and high-carbon (HC) was 11.9 mmol l^{-1}.

Fig. 7 CO_2-response curves for percentage of xylem-transported CO_2 assimilation ($^{13}A_x$) to total rates of photosynthesis under LC (light gray hexagons), MC (dark gray hexagons) and HC (closed hexagons) for (a) *B. napus* and (b) *P. deltoides*. Light-response curves for the efflux of $^{13}CO_2$ exiting the leaf in the light ($^{13}C_{light\ efflux}$) under LC (light gray diamonds), MC (dark gray diamonds), HC (closed diamonds) for (c) *B. napus* and (d) *P. deltoides*. In plots c and d the black line represents the average respiration in the dark (R_d) across all treatments for each species, 2.08 µmol CO_2 m^{-2} s^{-1} and 1.86 µmol CO_2 m^{-2} s^{-1} for *B. napus* and *P. deltoides*, respectively. While the dotted lines represent ½*R_d averaged across all treatments for each species, 1.04 µmol CO_2 m^{-2} s^{-1} and 0.93 µmol CO_2 m^{-2} s^{-1}, for *B. napus* and *P. deltoides*, respectively. Measurements represent means and ±1 SD of five replicates for each treatment. The low-carbon (LC) was 1.19 mmol l^{-1}, medium-carbon (MC) was 5.95 mmol l^{-1} and high-carbon (HC) was 11.9 mmol l^{-1}.

FIGURE 1

FIGURE 2

FIGURE 3

FIGURE 4

FIGURE 5

FIGURE 6

71

FIGURE 7

Chapter 4

What is the fate of xylem-transported CO_2 in Kranz-type C_4 plants?

Samantha S. Stutz[1]

[1]University of New Mexico, Department of Biology, MSC03-2020, Albuquerque,

NM 87131, USA

SUMMARY

- Concentrations of dissolved inorganic carbon are high in stems of trees and herbaceous C_3 plants; this inorganic carbon can exit the plant in the dark, contributing errors to measurements of leaf respiration. However, it is unknown if xylem-transported CO_2 will also affect plants with Kranz anatomy. C_3 species use a small portion of xylem-transported CO_2 for leaf photosynthesis; however, Kranz-type C_4 species may use more xylem-transported CO_2 for photosynthesis due to the tight junctions around the vascular bundles.

- In the dark cut leaves of *Amaranthus hypochondriacus* were placed in one of three solutions of $[NaH^{13}CO_3]$ dissolved in water while simultaneously measuring the efflux of xylem-transported CO_2 exiting the leaf in the dark in real-time using a tunable diode laser absorption spectroscope. The same method was used in the light to determine how much xylem-transported CO_2 was used for photosynthesis across light- or CO_2-response curves.

- In the dark the efflux of xylem-transported CO_2 increased with increasing rates of transpiration and $[^{13}CO_2^*]$; however, rates of $^{13}C_{efflux}$ in *A. hypochondriacus* were lower compared to C_3 species. Rates of xylem-transported CO_2 assimilation were higher in *A. hypochondriacus* compared to the C_3 species.

- Kranz anatomy likely influences the efflux of xylem-transported CO_2 out of cut leaves of *A. hypochondriacus* in the dark and likely rates of assimilation using xylem-transported CO_2 are high in the light. This may increase the carbon use efficacy of Kranz-type C_4 species over C_3 species.

74

INTRODUCTION

In Kranz-type C_4 species vascular bundles in the leaves are surrounded by bundle-sheath cells, which in turn are surrounded by mesophyll cells (Sage, 2004). Kranz anatomy allows C_4 species to compartmentalize and concentrate CO_2 around ribulose-1,5-bisphosphate-carboxylase/oxygenase (Rubisco), in the bundle-sheath cells, while isolating phosphoenolpyruvate carboxylase (PEPC), to the mesophyll cells (Hatch, 1987). CO_2 is moved from the mesophyll cells into the bundle-sheath cells as C_4 acids (Hatch *et al*., 1967). This biochemical pump reduces rates of photorespiration while increasing rates of photosynthesis (Hatch, 1987; von Caemmerer & Furbank, 1999) but at the energetic cost of regenerating phosphoenolpyruvate (PEP) (Hatch, 1987; Kanai & Edwards, 1999; Ubierna *et al*., 2011). In order for Kranz-type C_4 plants to reduce the energetic cost of regenerating PEP they must have high bundle-sheath resistance to CO_2 diffusion, or low leakiness (ϕ). Leakiness is the proportion of carbon fixed by PEPC that subsequently diffuses out of the bundle-sheath cells instead of being fixed by Rubisco (Farquhar, 1983; Hatch *et al*., 1995). The traditional understanding of photosynthesis in Kranz-type C_4 species is that CO_2 diffuses through the stomata into the substomatal cavity of the leaf where it will then diffuse into the mesophyll cells to be carboxylated into C_4 acids by PEPC before being shuttled into and decarboxylated in the bundle-sheath cells (Hatch *et al*., 1967). However, studies in C_3 species show that CO_2 can be transported in the xylem and used for photosynthesis by stems (Teskey *et al*., 2008, Bloemen *et al*., 2013a), branches (McGuire *et al*., 2009; Bloemen *et al*., 2013a, b), and leaves (Stringer & Kimmerer, 1993; McGuire *et al*., 2009; Bloemen *et al*., 2013a, b; Bloemen *et al*., 2015, Stutz, Chapter 3).

Concentrations of dissolved inorganic carbon ($[CO_2^*]$, the sum of $[CO_2]_{aq}$, $[H_2CO_3]$, $[HCO_3^-]$ and $[CO_3^{2-}]$) in the stems of trees can be between ~0.05 mmol l^{-1} and ~13 mmol l^{-1} (Teskey *et al*., 2008). This inorganic carbon is generated from cellular respiration and dissolves in the xylem and moves in bulk flow along with water through the plant to the leaf where it is either used for photosynthesis (Stringer & Kimmerer, 1993; Teskey & McGuire, 2002; Teskey *et al*., 2008; Bloemen *et al*., 2013a, b; Bloemen *et al*., 2015) or exits via transpiration (Stringer & Kimmerer, 1993; Bloemen *et al*., 2013a; Stutz *et al*., 2017). However, it is not just trees that have high $[CO_2]$ in stems, Stutz *et al*. (2017) found $[CO_2]$ in bolted stems of *Brassica napus* were 0.7 mmol l^{-1}, indicating that xylem-transported CO_2 is also concentrated in stems of herbaceous plants.

In *Populus deltoides* the efflux of xylem-transported CO_2 out of branches and stems of labeled saplings ranges from 82.6% in a low-label treatment (1.4 mmol l^{-1} [$^{13}CO_2^*$]) to 94.4% in a high-label treatment (12 mmol l^{-1} [$^{13}CO_2^*$]) (Bloemen *et al*., 2013a) while Stringer & Kimmerer (1993) found that 83% of the labeled $H^{14}CO_3^-$ diffused out of cut *P. deltoides* leaves in the dark. Stutz *et al*. (2017) found in cut leaves of *P. deltoides* across three [$^{13}CO_2^*$] that ~80% of the added xylem-transported CO_2 exited the leaf as $^{13}CO_2$. However, the amount of xylem-transported CO_2 that exited cut leaves of the herbaceous C_3 plant *B. napus* were only between 50% and 75% across the range of [$^{13}CO_2^*$]. As expected, the consumption of xylem-transported CO_2 in the dark was about two times higher in *B. napus* compared to *P. deltoides* (Stutz *et al*., 2017). However, in C_4 species: 1) higher concentrations of PEPC may lead to higher consumption of xylem-transported CO_2, in particular bicarbonate, 2) Kranz anatomy may hinder the amount of xylem-transported CO_2 exiting the leaf in the dark compared to C_3 species

and 3) any xylem-transported CO_2 exiting the leaf in the light could cause an overestimation of leakiness.

In C_3 plants, rates and utilization of xylem-transported CO_2 were mostly low compared to the amount of xylem-transported CO_2 available for photosynthesis in the light. Bloemen *et al*. (2013a) found only 17.4% and 5.6% of a low- and high-label $^{13}CO_2$ were assimilated by plant tissues over the course of 48 hours; the highest concentrations of the label were found in the branch and stem tissues while only a small portion was found in the leaf tissues from both treatments. When rates of xylem-transported CO_2 assimilation are studied on the scale of an individual leaf most of the label is found in the petiole and the tissues most proximal to the label with a small portion found in minor veins and mesophyll cells (Stringer & Kimmerer, 1993; Bloemen *et al*., 2015). When intercellular [CO_2] was low (*i.e.* high irradiance or low [CO_2]), rates of assimilation using xylem-transported CO_2 were highest in cut leaves of *B. napus* and *P. deltoides*; however, when the total rate of assimilation was lowest (*i.e.* low irradiance or low [CO_2]) the percentage of xylem-transported CO_2 to total assimilation was highest (Stutz, chapter 3).

Previous studies have focused on how trees utilize xylem-transported CO_2 while ignoring C_4 species. Therefore, the objectives of this study were to estimate: 1) the rate and total efflux of xylem-transported CO_2 exiting a cut leaf of the Kranz-type C_4 species, *Amaranthus hypochondriacus*, in the dark and 2) the rate and contribution of xylem-transported CO_2 to total assimilation in the light for *A. hypochondriacus*. These goals were accomplished using a LI-6400 with a custom leaf chamber coupled to a tunable diode laser absorption spectroscope (TDL) to measure how much xylem-transported CO_2 entered a cut leaf and exited the leaf in the dark or was used for photosynthesis in the light using light- and CO_2-response curves (Stutz *et al*., 2017;

Stutz, chapter 3). We hypothesized that Kranz-type anatomy found in *A. hypochondriacus* would prohibit much of the xylem-transported CO_2 from exiting cut leaves in the dark; in the light we hypothesized that the rate of xylem-transported CO_2 assimilation would be higher in *A. hypochondriacus* compared to the rate of xylem-transported CO_2 assimilation in *B. napus*.

MATERIALS & METHODS

Plant propagation and growth

Amaranthus hypochondriacus (L.) was grown under SPYDR 1200 GROW-MAX LED lights (Fluence Bioengineering, Austin, TX, USA) with 500 μmol quanta m^{-2} s^{-1} and a day/night cycle of 12 hours, in a greenhouse at the University of New Mexico in Albuquerque, NM in ambient CO_2. The greenhouse temperature varied between 20ºC-23.9ºC across a day. *A. hypochondriacus* was started from seed. The seeds were sowed in 500 mL pots with Metro-Mix 300 potting soil (Sun Gro Horticulture, Seba Beach, AB, Canada). Once the seedlings were larger they were transferred to 3.7 L pots filled with Metro-Mix 300 potting soil approximately 30 days after germination. Plants were fertilized twice weekly with Peter 20-20-20 fertilizer (Scotss Miracle-Gro, Marysville, OH, USA) and once weekly with chelated liquid iron (ferti-lome, Bonham, TX, USA). Plants were measured between 50 and 80 days after geminating.

Brassica napus (L. stellar DH GT060615) was propagated according to Stutz *et al*. (2017). *B. napus* was grown under natural light in an unshaded greenhouse, with mid-day photosynthetically active radiation (PAR) at pot level of 1200 μmol m^{-2} s^{-1} at the University of New Mexico in Albuquerque, NM, USA, under ambient CO_2, 24ºC/21ºC day/night.

Dark efflux measurements

A LI-6400 (LI-COR Biosciences, Lincoln, NE, USA) was coupled to a tunable diode laser absorption spectroscope (TDL—model TGA 100; Campbell Scientific, Inc., Logan, UT, USA) to measure online $^{12}CO_2$ and $^{13}CO_2$ exchange. Isotope calibration consisted of a high and low CO_2 tank that spanned the expected range of $[CO_2]$ of each isotopologue for the LI-COR reference and sample (Barbour *et al.,* 2007; Stutz *et al*., 2017). The TDL cycled among calibrations of the high and low CO_2 tank along with the LI-COR reference and sample line measuring for one minute at each site. However, only the last 10 seconds of data were used for calculations via the TDL LI-COR processing package (Erhardt & Hanson, 2013) in R (R Core Development Team, 2011). The TDL measures $[^{12}CO_2]$ and $[^{13}CO_2]$, so the net fluxes of each were calculated as in normal gas exchange where total $[CO_2]$ is measured in the air supplied to the leaf chamber and within the well-mixed leaf chamber.

The highest fully expanded leaf was placed in a large (80 cm^2) clear toped, custom leaf chamber with an RGB LED light source (LI-COR Biosciences) attached to a LI-6400 at 25ºC (leaf temperature) and 380 µmol mol^{-1} CO_2 reference with the RGB light source set at 1600 µmol quanta m^{-2} s^{-1}. The leaves were photographed, and projected leaf area was estimated using ImageJ (US National Institutes of Health, Bethesda, MD, USA). The leaves fit width-wise in the chamber but extended ~4-7 cm beyond the edge of the chamber. The petiole length was between 5 and 10 cm.

Once photosynthesis reached a steady state, the leaf was cut under water and the petiole was placed in a 40 mmol l^{-1} KCl solution. Stomatal conductance and photosynthesis decreased when the leaf was cut. The leaf remained in the KCl solution for ~30 minutes till the rate of photosynthesis reached the rate before the leaf was cut. The KCl solution was swapped for 99%

[13]C sodium bicarbonate dissolved in 40 mmol l^{-1} KCl at one of three [$^{13}CO_2^*$]: 1.19 (low-carbon—LC), 5.95 (medium-carbon—MC), or 11.9 mmol l^{-1} (high-carbon—HC). Individual leaves were only provided a single [$^{13}CO_2^*$] (see Stutz et al., 2017). These concentrations span the range of observed values for tree xylem inorganic carbon concentration ($CO_2 + HCO_3^-$). In the HC and MC treatments approximately 8 minutes after adding the $^{13}CO_2^*$ a small increase in $^{13}CO_2$ efflux was observed with the TDL and the light on the LI-6400 was turned off. There was no increase in $^{13}CO_2$ efflux under the LC treatment so the light was turned off after approximately 10-15 minutes. Throughout the measurement period, the rate of transpiration was manipulated by switching the LI-COR desiccant between full scrub (i.e., high VPD and higher rates of transpiration) and full bypass (i.e., low VPD and lower rates of transpiration). To further increase the relative humidity when the desiccant was on full bypass, a condensing tube in a water bath (VWR Scientific products, West Chester, PA, USA) was attached to the LI-COR inlet to decrease VPD to 0.5 kPa or less. The desiccant was left on full scrub or full bypass for approximately one hour. The measurement cycle consisted of approximately 3-4 alternating dry and wet periods. This procedure was used to gain the widest range of transpiration values possible in the dark for comparisons of transpiration and $^{13}CO_2$ efflux. Each treatment consists of five replicates.

Estimating the consumption rate of xylem-transported CO_2 in the dark

The rate of consumption of xylem-transported CO_2 was calculated according to Stutz et al. (2017) by multiplying the rate of ^{12}C leaf respiration ($^{12}C_{RL}$) by 1.1%, the natural abundance of $^{13}CO_2$ in the atmosphere compared to $^{12}CO_2$ in the atmosphere (Girffis et al., 2004). We calculated an expected ^{13}C efflux ($^{13}C_{cal\ efflux}$) that would occur if all the $^{13}CO_2$ added to the cut

leaf exited the leaf as $^{13}CO_2$. This was accomplished by multiplying the $[^{13}CO_2{}^*]$ in the solution fed to the leaves by the rate of transpiration and adding it to the background $^{13}C_{RL}$. We used the ratio of observed $^{13}CO_2$ efflux ($^{13}C_{efflux}$) to $^{13}C_{cal\ efflux}$ to determine the fraction of supplied $^{13}CO_2$ exiting the leaf and expressed it as a percentage. We estimated the rate of consumption of xylem-transported CO_2 by taking the difference between the $^{13}C_{cal\ efflux}$ and observed $^{13}C_{efflux}$. For these calculations we assumed the transpiration rate along with the rate of ^{12}C and ^{13}C effluxes were constant across one TDL/LI-COR cycle i.e. 4 minutes. We excluded the first 45 minutes after the light was turned off for these calculations to see that enzymes were deactivated in the C_3 species, *Brassica napus* but not fully deactivated in the C_4 species *A. hypochondriacus* and to allow the water in the leaf to be replaced with the water supplied to the petiole. Data from *B. napus* were modified from Stutz *et al.* (2017).

Light-response curves

The highest fully expanded leaf was placed in a clear toped, 38.5 cm^2, circular custom leaf chamber made to fit an RGB LED light source (LI-COR Biosciences, Lincoln, NE, USA) attached to a LI-6400 at 23°C (leaf temperature), 380 µmol mol^{-1} CO_2 reference at 1600 µmol quanta $m^{-2}s^{-1}$. Leaves were left in the chamber for approximately 60 minutes before being cut and placed in a 40 mmol l^{-1} KCl solution. The leaf remained in the KCl solution for ~30 minutes till the rate of photosynthesis reached the rate before the leaf was cut. As with the dark efflux measurements the KCl solution was swapped for 99% ^{13}C sodium bicarbonate dissolved in 40 mmol l^{-1} KCl at one of three $[^{13}CO_2{}^*]$: LC, MC, or HC. As with the dark efflux measurements, an individual leaf was only provided a single $[^{13}CO_2{}^*]$. There was an additional treatment where the cut leaves remained in the KCl solution instead of being transferred to a $[^{13}CO_2{}^*]$ solution.

The light response curves were measured in the following order: 1600, 1300, 1000, 800, 500, 250, 200, 175, 150, 125, 100, 75, 50, 35, 0 μmol quanta m^{-2} s^{-1}. Five measurements were made at each irradiance except for the highest irradiance where we waited for the $^{13}CO_2$ efflux to level out and only took the last five measurements for the averages. Five replicate leaves were measured for each [$^{13}CO_2^*$] and KCl solutions. The measurements for *B. napus* are described in Stutz (Chapter 3).

CO$_2$-response curves

For the CO$_2$-response curves, an attached leaf was placed in the same LI-6400 custom leaf chamber as was used for the light-response curves at 23ºC (leaf temperature) at 1600 μmol quanta m^{-2}s^{-1}. The CO$_2$ reference on the LI-6400 was set so the [CO$_2$] at the leaf level was approximately 400 μmol mol^{-1}, which was between 500 and 650 μmol mol^{-1} CO$_2$ reference [CO$_2$]. As with the light-response curves, leaves were left in the chamber for approximately 60 minutes before being cut and placed in a 40 mmol l^{-1} KCl solution for ~30 minutes. The KCl solution was swapped for 99% ^{13}C sodium bicarbonate (NaH^{13}CO$_3$) dissolved in 40 mmol l^{-1} KCl at one of three [$^{13}CO_2^*$]: LC, MC, HC or remaining in the KCl solution for the measurement. As with the light-response curves the individual leaves were only provided a single [$^{13}CO_2^*$] or left in the 40 mmol l^{-1} KCl solution according to Stutz *et al*. (2017). As with the light-response curves, the leaf was left at the starting [CO$_2$] till the δ^{13}C and [$^{13}CO_2$] reading on the TDL stabilized approximately 20 to 30 minutes for each leaf. The [CO$_2$] on the LI-6400 reference were applied to the leaf in the following order: starting [CO$_2$], 200, 100, 50, 150, 300, starting [CO$_2$], 1000, 2000, 1500, 700 and starting [CO$_2$]. The leaf was left at each [CO$_2$] for three cycles on the TDL except for the starting [CO$_2$] where the leaf was left until it reached the

starting rate of photosynthesis. Following the CO_2-response curve the light was turned off and

respiration was measured when the leaf had been in the dark for at least 30 minutes, to avoid

light enhanced dark respiration (LEDR). Fives leaves from each species were measured for each

[$^{13}CO_2^*$] and the KCl solution. The measurements for *B. napus* are described in Stutz (Chapter

3).

Estimating the amount of xylem-transported CO_2 entering the cut leaves and rate of

consumption of xylem-transported CO_2 in the light

The rate of xylem-transported CO_2 consumption in the light in the Kranz-type C_4 species,

A. hypochondriacus was calculated as:

$$Consumption\ in\ the\ light = Rate\ of\ ^{13}CO_2\ entering\ leaf - ^{13}C_{pred\ light\ efflux}$$ (Equation

1)

where, the rate of $^{13}CO_2$ entering the leaf is estimated based on the rate of transpiration

and the [$^{13}CO_2^*$] added to the cut leaf and where $^{13}C_{pred\ light\ efflux}$ is the predicted rate of xylem

transported CO_2 exiting the leaf in the absence of assimilation and is estimated from linear

regression models of xylem CO_2 effluxes in the dark across the three different [$^{13}CO_2^*$] from the

first part of this study.

Statistical analyses

Analysis of covariance (ANCOVA) was used to compare slopes among [$^{13}CO_2^*$]

treatments in *A. hypochondriacus*, followed by Tukey post-hoc multiple comparisons of means

to determine which slopes were significantly different among the three treatments. The

percentage of xylem-transported CO_2 exiting the leaf and the rate of consumption of xylem-

transported CO_2 were compared between species, *B. napus* and *A. hypochondriacus* and among treatments (LC, MC and HC) using a two-way analysis of variance (ANOVA) followed by Tukey HSD post-hoc comparisons.

Linear mixed effects models were produced for the following variables: $^{12}A_{obs}$, consumption in the light, and photosynthetic discrimination ($\Delta^{13}C$) for both the light- and CO_2-response curves. The fixed effects were *A. hypochondriacus* and [$^{13}CO_2^*$] while the random effects were irradiance and [CO_2], for the light- and CO_2-response curves, respectively. The amount of xylem-transported CO_2 entering the leaf and consumption in the light were compared to the C_3 species, *B. napus*, the fixed effects were species and [$^{13}CO_2^*$] while the random effects were irradiance and [CO_2], for the light- and CO_2-response curves respectively. Results were deemed significant at *P<0.05*. All statistical analyses were performed in R (version 3.4.2, R Development Core Team 2012).

RESULTS

Retention and magnitude of xylem-transported CO_2 in the dark

In the Kranz-type C_4 species, *Amaranthus hypochondriacus*, rates of xylem-transported CO_2 dark efflux ($^{13}C_{efflux}$) increased with increasing rates of transpiration and [$^{13}CO_2^*$] (Fig. 1b). There were significant differences between the low-carbon (LC) and high-carbon (HC) treatments ($P<0.001$), however, there were no significant differences between the medium-carbon (MC) and HC treatments ($P=0.34$), or between the LC and MC treatments ($P=0.097$). The rate of leaf respiration ($^{12}C_{RL}$) increased slightly with increasing rates of transpiration (Fig. 1a), but was not significantly different across the range of transpiration ($P=0.05$). When rates of $^{13}C_{efflux}$ were compared to the herbaceous C_3 species, *Brassica napus* following the light being

off for forty-five minutes rates of transpiration were similar between the two species but the rates of $^{13}C_{efflux}$ were considerably lower in *A. hypochondriacus* compared to *B. napus* (Fig. 1c), in the HC treatment.

When the $^{12}C_{RL}$ and $^{13}C_{efflux}$ rate were compared at a single rate of transpiration, 0.75 mmol H_2O m^{-2} s^{-1}, the rate of $^{12}C_{RL}$ was ~1.4 μmol CO_2 m^{-2} s^{-1} across all [$^{13}CO_2^*$] (Fig. 2b) and were not significantly different among [$^{13}CO_2^*$] (P=0.89). However, the rate of $^{13}C_{efflux}$ increased from ~0.015 μmol CO_2 m^{-2} s^{-1} in the LC treatment to ~0.04 μmol CO_2 m^{-2} s^{-1} in the MC and HC treatments (Fig. 2a) there were no significant differences among rates of $^{13}C_{efflux}$ across [$^{13}CO_2^*$] (P=0.08).

Xylem-transported CO$_2$ that exited the leaf in the dark

The calculated amount of [$^{13}CO_2^*$] that entered the darkened leaf and subsequently exited the leaf as CO_2 in the dark was calculated following the first 90 minutes after turning off the light across all [$^{13}CO_2^*$] in the dark for both *B. napus* and *A. hypochondriacus*. The percentage of xylem-transported CO_2 exiting the leaf in the dark increased with increasing [$^{13}CO_2^*$], in both species (P<0.001) and was significantly different among [$^{13}CO_2^*$] (P<0.001). In the LC treatment there was a significant difference in the percentage of xylem-transported CO_2 that exited cut *A. hypochondriacus* (~4%) compared to cut *B. napus* leaves (~8%) (P<0.001) (Fig. 3a, b). There was also a significant difference in the percentage of xylem-transported CO_2 that exited the leaves in the MC treatment ~20% and ~21% in *A. hypochondriacus* and *B. napus*, respectively (P<0.001). In *A. hypochondriacus* the percentage of xylem-transported CO_2 exiting the leaf was similar between the MC (~20%) and HC (~23%) but was significantly different

between the treatments ($P<0.001$) (Fig. 3a); however, the percentage of xylem-transported CO_2 that exited the leaf in *B. napus* increased 43% going from the MC to HC treatment ($P<0.001$)..

The rate of consumption of xylem-transported CO_2 was ~5 times higher in *A. hypochondriacus* compared to *B. napus* across all [$^{13}CO_2^*$] and was significantly different between species ($P<0.001$) and among [$^{13}CO_2^*$] ($P<0.001$) (Fig. 3c, d). In *A. hypochondriacus* the estimated retention rate of xylem-transported CO_2 was ~0.25 μmol CO_2 m^{-2} s^{-1} in the LC and MC treatments and was ~0.20 μmol CO_2 m^{-2} s^{-1} in the HC treatment (Fig. 3c). The rate of xylem-transported retention was significantly different among all [$^{13}CO_2^*$] ($P<0.01$). In *B. napus* the rate of consumption of xylem-transported CO_2 was ~0.02 μmol CO_2 m^{-2} s^{-1} in the LC treatment and significantly different from the other [$^{13}CO_2^*$] treatments ($P<0.001$), but the rates in the MC and HC treatments were similar ~0.06 μmol CO_2 m^{-2} s^{-1} and not significantly different ($P=0.99$) (Fig. 3d).

Did xylem-transported CO_2 reach the leaf in the light?

As expected, photosynthetic discrimination ($\Delta^{13}C$), in the KCl and LC treatments was ~4‰ under high irradiance and increased with decreasing irradiance to ~8‰ in the KCl treatment and ~5‰ in the LC treatment (Fig. 4a). Before placing the cut leaf in the MC or HC treatments $\Delta^{13}C_{obs}$ was ~4‰ (data not shown) but after placing the leaf in the [$^{13}CO_2^*$] solution $\Delta^{13}C_{obs}$ was ~49‰ and ~141‰ (Fig. 4c) under high irradiance in the MC and HC treatments, respectively. As in the KCl and LC treatments, $\Delta^{13}C_{obs}$ increased with decreasing irradiance to ~107‰ and ~420‰ (Fig. 4c) at the lowest irradiance in the MC and HC treatments, respectively. Based on $\Delta^{13}C_{obs}$ in the MC and HC treatments xylem-transported CO_2 exited the leaf as $^{13}CO_2$.

However, there were no significant differences among treatments across irradiance ($P=0.66$) or among [$^{13}CO_2^*$] ($P=0.96$).

In the CO_2-response curves, $\Delta^{13}C$ in the KCl and LC treatments were ~4‰ under high [CO_2]; and increased to ~13‰ under the lowest [CO_2] (Fig. 4b). There were no significant differences between the LC and KCl treatments across any intercellular [CO_2] in the CO_2-response curves. Photosynthetic discrimination in the MC and HC treatments was ~4‰ before cutting the leaf (data not shown) but increased to ~90‰ in the MC and ~450‰ in the HC treatment (Fig. 4d). The HC treatment was significantly different from the KCl, LC and MC treatments ($P<0.001$) when intercellular [CO_2] was less than 200 μmol mol^{-1}. The MC and LC treatments were only significantly different under the lowest intercellular [CO_2] ($P<0.05$).

How much xylem-transported CO_2 entered the leaf?

By knowing the rate of transpiration, and the concentration of [$^{13}CO_2^*$] added to a cut leaf we were able to calculate how much xylem-transported CO_2 entered the leaf in both the herbaceous C_3 species, *B. napus*, and the C_4 *A. hypochondriacus*. Rates of xylem-transported CO_2 entering the leaf increased with increasing transpiration and increasing [$^{13}CO_2^*$] for both species (Fig. 5). In the light-response curves the highest rates of xylem-transported CO_2 entering the leaf occurred when irradiance and stomatal conductance were high, this also coincided with higher rates of carbon fixation in the light ($^{13}A_x$) (Fig. 6a, b). The highest rate of $^{13}CO_2$ entering the leaf in *A. hypochondriacus* were ~0.07 μmol CO_2 m^{-2} s^{-1}, ~0.42 μmol CO_2 m^{-2} s^{-1}, and ~0.68 μmol CO_2 m^{-2} s^{-1} in the LC, MC and HC treatments, respectively (Fig. 5a). Rates of xylem-transported CO_2 entering the leaf was significantly different among treatments when irradiance was greater than 500 μmol quanta m^{-2} s^{-1} ($P<0.001$). In *B. napus* the highest rates of $^{13}CO_2$

entering the leaf were ~0.09 μmol CO_2 m^{-2} s^{-1}, ~0.52 μmol CO_2 m^{-2} s^{-1} and ~0.84 μmol CO_2 m^{-2} s^{-1} (Fig. 5c). The amount of xylem-transported CO_2 entering the leaf was significantly different between LC and HC treatments above the light compensation point (75 μmol quanta m^{-2} s^{-1}); when irradiance was above 800 μmol quanta m^{-2} s^{-1} there were significant differences among all [$^{13}CO_2^*$]. In *A. hypochondriacus* the highest rate of transpiration was ~3.5 mmol H_2O m^{-2} s^{-1} across all [$^{13}CO_2^*$]; however in *B. napus* the highest rate of transpiration was ~4.5 mmol H_2O m^{-2} s^{-1} allowing more xylem-transported CO_2 to enter the cut leaves of *B. napus* compared to *A. hypochondriacus*. The amount of xylem-transported CO_2 entering the cut leaves was significantly different between the species in the MC and HC treatments across all irradiances above the light compensation point (*P*<0.001); however, the LC treatment was not significantly different between species across any irradiance.

In the CO_2-response curves, for both species, rates of $^{13}CO_2$ entering the leaf were highest when the rate of transpiration and stomatal conductance were highest (Fig. 5b, d). Rates of $^{13}CO_2$ entering the leaf for *A. hypochondriacus* were ~0.08 μmol CO_2 m^{-2} s^{-1}, ~0.40 μmol CO_2 m^{-2} s^{-1}, and ~0.58 μmol CO_2 m^{-2} s^{-1}, in the LC, MC and HC treatments, respectively. The amount of $^{13}CO_2$ entering the leaf was significantly different in the LC treatment compared to the MC and HC treatments across all intercellular [CO_2] (*P*<0.05). The MC and HC treatments were significantly different when the [CO_2] was sub-saturating (*P*<0.001); however, these treatments were not significantly different when [CO_2] was saturating. Rates of $^{13}CO_2$ entering the leaf in *B. napus* were ~0.06 μmol CO_2 m^{-2} s^{-1}, ~0.31 μmol CO_2 m^{-2} s^{-1}, and ~0.71 μmol CO_2 m^{-2} s^{-1} in the LC, MC and HC treatments, respectively (Fig. 5d). The amount of xylem-transported CO_2 entering the leaf in the LC treatment was significantly different from the MC and HC treatments across all [CO_2] (*P*<0.001). The amount of xylem-transported CO_2 entering the leaf was

significantly different in the HC treatment between the species ($P<0.01$) but not significantly different between the species in the LC treatment across any $[^{13}CO_2^*]$.

Rates of $^{12}A_{obs}$

Rates of assimilation using the ^{12}C isotope ($^{12}A_{obs}$) increased with increasing irradiance across the KCl, LC, MC and HC treatments, the saturating rate of assimilation was ~22 µmol CO_2 m^{-2} s^{-1} which occurred at an irradiance of 1600 µmol quanta m^{-2} s^{-1} (Fig. 6c). There were no significant differences among rates of $^{12}A_{obs}$ across the light-response curve in the four treatments ($P=0.84$). As expected, in the CO_2-response curves, rates of $^{12}A_{obs}$ increased with increasing rates of intercellular $[CO_2]$ and saturated at an intercellular $[CO_2]$ of ~200 µmol CO_2 mol^{-1} at a rate of ~30 µmol CO_2 m^{-2} s^{-1} (Fig. 6d), there were no significant differences in $^{12}A_{obs}$ among the four treatments ($P=0.66$).

Rates of carbon fixation in the light

Rates of carbon fixation in the light increased with increasing irradiance and $[^{13}CO_2^*]$ (Fig. 6a). Rates of carbon fixation were 0.05 µmol CO_2 m^{-2} s^{-1}, 0.24 µmol CO_2 m^{-2} s^{-1}, and 0.47 µmol CO_2 m^{-2} s^{-1} in the LC, MC, and HC treatment, respectively (Fig. 6a). The rate of photosynthesis of $^{13}CO_2$ in the KCl treatment was and 0.30 µmol CO_2 m^{-2} s^{-1} (Fig. 6a). Rates of carbon fixation were significantly different between the LC and HC treatments across all irradiances ($P<0.001$) and all treatments were significantly different when irradiance was greater than 800 µmol quanta m^{-2} s^{-1} ($P<0.001$). The rate of $^{13}A_{obs}$ in the KCl treatment are 1.1% the rate of $^{12}A_{obs}$, the rate that would be expected based on the background $[^{13}CO_2]$ in the atmosphere (Griffiths *et al*., 2004).

In the CO_2-response curves, rates of $^{13}A_{obs}$ increased with increasing intercellular $[CO_2]$ in the KCl treatment saturating at a rate of ~0.35 μmol CO_2 m^{-2} s^{-1} (Fig. 6b), again this rate was ~1.1% the rate of $^{12}A_{obs}$. Rates of carbon fixation in the light increased with increasing $[^{13}CO_2^*]$ and were highest when intercellular $[CO_2]$ was low but decreased with increasing intercellular $[CO_2]$ (Fig. 6b). The highest rates of non-Rubisco activity in the light were ~0.06 μmol CO_2 m^{-2} s^{-1}, ~0.23 μmol CO_2 m^{-2} s^{-1}, and ~0.4 μmol CO_2 m^{-2} s^{-1} in the LC, MC and HC treatments, respectively. The decrease in non-Rubisco activity occurred when intercellular $[CO_2]$ was 200 μmol mol^{-1}, which was near the CO_2 saturation point for $^{12}A_{obs}$ (Fig. 6b). There were significant differences in rates of carbon fixation in the light across $[CO_2]$ ($P<0.05$) and among $[^{13}CO_2^*]$ ($P<0.001$). The rates of carbon fixation in the light were significantly different between the LC and MC treatments ($P<0.01$) across all $[CO_2]$.

DISCUSSION

Efflux of xylem-transported CO_2 in the dark

Our method, of placing a cut leaf of the Kranz-type C_4 species, *Amaranthus hypochondriacus*, in a solution of $[^{13}CO_2^*]$ in a LI-6400 leaf chamber coupled to a tunable diode laser absorption spectroscope (TDL), allowed us to measure the rate of $^{13}CO_2$ efflux out of the leaf in the dark among all $[^{13}CO_2^*]$. As with the herbaceous C_3 species, *Brassica napus*, rates of $^{13}C_{efflux}$ in *A. hypochondriacus*, were dependent upon the rate of transpiration and the $[^{13}CO_2^*]$, with the highest rates of $^{13}C_{efflux}$ occurring when both the rate of transpiration and $[^{13}CO_2^*]$ were high (Fig. 1b). However, compared to *B. napus* (Stutz *et al*., 2017), rates of $^{13}C_{efflux}$ were ~1.5 and ~2 times lower when at the same rate of transpiration in *A. hypochondriacus* in the medium-carbon (MC) and high-carbon (HC) treatments, respectively (Fig. 1b, c).

The highest percentage of xylem-transported CO_2 that exited the leaf of *A. hypochondriacus* was 30%, which occurred in the MC and HC treatments; while the highest percentage of xylem-transported CO_2 that exited the leaf in *B. napus* was 75%, which occurred in the HC treatment (Fig. 3a, b). Stringer & Kimmerer (1993) and Stutz *et al*. (2017) observed that ~83% of xylem-transported CO_2 exited cut leaves of *Populus deltoides* in the dark. Rates of xylem-transported CO_2 consumption were higher in the Kranz-type C_4 species (~0.25 µmol CO_2 m^{-2} s^{-1}) compared to *B. napus* (~0.08 µmol CO_2 m^{-2} s^{-1}), in the first 90 minutes after turning off the light, indicating one of several possibilities: 1) it takes longer and there are more photosynthetic enzymes to be deactivated in the dark in *A. hypochondriacus*, 2) lower stomatal conductance in *A. hypochondriacus* which lead to lower efflux of xylem-transported CO_2 entering and exiting the leaf, or 3) Kranz anatomy prevented xylem-transported CO_2 from exiting the leaf.

Following deactivation of photosynthetic enzymes, 90 to 120 minutes in C_4 species and 30 to 60 minutes in C_3 species (Rajagopalan *et al.*, 1993), the rate of consumption of xylem-transported CO_2 should decrease. Rates of xylem-transported CO_2 consumption in the dark were similar between *B. napus* (~0.07 µmol CO_2 m^{-2} s^{-1}) and *A. hypochondriacus* (~0.07 µmol CO_2 m^{-2} s^{-1}) when rates of xylem-transported CO_2 consumption were averaged following the light being turned off for at least 120 minutes; indicating that deactivation of PEPC took longer in the C_4 species but once PEPC was deactivated the consumption rate of xylem-transported CO_2 were similar between the C_3 and C_4 species. Additionally, Alanso-Cantabrana & von Caemmerer (2016) found *in vitro* PEPC activities were 32 times higher in *Flaveria bidentis* (C_4 species) compared to *F. pringlei* (C_3 species). It is likely that a combination of the quantity of PEPC and

the time to deactivate PEPC in the Kranz-type C_4 species that caused the higher consumption of xylem-transported CO_2 observed in *A. hypochondriacus* compared to *B. napus* in the dark.

Another possibility for why *A. hypochondriacus* has a lower $^{13}C_{efflux}$ compared to *B. napus* could be stomatal conductance in the dark. In *B. napus* and *A. hypochondriacus* stomatal conductance was ~0.5 mol H_2O m^{-2} s^{-1} before cutting the leaf. When the light was turned off stomatal conductance dropped in *B. napus* to between ~0.01 mol H_2O m^{-2} s^{-1} and ~0.02 mol H_2O m^{-2} s^{-1} (data not shown) and remained at these conditions throughout the experiment. However, when the *A. hypochondriacus* leaf was cut stomatal conductance declined to ~0.1 mol H_2O m^{-2} s^{-1} before the light was turned off; but once the light was turned off stomatal conductance declined to ~0.008 mol H_2O m^{-2} s^{-1} within an hour (data not shown). The low stomatal conductance in the dark observed in *A. hypochondriacus* may have contributed to the low amount of xylem-transported CO_2 that exited the leaf in the dark. Snyder *et al*. (2003) observed that stomatal conductance at night was between 0.012 mmol H_2O m^{-2} s^{-1} and 0.025 mmol H_2O m^{-2} s^{-1} in two Kranz-type C_4 *Atriplex* shrubs and a Kranz-type C_4 grass in a warm desert habitat. However, in the same location stomatal conductance was higher in the C_3 species 0.1 mmol H_2O m^{-2} s^{-1} compared to the C_4 species. The dark stomatal conductance we observed in *A. hypochondriacus* was considerably lower than stomatal conductance on attached leaves from closely related C_4 species. Possibly the low stomatal conductance observed in our experiment is the result of cutting the leaf. Recent work shows night stomatal conductance and rates of dark transpiration are higher than previously thought in both C_3 and C_4 species (Caird *et al*., 2007; Resco de Dios *et al*. 2015). However, a third possibility is that Kranz anatomy impedes the flow of xylem-transported CO_2 out of the leaf.

In Kranz-type C_4 species the vascular bundle is surrounded by a ring of bundle-sheath cells which are surrounded by a ring of mesophyll cells. If xylem-transported CO_2 travels symplastically through the plasmodesmata or plasma membrane then the CO_2 has the potential to interact with enzymes located in the mesophyll and bundle-sheath cells. Instead, if water travels apoplastically, it will not have an opportunity to interact with the cellular enzymes. When rates of transpiration are compared between *A. hypochondriacus* and *B. napus* 45 minutes after turning off the light, rates of transpiration are similar between the two species but the efflux of xylem-transported CO_2 is two times greater in *B. napus* compared to *A. hypochondriacus* (Fig 1c), indicating that it is likely Kranz anatomy and not stomatal conductance or deactivation of photosynthetic enzymes in the dark that is responsible for the lower rate of $^{13}C_{efflux}$ observed in *A. hypochondriacus* in the dark.

Did the Kranz-type C_4 plant use xylem-transported CO_2 for photosynthesis?

Our method, of placing a cut Kranz-type C_4 leaf in a solution of $[^{13}CO_2^*]$ in a LI-6400 leaf chamber coupled to a TDL, allowed us to estimate how much xylem-transported CO_2 was used for carbon fixation in the light. Little if any xylem-transported CO_2 exited the leaf in the light; however, it is impossible to know if xylem-transported CO_2 was captured by Rubisco or PEPC. Photosynthetic discrimination confirms that little if any xylem-transported CO_2 exited the leaf in the low-carbon (LC) treatment in either the light- or CO_2-response curves (Fig. 4a, b). However, some xylem-transported CO_2 exited the leaf in the MC and HC treatments as evidenced by the high $\Delta^{13}C$ values observed in both the light- and CO_2-response curves (Fig. 4c, d).

We know the rate of transpiration, which allows us to calculate the amount of $[^{13}CO_2^*]$ entering the cut leaf for both *B. napus* and *A. hypochondriacus* (Fig. 5). As expected, the rate of xylem-transported CO_2 entering the leaf was dependent upon the rate of transpiration and $[^{13}CO_2^*]$ for both species. Since rates of transpiration were higher in *B. napus* compared to *A. hypochondriacus* the rate of xylem-transported CO_2 entering the leaf was also higher (Fig. 5); however, we detected little xylem-transported CO_2 exiting the leaf of *A. hypochondriacus* in the light but a large amount of xylem-transported CO_2 exiting *B. napus* in the light indicating that the capacity for *B. napus* to utilize xylem-transported CO_2 is lower than the capacity for *A. hypochondriacus*. If none of the xylem-transported CO_2 that enters the leaf exits the leaf then xylem-transported CO_2 is consumed by enzymes in the light. Little if any xylem-transported CO_2 exited the leaves of *A. hypochondriacus* in the LC treatment (Fig. 4) indicating that all added xylem-transported CO_2 was used for photosynthesis; however, it is impossible to detect if the xylem-transported CO_2 was captured by Rubisco or PEPC. In the MC and HC treatments $\Delta^{13}C$ indicates that some xylem-transported CO_2 exited the leaf, however, based on calculations using data from the TDL the efflux of xylem-transported CO_2 was minimal in both the MC and HC treatments.

Concentrations of CO_2 are high in stems of trees (Teskey *et al*., 2008), yet prior work has shown that little of the xylem-transported CO_2 is used for photosynthesis compared to what is available (Bloemen *et al*., 2013a). Our data show that this is not the same for Kranz-type C_4 plants, especially at lower concentrations. We found it was hard to detect any efflux of xylem-transported CO_2 from *A. hypochondriacus* such that labeled leaves in the LC treatment had photosynthetic discrimination values which are identical to the KCl control. However, in the MC and HC treatments $\Delta^{13}C$ values are different from the KCl values indicating that some

xylem-transported CO_2 exited the leaves. Compared to *B. napus* very little xylem-transported CO_2 exited the Kranz-type C_4 leaf.

In order for xylem-transported CO_2 to exit the leaf of the Kranz-type C_4 plant CO_2 must exit the vascular bundle and then exit through the ring of bundle-sheath and mesophyll cells. The water with the dissolved CO_2 has three possibilities for exiting the leaf: 1) traveling apoplastically, traveling along the cells walls, 2) traveling symplastically, crossing the plasma membrane of the cell, or 3) traveling in gas phase (Buckley, 2015). While it was traditionally thought that water traveled apoplastically (Strugger, 1943); recent work has shown the existence of aquaporins (Chrispeels & Agre, 1994) and tracer studies show the accumulation of a tracer at the proximal margins of living cells and the xylem (Canny, 1986, 1990) indicating that water may move symplastically through cells. Aquaporins allow water, CO_2 and other small uncharged molecules to quickly and easily pass through membranes (Uehlein *et al*., 2003; Flexas *et al.*, 2006; Maurel *et al*., 2008; Sade *et al*., 2013). In order for water to move symplastically it must cross two sets of membranes per cell as well as diffuse through the cytoplasm of the cell (Buckley, 2015). However, if water traveled out of the xylem and symplastically into the bundle-sheath cells it will likely add to the high concentration of CO_2 around Rubisco or it could travel apoplastically through the layer of bundle-sheath cells and be carboxylated by PEPC in the mesophyll cell and travel into to the bundle-sheath cell as a C_4 acids. If water with dissolved xylem-transported CO_2 traveled symplastically through the cells then very little xylem-transported CO_2 would exit the leaf and a high percentage of xylem-transported CO_2 would be used for photosynthesis but not be detected with our TDL technique. If water with dissolved CO_2 traveled apoplastically through the leaf before reaching the intercellular air spaces where the water will evaporate and either the CO_2 will move out of solution and remain in the intercellular

95

air space or exit the leaf as CO_2. A third possibility is that water will enter the gas phase

between the bundle-sheath cell and xylem interphase and then enter the leaf in the vapor phase.

If this was the case then the CO_2 would also be in gas phase and would either be captured in the

bundle-sheath cells or mesophyll cells or exit the leaf as CO_2. Buckley (2015), in modeling the

three possibilities of water movement through the leaf concluded that most of the water traveled

apoplastically through the leaf. Based on how little xylem-transported CO_2 exited the Kranz-

type C_4 leaf it appears that much of the water could have traveled symplastically through the

leaf. However, our method does not allow us to determine how water with dissolved CO_2

traveled through a leaf and the only conclusion that can be drawn is that most xylem-transported

CO_2 was captured and used for carbon fixation.

Significance for the evolution to C_4 photosynthesis?

C_4 photosynthesis is spread across 19 plants families reflecting 61 independent origins

(Sage, 2016) in both eudicots and monocots. In order for C_4 photosynthesis to work a separation

of enzymes is required. Separation of C_3 and C_4 enzymes occurs in one of two ways: 1) Kranz-

type C_4 plants that separate Rubisco and PEPC into two distinct cells, bundle-sheath and

mesophyll respectively, termed Kranz anatomy (Edwards *et al*., 2004) or 2) single-cell C_4 plants

that use a single-cell with partitions for C_3 and C_4 enzymes (Voznesenskaya *et al*., 2001;

Edwards *et al*., 2004). Both anatomical types of C_4 photosynthesis effectively concentrate CO_2

around Rubisco while reducing rates of photorespiration. In Kranz-type C_4 plants the bundle-

sheath cells have low conductance to CO_2 (high resistance to CO_2 diffusion and low ϕ). Several

anatomical features are required to advance to Kranz-type C_4 photosynthesis such as increased

vein densities, and enhancement of bundle-sheath organelles in addition to the biochemical

requirements such as photorespiratory CO_2 pumps and increased PEPC activity before the finial optimization can occur (Monson, 1999; Sage, 2004). While increasing vein densities may only increase structural integrity or enhance leaf water status (Sage, 2004) it may also allow xylem-transported CO_2 to be utilized for photosynthesis by reducing the distance between vascular bundles and photosynthetic cells. Many C_3 and intermediate C_3-C_4 species have developed Kranz anatomy with closely spaced veins and development of bundle-sheath cells which may provide these plants an advantage that was previously overlooked, the ability to utilize and recycle xylem-transported CO_2 for leaf photosynthesis.

CONCLUSION

Our technique, of using an LI-6400 coupled to a TDL, allowed us to measure the efflux of xylem-transported CO_2 out of cut leaves in the Kranz-type C_4 species, *Amaranthus hypochondriacus* in the dark. Rates of $^{13}C_{efflux}$ in the dark increased with increasing rates of transpiration and $[^{13}CO_2{}^*]$, however, when compared to a herbaceous C_3 species, *Brassica napus*, rates of $^{13}C_{efflux}$ were lower in *A. hypochondriacus* when compared at the same rates of transpiration and $[^{13}CO_2{}^*]$ indicating that leaf anatomy or enzymatic activity in the dark was decreasing the flux of xylem-transported CO_2 out of the leaf. Because of the high carbon fixation in the dark, we cannot prove that carbon fixation in the light utilized the full C_4 cycle, though we think it is likely as even less xylem-transported CO_2 exited the leaf in the light. Since the amount of xylem-transported CO_2 that entered the leaf was dependent upon the rate of transpiration and $[^{13}CO_2{}^*]$, more ^{13}C entered the leaf in the light, but less than in *B. napus*. However, the low efflux rate of xylem-transported CO_2 means that leaves of *A. hypochondriacus*

likely use more of it. Potentially Kranz anatomy is one way C_4 species are able to increase photosynthetic efficiency over their C_3 counterparts.

AUTHOR CONTRIBUTIONS

S.S.S. performed experiments and analyzed data. D.T.H. provided conceptual framework.

S.S.S. and D.T.H. wrote the manuscript.

REFERENCES

Alonso-Cantabrana H, von Caemmerer S. 2016. Carbon isotope discrimination as a diagonostic tool for C_4 photosynthesis in C_3-C_4 intermediate species. *Journal of Experimental Botany* **67:** 3109-3121.

Barbour MM, McDowell NG, Tcherkez G, Bickford CP, Hanson DT. 2007. A new measurement technique reveals rapid post-illumination changes in the carbon isotope composition of leaf-respired CO_2. *Plant, Cell & Environment* **30**: 469-482.

Bloemen J, McGuire MA, Aubrey DP, Teskey RO, Steppe K. 2013a. Transport of root-respired CO_2 via the transpiration stream affects aboveground carbon assimilation and CO_2 efflux in trees. *New Phytologist* **197**: 555-565.

Bloemen J, McGuire MA, Aubrey DP, Teskey RO, Steppe K. 2013b. Assimilation of xylem-transported CO_2 is dependent on transpiration rate but small relative to atmospheric fixation. *Journal of Experimental Botany* **64**: 2129-2138.

Bloemen J, Bauweraerts I, De Vos F, Vanhove C, Vandenberghe S, Boeckx P, Steppe K. 2015. Fate of xylem-transported [11]C- and ^{13}C-labeled CO_2 in leaves of poplar. *Physiologia Plantarum* **153**: 555-564.

Buckley TN. 2015. The contributions of apoplastic, symplastic and gas phase pathways for water transport outside the bundle sheath in leaves. *Plant, Cell & Environment* **38**: 7-22.

von Caemmerer S, Furbank RT. 2003. The C_4 pathway: an efficient CO_2 pump. *Photosynthesis Research* **77**: 191-207.

Caird MA, Richards JH, Donovan LA. 2007. Nighttime stomatal conductance and transpiration in C_3 and C_4 plants. *Plant Physiology* **143**: 4-10.

Canny M. 1986. Water pathways in wheat leaves. III. The passage of the mestome sheath and the function of the suberized lamellae. *Physiologia Plantarum* **66**: 637-647.

Canny M. 1990. What becomes of the transpiration stream? *New Phytologist* **114**: 341-368.

Chrispeels MJ, Agre P. 1994. Aquaporins: water channel proteins of plant and animal cells. *Trends in Biochemical Sciences* **19**: 421-425.

Erhardt EB, Hanson DT. 2013. Tdllicor: TDL/Licor processing. R package version 0.1-22.

Edwards GE, Franceschi VR, Voznesenskaya EV. 2004. Single cell C_4 photosynthesis versus the dual-cell (Kranz) paradigm. *Annual Review of Plant Biology* **55**: 173-196.

Farquhar GD. 1983. On the nature of carbon isotope discrimination in C_4 species. *Australian Journal of Plant Physiology* **10**: 205-226.

Flexas J, Ribas-Carbo M, Hanson DT, Bota J, Otto B, Cifre J, McDowell N, Medrano H, Kaldenhoff R. 2006. Tobacco aquaporin NtAQP1 is involved in mesophyll conductance to CO_2 *in vivo*. *Plant Journal* **48**: 427-439.

Griffis T, Baker J, Sargent S, Tanner B, Zhang J. 2004. Measuring field-scale isotopic fluxes with tunable diode laser absorption spectroscopy and micrometeorological techniques. *Agricultural and Forest Meterology* **124**: 15-29.

Hatch MD. 1987. C_4 photosynthesis—a unique blend of modified biochemistry, anatomy and ultrastructure. *Biochimica et Biophysica Acta* **895**: 81-106.

Hatch MD, Agostino A, Jenkins CLD. 1995. Measurement of the leakage of CO_2 from bundle-sheath cells of leaves during C_4 photosynthesis. *Plant Physiology* **108**: 173-181.

Hatch MD, Slack CR, Johnson HS. 1967. Further studies on a new pathway of photosynthetic carbon dioxide fixation in sugarcane and its occurrence in other plant species. *Biochemical Journal* **102**: 417-422.

Kanai R, Edwards GE. 1999. The biochemistry of C_4 photosynthesis in: Sage RF, Monson RK, eds. C_4 plant biology. London: Academic Press, 49-87.

Maurel C, Verdoueq L, Luu DT, Santoni V. 2008. Plant aquaporins: membrane channels with multiple integrated functions. *Annual Review of Plant Biology* **59**: 595-624.

McGuire MA, Marshall JD, Teskey RO. 2009. Assimilation of xylem-transported ^{13}C-labelled CO_2 in leaves and branches of sycamore (*Platanus occidentalis* L.). *Journal of Experimental Botany* **60**: 3809-3817.

Monson RK. 1999. The origins of C_4 genes and evolutionary pattern in the C_4 metabolic phenotype. In Sage RF, Monson RK, eds. *C_4 plant biology*. San Diego, CA, USA: Academic Press, 377-410.

R Core Development Team. 2012. R: A language and environment for statistical computing. Vienna, Austria: Ro Foundation for Statistical Computing. ISBN 3-900051-0700. Aviailable at: http://www.R-project.org (Accessed 19 August 2012).

Rajagopalan AV, Devi MT, Raghavendra AS. 1993. Patterns of phosphoenolpyruvate carboxylase activity and cytosolic pH during light activation and dark deactivation in C_3 and C_4 plants. *Photosynthesis Research* **38**: 51-60.

Resco de Dios V, Roy J, Ferrio JP, Alday JG, Landais D, Milcu A, Gessler A. 2015. Processes driving nocturnal transpiration and implications for estimating land evapotranspiration. *Scientific Reports* **5**: 10975.

Sade N, Galle A, Flexas J, Lerner S, Peleg G, Yaaran A, Moshelion M. 2013. Differential tissue-specific expression of NtAQP1 in *Arabidopsis thaliana* reveals a role for this protein in stomatal and mesophyll conductance of CO_2 under standard and salt-stress conditions. *Planta* **239**: 357-366.

Sage RF. 2004. The evolution of C_4 photosynthesis. *New Phytologist* **161**: 341-370.

Sage RF. 2016. A portrait of the C_4 photosynthetic family on the 50th anniversary of its discovery: species number, evolutionary lineages, and Hall of Fame. *Journal of Experimental Botany* **67**: 4039-4056.

Snyder KA, Richards JH, Donovan LA. 2003. Night-time conductance in C_3 and C_4 species: do plants lose water at night? *Journal of Experimental Botany* **54**: 861-865.

Stringer JW, Kimmerer TW. 1993. Refixation of xylem sap CO_2 in *Populus deltoides*. *Physiologia Plantarum* **89**: 243-251.

Strugger S. 1943. Der aufsteigende Saftstrom in der Pflanze. *Naturwisenschaft* **31**: 181-191.

Stutz SS, Anderson J, Zulick R, Hanson DT. 2017. Inside out: efflux of carbon dioxide from leaves represents more than leaf metabolism. *Journal of Experimental Botany* **68**: 2849-2857.

Teskey RO, McGuire MA. 2002. Carbon dioxide transport in xylem causes errors in estimation of rates of respiration in stems and branches of trees. *Plant, Cell and Environment* **25:** 1571-1577.

Teskey RO, Saveyn A, Steppe K, McGuire MA. 2008. Origin, fate and significance of CO_2 in tree stems. *New Phytologist* **177**: 17-32.

Ubierna N, Sun W, Cousins AB. 2011. The efficiency of C_4 photosynthesis under low light conditions: assumptions and calculations with CO_2 isotope discrimination. *Journal of Experimental Botany* **62**: 3119-3134.

Uehlein, Lovisolo C, Siefritz F, Kaldenhoff R. 2003. The tobacco aquaporin NtAQP1 is a membrane CO_2 pore with physiological functions. *Nature* **425**: 734-737.

Voznesenskaya EV, Franceschi VR, Kiirats O, Freitag H, Edwards GE. 2001. Kranz anatomy is not essential for terrestrial C_4 plant photosynthesis. *Nature* **414**: 543-546.

FIGURES

Fig. 1 (a) Transpiration dependence of leaf respiration ($^{12}C_{RL}$) for three [$^{13}CO_2^*$]—light gray triangles represents the low-carbon (LC—1.19 mmol l^{-1}) treatment (y=0.1413x + 1.234, R^2=0.1337), dark gray triangles represent the medium-carbon (MC—5.95 mmol l^{-1}) treatment (y=0.2046x + 1.215, R^2=0.3945) and filled triangles represent the high-carbon (HC—11.9 mmol l^{-1}) treatment (y=0.3013x + 1.048, R^2=0.7326). (b) Transpiration dependence of $^{13}C_{efflux}$ in the dark for three [$^{13}CO_2^*$] light gray circles represent the LC (y=0.002446x + 0.01554, R^2=0.2740), dark gray circles represent the MC (y=0.04432x + 0.001913, R^2=0.9019) and filled circles represent the HC (y=0.06925x -0.007001, R^2=0.9661). (c) Transpiration dependence of $^{13}C_{efflux}$ in the HC treatment from *Brassica napus* (green diamonds) and *Amaranthus hypochondriacus* (gray circles) from the HC treatment. Measurements represent 45 minutes after the light was turned off. Measurements were made on excised leaves of *A. hypochondriacus* or *B. napus* placed in one of the three [$^{13}CO_2^*$] solutions. Measurements represent averages and ±1 SD of five replicates for *A. hypochondriacus* and four replicates for *B. napus*. Transpiration was averaged over 0.1 mmol H$_2$O m^{-2} s^{-1} increments and represents rates of transpiration and $^{13}C_{efflux}$ at least 45 minutes after the light was turned off. *B. napus* data modified from Stutz *et al*. (2017).

Fig. 2 Response of gross (a) $^{13}C_{efflux}$ (circles) and (b) $^{12}C_{RL}$ (triangles) in *A. hypochondriacus* at a transpiration rate of 0.75 mmol H$_2$O m^{-2} s^{-1} for each [$^{13}CO_2^*$]. Measurements were made on cut leaves of *A. hypochondriacus* placed in one of three [$^{13}CO_2^*$] solutions—LC, MC, and HC. Measurements represent averages and ±1 SD of five replicates for each [$^{13}CO_2^*$]. The low-carbon (LC) was 1.19 mmol l^{-1}, medium-carbon (MC) was 5.95 mmol l^{-1} and high-carbon (HC) was 11.9 mmol l^{-1}.

Fig. 3 The percentage of gross xylem-transported $^{13}CO_2$ exiting the leaf in the transpiration stream in (a) *A. hypochondriacus* and (b) *Brassica napus* across three $[^{13}CO_2{}^*]$ averaged over the first 90 minutes after turning off the light. Estimated rates xylem-transported $^{13}CO_2$ consumption in cut leaves of (c) *A. hypochondriacus* and (d) *B. napus* across three $[^{13}CO_2{}^*]$ averaged over the first 90 minutes after turning off the light. Measurements represent averages and ± 1 SD of five replicates for *A. hypochondriacus* and four replicates for *B. napus* made on cut leaves under the following concentrations: LC, MC, and HC. The low-carbon (LC) was 1.19 mmol l^{-1}, medium-carbon (MC) was 5.95 mmol l^{-1} and high-carbon (HC) was 11.9 mmol l^{-1}. *B. napus* data modified from Stutz *et al*. (2017).

Fig. 4 Photosynthetic discrimination ($\Delta^{13}C$) across (a,c) light- and (b, d) CO_2-response curves in *Amaranthus hypochondriacus*. Light-response curves (a) KCl control (open diamonds) and LC (light gray diamonds) and (c) MC (dark gray diamonds) and HC (filled diamonds) treatments. CO_2-response curves (b) KCl control (open diamonds) and LC (light gray diamonds) and (d) MC (dark gray diamonds) and HC (filled diamonds) treatments. Measurements represent means and ± 1 SD of five replicates for each treatment on cut leaves of *A. hypochondriacus*. The low-carbon (LC) was 1.19 mmol l^{-1}, medium-carbon (MC) was 5.95 mmol l^{-1} and high-carbon (HC) was 11.9 mmol l^{-1}.

Fig. 5 Calculated rates of $^{13}CO_2$ entering cut leaves of the (a, b) C_4 species *A. hypochondriacus* and (c, d) the C_3 species *B. napus* in (a, c) light- and (b, d) CO_2-response curves. LC (light gray diamonds), MC (dark gray diamonds) and HC (closed diamonds) for both species. Measurements represent means and ± 1 SD of five replicates for each treatment in *A.*

hypochondriacus and *B. napus*. The low-carbon (LC) was 1.19 mmol l^{-1}, medium-carbon (MC) was 5.95 mmol l^{-1} and high-carbon (HC) was 11.9 mmol l^{-1}.

Fig. 6 Light- and CO_2-response curves for rates of photosynthesis with (a, b) ^{13}Carbon ($^{13}A_x$—photosynthesis using xylem-transported CO_2, or background rates of $^{13}A_{obs}$ in KCl treatment) and (c, d) ^{13}Carbon ($^{12}A_{obs}$—photosynthesis CO_2 derived from the atmosphere). $^{13}A_x$ in *A. hypochondriacus* KCl (open circles), LC (light gray circles), MC (dark gray circles) and HC (closed circles) and $^{12}A_{obs}$ for *A. hypochondriacus*, for KCl (open triangles), LC (light gray triangles), MC (dark gray triangles) and HC (closed triangles). Measurements represent means and ±1 SD of five replicates for each treatment. The low-carbon (LC) was 1.19 mmol l^{-1}, medium-carbon (MC) was 5.95 mmol l^{-1} and high-carbon (HC) was 11.9 mmol l^{-1}.
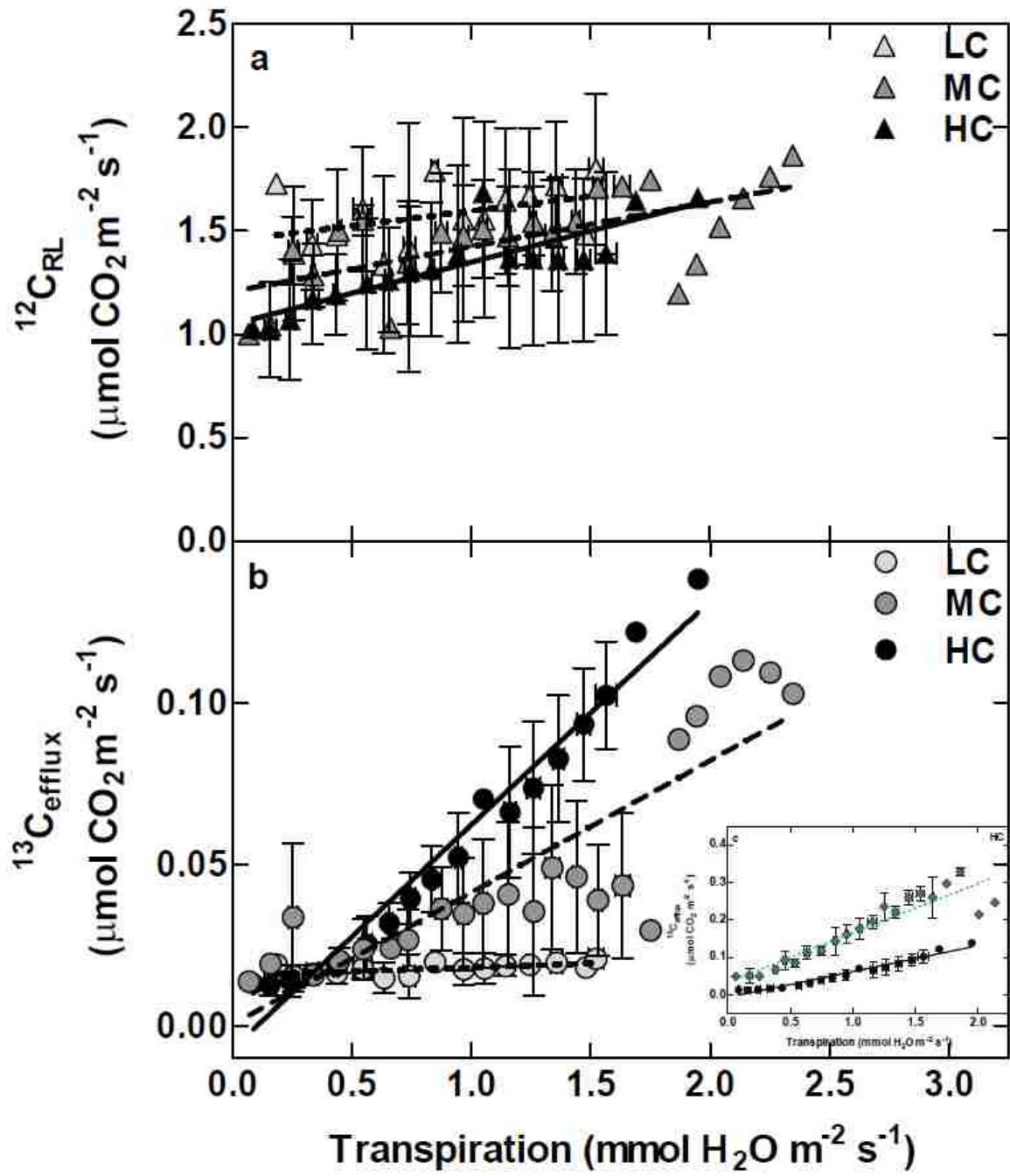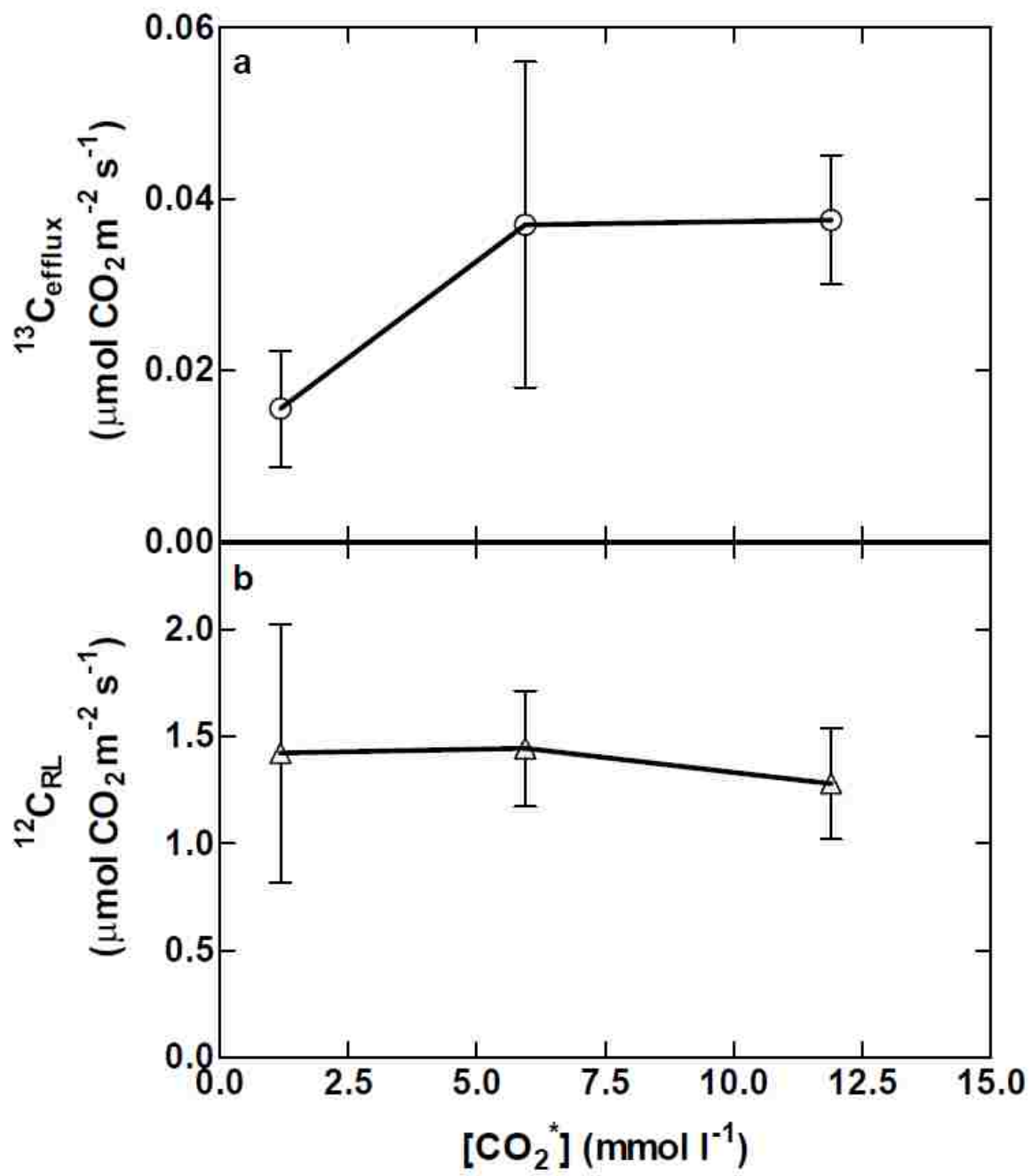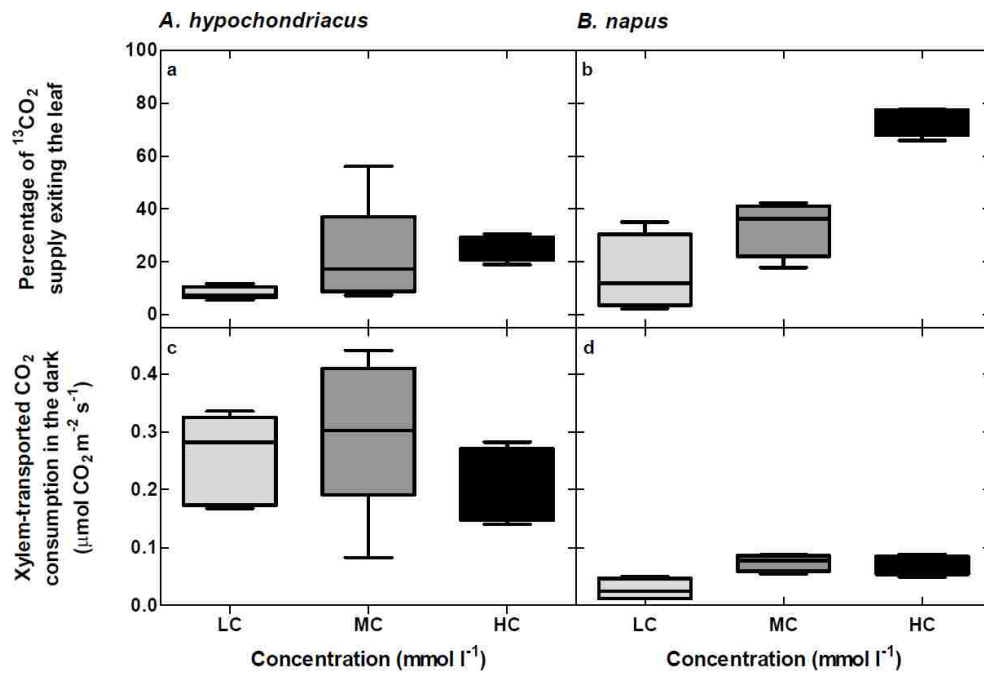
FIGURE 1

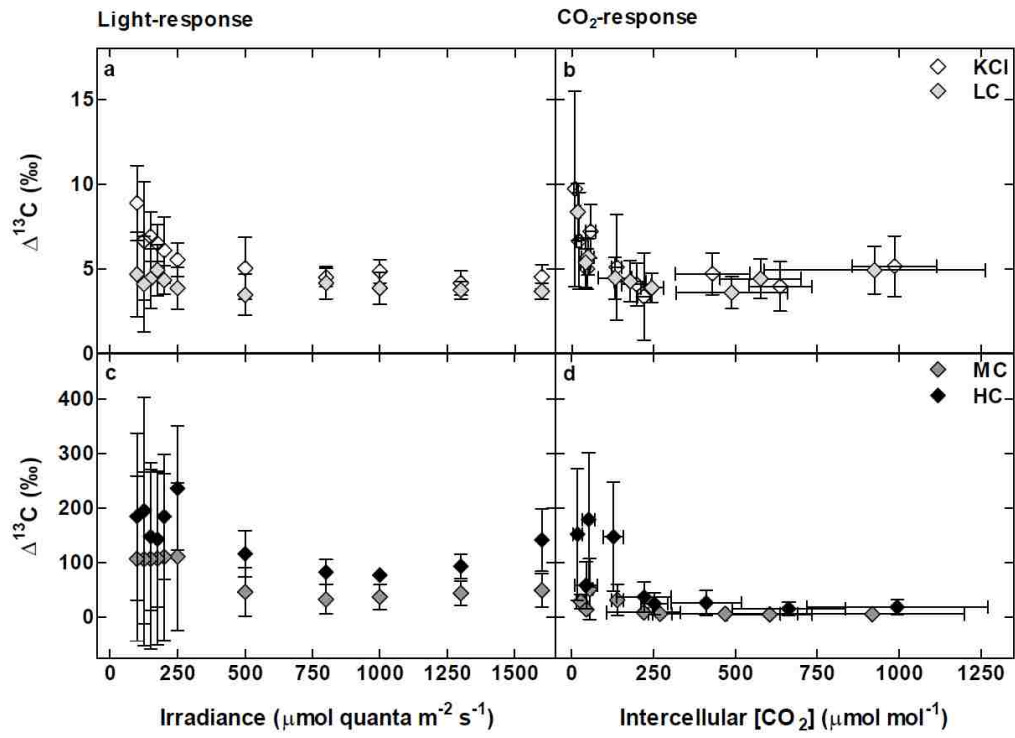**FIGURE 2**

FIGURE 3

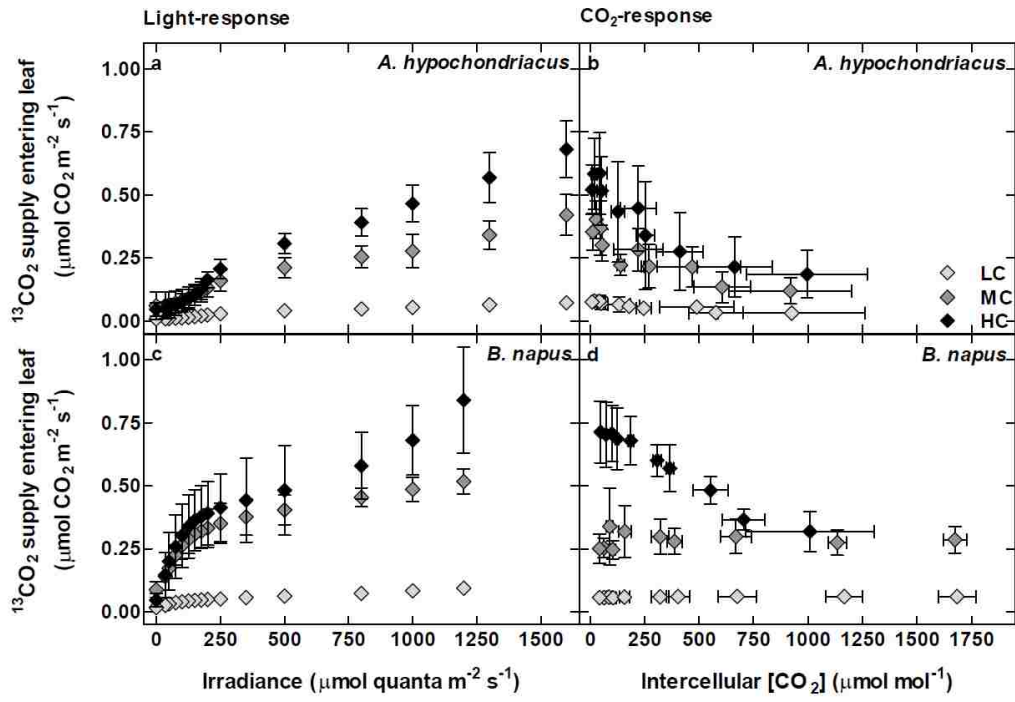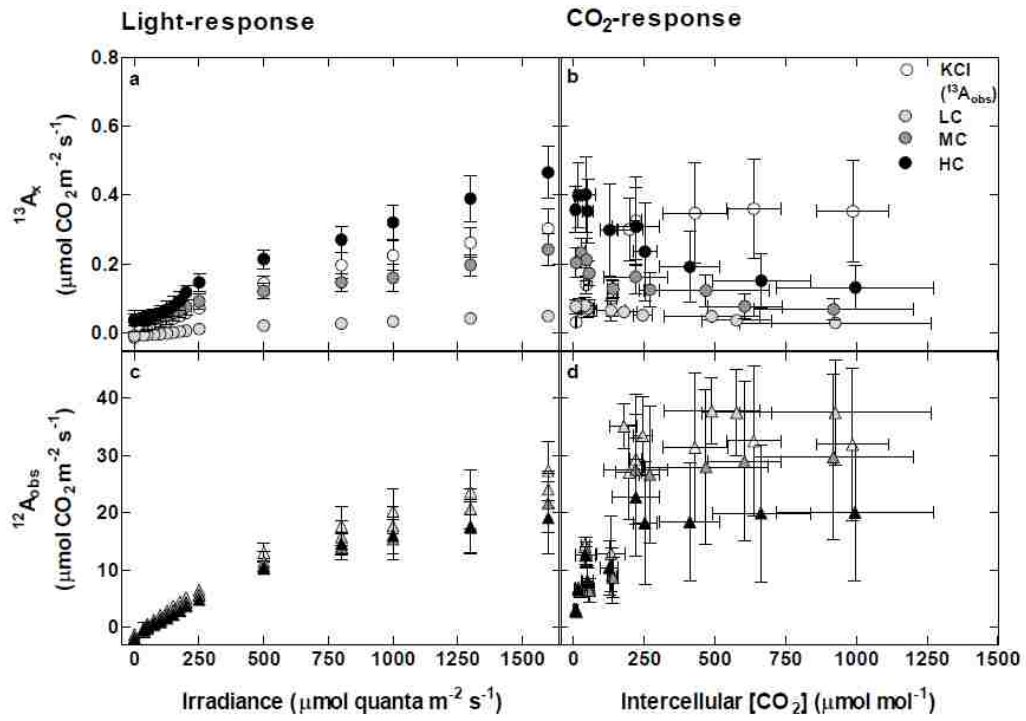**FIGURE 4**

FIGURE 5

FIGURE 6

Chapter 5

Conclusions

The aims of this study were to utilize a novel method that couples a tunable diode absorption spectroscope (TDL) to a portable photosynthesis machine (LI-6400) to explore: 1) how much xylem-transported CO_2 effluxes through cut leaves in the dark, 2) how much xylem-transported CO_2 is used for photosynthesis and 3) how much xylem-transported CO_2 effluxes out of a leaf in the light in a woody and herbaceous C_3 species and Kranz-type C_4 species. Previous methods for measuring rates of xylem-transported CO_2 assimilation have utilized radioactive or stable isotopes. However, these methods only allow measurements of xylem-transported CO_2 assimilation at discrete time points; require complete destruction of the tissues, followed by lengthy work to determine how much xylem-transported CO_2 is incorporated into plant tissues. Using a LI-6400 coupled to a TDL allows for real-time measurements of respiration (chapters 2 and 4) or assimilation (chapters 3 and 4) for both $^{12}CO_2$ and $^{13}CO_2$. In this study, the petiole of a cut leaf was placed in a solution of ^{13}C sodium bicarbonate dissolved in potassium chloride to simulate uptake and utilization of xylem-transported CO_2. However, with leaf, branch and stem chambers it would be possible to measure rates of xylem-transported CO_2 assimilation and efflux across an entire plant using non-destructive techniques.

In the dark, the efflux of xylem-transported CO_2 was greatest when both the rate of transpiration and $[^{13}CO_2{}^{*}]$ were high. Despite differences in leaf and stem anatomies the efflux of xylem-transported CO_2 assimilation was similar between the woody and herbaceous C_3 species; but it was lower in the Kranz-type C_4 species. However, several

111

unknowns still exist, such as stem [CO_2] across the height of woody and herbaceous plants and how branch CO_2 concentrations with attached leaves compare to the concentration of CO_2 in stems.

The LI-6400 coupled to the TDL can also be used to estimate rates of consumption of xylem-transported CO_2 in the dark. By knowing how much CO_2 is supplied to the leaf along with the rate of CO_2 entering and exiting the leaf it is possible to estimate how much xylem-transported CO_2 is consumed by enzymes in the dark. Rates of consumption of xylem-transported CO_2 were similar between the C_3 species; however, the rate of consumption was higher in the Kranz-type C_4 species following turning off the light. These differences are likely a result of the higher concentrations and slower deactivation of phosphoenolpyruvate carboxylase (PEPC). Enzyme assays could be used to determine the concentrations of PEPC in the C_3 and C_4 species and activity of PEPC going from illumination to darkness in C_3 and C_4 plants.

In the light, the flux of atmospheric CO_2 entering the leaf and the efflux of CO_2 generated from mitochondrial respiration are coupled with the addition of xylem-transported CO_2 entering the leaf with the water stream. In the C_3 species, rates of photosynthesis using xylem-transported CO_2 were highest when the intercellular CO_2 concentration was lowest, which occurred under high irradiance and low CO_2 concentrations in the light- and CO_2-response curves, respectively. However, in the Kranz-type C_4 species, it was only possible to determine how much xylem-transported CO_2 entered the leaf and estimate how much of the xylem-transported CO_2 would be used in the dark and equate that to enzymatic processes occurring in the light. Despite differences in leaf structure and petiole anatomy the woody and herbaceous C_3 species

had similar rates of assimilation using xylem-transported CO_2. However, it is likely that Kranz anatomy increased rates of xylem-transported CO_2 assimilation in the C_4 species compared to the C_3 species.

In the C_3 species, the highest rates of $^{13}C_{light\ efflux}$ occurred when rates of transpiration were highest, which coincided with the highest rates of xylem-transported CO_2 assimilation. However, very little xylem-transported CO_2 exited the Kranz-type C_4 leaf in the light compared to what exited the leaf in the dark. Kranz anatomy maybe another way C_4 species are able to increase photosynthetic efficiency over their C_3 counter parts. The first way to test this would be to label Kranz-type C_4 leaves with ^{14}C xylem-transported CO_2, collect the efflux and radiograph a labeled leaf to see how much xylem-transported CO_2 exited or remained in the leaf. Another way to test the influence of Kranz anatomy on xylem-transported CO_2 would be to use the single-cell C_4 species *Suaeda aralocaspica*. In *Suada* anatomy, the vascular bundles surround water storage cells which are surrounded by photosynthetic cells. However, both ribulose-1,5-bisphosphate-carboxylase/oxygenase (Rubisco) and PEPC are located in the same cell, with Rubisco located in the proximal and PEPC located in the distal end of the cell thus eliminating Kranz anatomy, but as in Kranz anatomy, xylem-transported CO_2 would first interact with Rubisco before interacting with PEPC.

The first project demonstrated that xylem-transported CO_2 effluxes from cut leaves of a woody and herbaceous C_3 species with different leaf anatomies, as well as Kranz-type C_4 species; however the rates of $^{13}CO_2$ efflux were lower in Kranz-type C_4 species compared to both C_3 species. Rates of $^{13}CO_2$ efflux in the dark, assuming low rates of transpiration and low $[CO_2^*]$, are just over 1.5% of the rate respiration in the C_3

species. While this efflux is small on the scale of an individual leaf, when scaling to include all the trees on Earth it may have a profound impact on models for the global carbon cycle. The second project demonstrated that the contribution of xylem-transported CO_2 to total photosynthesis in C_3 plants is considerably smaller than the contribution of atmospheric CO_2 to photosynthesis; however, xylem-transported CO_2 maybe like compound interest in a bank account. The amount of xylem-transported CO_2 that the plant uses is small at any given time but through time the contribution of xylem-transported CO_2 to total assimilation will be significant. The addition of xylem-transported CO_2 to photosynthesis may allow a plant to grow more in a season, allow a plant to produce more seeds or use the fixed carbon for respiration. The second project was also able to measure the efflux of xylem-transported CO_2 in the light. This efflux was small but should be explored more to assess the implications for modeling rates of respiration in the light. The third project demonstrated that Kranz-type C_4 plants likely use almost all xylem-transported CO_2 for photosynthesis. It is possible to determine how much xylem-transported CO_2 entered the Kranz-type C_4 leaves; however, little if any xylem-transported CO_2 exited the leaf indicating that nearly all of the xylem-transported CO_2 remained in the leaf. Kranz anatomy maybe another way C_4 plants are able to increase their carbon and water use efficiency over their C_3 counterparts.

Future work on xylem-transported CO_2 must determine the branch [CO_2] near attached leaves to determine how much xylem-transported CO_2 reaches leaves in the light and dark. This measurement has implications for understanding how xylem-transported CO_2 contributes to global models of leaf respiration and photosynthesis along with implications for understanding and improving global carbon models to understand the

responses of respiration and photosynthesis to climate change. Xylem-transported CO_2 has not previously been studied in C_4 species but many important agricultural crops such as maize, sugarcane, and sorghum are C_4 species. Understanding how Kranz-type C_4 plants improve their water and carbon use efficiency over C_3 plants has implications for improving photosynthesis in both C_4 and C_3 crop species.